Immunoglobulins and their Fragments on Solid Surfaces

Promotor: dr. J. Lyklema
hoogleraar in de fysische chemie, met bijzondere
aandacht voor de grensvlak- en kolloïdchemie

Co-promotor: dr. ir. W. Norde
universitair hoofddocent bij de
vakgroep Fysische en Kolloïdchemie

Immunoglobulins and their Fragments on Solid Surfaces

J.A.G. Buijs

BIBLIOTHEEK
LANDBOUWUNIVERSITEIT
WAGENINGEN

Stellingen

1. Het IgG-molekuul wordt preferent geadsorbeerd via het Fc gedeelte doordat het Fc-fragment een lagere struktuurstabiliteit heeft dan het $F(ab')_2$-fragment.

    Dit proefschrift, Hoofdstukken 5 en 6.

2. Elektrostatische wisselwerkingen zijn in staat om de orientatie van een geadsorbeerd IgG-molekuul te beïnvloeden.

    Dit proefschrift, Hoofdstuk 6.

3. Maximale adsorptie van IgG vindt niet plaats in het i.e.p. van het eiwit [1] en ook niet in het i.e.p. van het eiwit/oppervlak complex [2] maar bij een pH tussen deze twee bovengenoemde waarden in [3].

    1. P. Bagchi and S.M. Birnbaum, J. Colloid Interface Sci., 83 (1981) 460.
    2 A.V. Elgersma (1990) proefschrift LUW, stelling 1.
    3 Dit proefschrift, Hoofdstuk 3.

4. Vorming van α-helices in eiwitten kan geïnduceerd worden als een eiwit in contact komt met een hydrofoob oppervlak.

    Dit proefschrift, Hoofdstuk 5

5. Er hoeft geen DNA aanwezig te zijn om een Scanning Tunneling Microscopy afbeelding van DNA te maken.

    C.R Clemmer, and T.P. Beebe, Jr., Science, 251 (1991) 640.

6. De met behulp van fotoakoestiek gemeten absorptiespectra van zwak-absorberende poeders kunnen niet zonder meer genormaliseerd worden met behulp van een alles-absorberend (zwart) poeder.

    J. Buijs, J.P. Favier, O. Dóka, A. Miklós, and A. Lörincz, Springer Series in Optical Sciences, Vol. 69, Photoacoustic and Photothermal Phenomena III, Ed. D. Bicanic, Springer Verlag 1991.

7. Door het voortgaande proces van verkorting en specialisatie van zowel studie als promotie zullen stellingen bij een proefschrift verder vervallen tot een inhoudsloze traditie.

8. Er is een omgekeerd evenredig verband tussen de consumptie van voedselproducten met een laag vetgehalte en het vetgehalte van de consument.

    (observatie tijdens het inkopen van levensmiddelen in de V.S.)

9. Gezien het grote aantal gekleurde illustraties in gerenommeerde tijdschriften als Science en Nature, lijkt het erop dat het wetenschappelijke gehalte van een artikel toeneemt als illustraties gekleurd worden.

10. Veel wetenschappers zijn zo gewend om het belang van hun eigen onderzoek te overwaarderen dat ze op den duur zelf in deze overwaardering gaan geloven.

11. Door de mechanistische visie op het leven wordt de invloed van de emotionele toestand van een persoon op zijn/haar gezondheid sterk onderschat in de medische wetenschappen.

12. Gezien de lange tijd die de katholieke kerk erover deed om Galileo Galilei te rehabiliteren, zal het ook nog lang duren voordat de emancipatie van vrouwen leidt tot het aanstellen van vrouwelijke priesters.

Stellingen behorend bij het proefschrift "Immunoglobulins and their Fragments on Solid Surfaces" van Jos Buijs, Landbouwuniversiteit Wageningen, 22 september 1995.

Contents

3 *Adsorption of Monoclonal IgGs and their F(ab')₂ fragments onto Polymeric Surfaces*

4 *Adsorption Dynamics of IgG and its F(ab')₂ and Fc fragments Studied by Reflectometry*

1 General Introduction

1.1 Introduction

When protein solutions are exposed to surfaces, more often than not the proteins accumulate at the interface. In nature, proteins are present in biological fluids such as cell plasma, blood, milk, fruit juices, sea water, urine, saliva, and tears. Proteins play important roles in many biological processes; for some of these adsorption is a prerequisite. A well-known example is blood clotting by the proteins thrombin and fibrinogen after these have accumulated at the blood/air interface of open wounds. The relevance of protein adsorption at solid surfaces stems in part from technical developments which involve the exposure of non-biological materials to biological substances. For instance, this is the case with implanted artificial organs upon which blood proteins may adsorb. Another example is biofouling of materials as diverse as contact lenses, haemodialysis membranes, teeth and dental restoratives, ship hulls, and food processing equipment.

The progress made in biotechnology has also led to the utilisation of the biological functions of proteins outside their natural environment. Proteins are used in a wide range of applications in the field of biomedical, pharmaceutical and food industry. Many of these applications rely on the fact that the proteins are adsorbed at an interface, including diagnostic test systems, biosensors, emulsions and foams, biochemical separation and purification methods, and laundry detergent systems. In order to control and manipulate protein adsorption in the above-mentioned applications, a detailed understanding of the adsorption process is required.

1.2 Immunological tests

The present study is focused on the fundamental aspects of the adsorption behaviour of immunoglobulin G (IgG) onto solid surfaces. The use of IgG stems from its ability to bind a large variety of molecules (antigens) in a highly specific way. Therefore, the IgG

molecules can be used in sensitive detection methods aimed at the diagnosis of biological substances such as pathogens and hormones. Over the past few decades, immobilised IgG molecules have extensively been applied in diagnostic test systems such as enzyme-linked immuno-sorbent assays (ELISA) [1], radio immuno assays (RIA) [2], and latex agglutination assays [3,4]. More recently, a growing interest for accurate, sensitive and fast methods in the fields of medical diagnostics, pollution science, and food analysis has led to the development of biosensors involving immobilisation of biosensitive proteins such as IgG molecules [5,6].

Immobilisation of the IgG molecules is very helpful in order to concentrate IgG-antigen complexes for visualisation of the antigen binding. Upon adsorption however, the IgG molecules may loose their ability to bind antigens. A reduction in the antigen binding capacity may be caused by a decreased accessibility of the binding sites to antigens in solution. This can for example happen when the binding sites are in close contact with the sorbent surface. Furthermore, the adsorption may induce structural changes in the IgG molecule resulting in a reduction of the antigen binding capacity. An ideal situation of the state in which the '"Y"-shaped IgG molecules are adsorbed is shown in Fig. 1a. In this adsorbed state, the IgG molecule is attached by its Fc part whereas the antigen binding sites, located at the top of each of the two Fab parts, are oriented towards the solution. The adsorbed states of the IgG molecules in which the antigen binding is reduced owing to an unfavourable orientation or to structural changes are schematically shown in Figs. 1b and 1c, respectively.
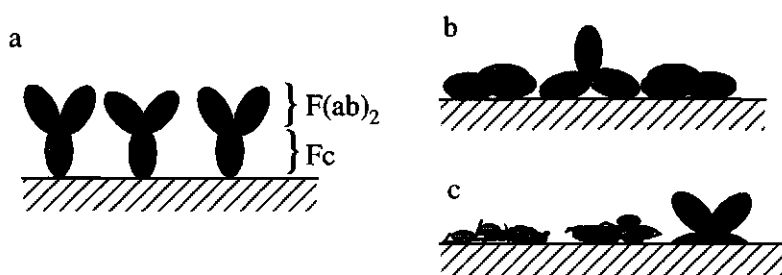
Fig. 1. Schematic representation of adsorbed states of IgG molecules. a) Ideal situation in which the antigen binding sites (dots at the top of the Fab parts) are directed towards the solution; b) orientation in which the antigen binding sites are inaccessible to antigens; c) adsorption-induced structural changes have occurred which in some cases can result in a loss of binding capacity.

1.3 Adsorption

Protein adsorption is determined by a delicate balance of several types of interaction between the different components in the system, i.e., the protein molecules, the sorbent surface the solvent and other solutes such as low molecular weight ions [7]. The interactions which are generally considered to be the most relevant ones for adsorption are:

hydrophobic interactions which emanate from the replacement of water molecules at the sorbent surface by proteins whereby the number of configurations, and hence the entropy of the water molecules increase. The more hydrophobic the surface, the stronger adsorption is promoted. This interaction is often the leading one, implying that it often overrules the other interactions.

electrostatic interactions, mainly Coulomb interactions between charged groups on the protein and the sorbent surface. These interactions are influenced by low molecular weight ions in solution because these can screen the electrostatic interactions and be incorporated in the adsorbed protein layer. Thus, at higher ionic strengths the influence of electrostatic interactions is reduced.

structural changes in the protein molecule which can be induced by the change in the environment of the proteins due to the presence of a sorbent surface. If these structural changes involve a loss of secondary and tertiary structure, it results in an increase in the conformational entropy of the protein. Moreover, a higher flexibility in the protein structure enables an optimisation of electrostatic and hydrophobic interactions.

The mechanism of adsorption can be studied by systematically changing the physical properties of the protein, the sorbent surface and the solution. In this way information is obtained about the nature of the interactions responsible for the adsorption process. A detailed understanding of the influence of the various interactions on the adsorbed state of the proteins is required in order to optimise the functioning of the immobilised proteins in their applications.

1.4 Outline of this thesis

The purpose of the present study is to require more insight in how IgG adsorption is affected by the interactions between IgG molecules and sorbent surfaces. In view of the practical applications this work is especially focused on how these protein-sorbent interactions determine the adsorbed state of the IgG molecules. Another important aspect

which is emphasised upon in the present study, is the influence of the different domains of the IgG molecule, i.e., the F(ab) and the Fc parts, on the adsorption behaviour.

An overview of the interactions involved in the adsorption of IgG together with the influence of these interactions on the adsorbed state of IgG molecules will be presented in Chapter 2. Furthermore, the IgG molecules used in the present study will be characterised with respect to some of their physical properties which are relevant for interpreting their adsorption behaviour.

In Chapters 3, 4, 5, and 6 various aspects of the adsorption process of IgG will be described. Information about the interactions involved is obtained by systematically changing the physical properties of the system. Hydrophobic interactions are studied by comparing adsorption at a hydrophilic and a hydrophobic sorbent surface. The electrostatic interactions are varied by performing adsorption experiments at different values for pH and ionic strength. Moreover, two monoclonal IgGs which differ in iso-electric point are studied. The influence of the F(ab) and the Fc parts on the adsorption behaviour is studied by comparing the adsorption of $F(ab')_2$ and Fc fragments with that of the whole IgG molecules. The fragmentation of the IgG molecules into $F(ab')_2$ and Fc fragments will be presented in Chapter 2.

Chapter 3 will be focused on the equilibrium adsorbed state of the two IgGs and their corresponding $F(ab')_2$ fragments onto three polymer latices which differ in hydrophobicity and charge. The influence of electrostatic interactions will be emphasised by characterising the protein-sorbent complexes with respect to their electrokinetic potential. Furthermore, special attention will be paid to the orientation of the adsorbed IgG and $F(ab')_2$ molecules.

The dynamic aspects of the adsorption process will be described in Chapter 4. The kinetic aspects are studied using reflectometry, a technique which enables a continuous monitoring of the adsorbed amount in time. The protein flux towards the surface is well-controlled which enables a quantification of the energy barriers which have to be overcome for the proteins to adsorb. In addition to monitoring the amount adsorbed in time, the desorption with respect to dilution is studied.

The results obtained from the adsorption studies, as reported in Chapters 3 and 4, yield a wealth of information about the influence of electrostatic and hydrophobic interactions on the adsorption behaviour. Nevertheless, these experimental data are not conclusive as to the role of structural changes in the adsorption process. Therefore, structural changes induced by the adsorption process are further studied using Fourier Transform Infrared spectroscopy (FTIR) in combination with Attenuated Total Reflection. This combination of techniques is a valuable tool for studying the secondary structure of proteins in the

adsorbed state [8,9]. Furthermore, the FTIR technique enables a quantification of the adsorbed amounts. The infrared spectra are recorded at certain time intervals of the adsorption process. In this way time-dependent information concerning the amounts adsorbed and the secondary structure of the adsorbed proteins is obtained under various adsorption conditions. These results will be presented in Chapter 5.

Finally, in Chapter 6 the effect of the various protein-sorbent interactions on the antigen binding capacity will be discussed. In this part of the study, first a layer of IgG or F(ab')$_2$ molecules is adsorbed, whereafter a solution containing the antigen is supplied. Both the amount of adsorbed IgG or F(ab')$_2$ and the amount of bound antigen are monitored using reflectometry.

The thesis is concluded by a summary and some perspectives for manipulating the adsorbed state of IgG based on the observed differences in adsorption behaviour of the F(ab')$_2$ and Fc fragments.

1.5 References

1   B. Longhi, B. Chichehian, A. Causse, and J. Caraux, *J. Immunol. Methods*, **92** (1986) 89.

2   L.A. Cole, D.B. Seifer, A. Kardana, and G.D. Braunstein, *Am. J. Obstet. Gynecol.*, **168** (1993) 1580.

3   S. Matsuzawa, Y. Itoh, H. Kimura, R. Kobayashi, and C. Miyauchi, *J. Immunol. Methods*, **60** (1983) 189.

4   B.L.J.C. Konings, E.G.M. Pelssers, A.J.C.M. Verhoeven, and K.M.P. Kamps, *Colloids Surfaces B: Biointerfaces*, **1** (1993) 69.

5   S. Löfas, B. Johnsson, K. Tegendal, and I. Rönnberg, *Colloids Surfaces B: Biointerfaces*, **1** (1993) 83.

6   I. Vikholm, and O. Teleman, *J. Colloid Interface Sci.*, **68** (1994) 125.

7   W. Norde, and J. Lyklema, *J. Biomater. Sci. Polymer Edn.*, **2** (1991) 183.

8   D.M. Byler, and H. Susi, *Biopolymers*, **25** (1986) 469.

9   W.K. Surewicz, and H.H. Mantsch, *Biochem. Biophys. Acta*, **952** (1988) 115.

2 Immunoglobulin G: Physical Properties and Adsorption Behaviour

Protein adsorption is mostly determined by physical interactions between the protein molecules and the sorbent surface. An overview is given of the different types of interactions between a protein and a sorbent surface, and on how these interactions influence the adsorption behaviour of immunoglobulin G (IgG). Furthermore, the two monoclonal IgGs used in the present study are characterised with respect to some of their physical properties which are relevant for their adsorption behaviour.

2.1 Structure of immunoglobulin G

The biological functioning of IgG stems from its ability to bind a large variety of molecules (antigens) in a highly specific way. The IgG molecule is composed of four polypeptide chains which are hold together by disulphide bonds and non-covalent forces. These four chains are divided into two groups of identical units; two heavy and two light chains. A schematic representation is shown in Fig. 1. The folded polypeptide chains are grouped together in three domains forming a "Y"-shaped configuration. The antigen binding sites are located at the far ends on two of the three domains. These two domains are identical and are called F(ab). The third domain is the Fc part which derived its name because this fragment readily crystallises. Among the physiological functions of the Fc part are interactions with specific receptors on the surface of a variety of cells. The three fragments are linked by a flexible hinge region, which allows the distance between the two antigen-binding sites to vary [1]. The biological significance of this segment flexibility is to facilitate the formation of IgG-antigen complexes. In the last few decades three-dimensional structures of crystallised IgG molecules and their fragments have been solved using X-ray diffraction. In this way the spatial structures of an Fc fragment [2], a Fab fragment [3,4] and an intact IgG molecule [5,6] have been obtained.
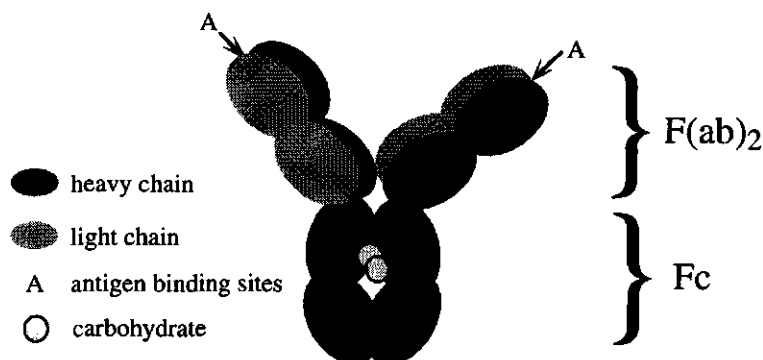
Fig. 1. schematic representation of an IgG molecule.

The IgG structures reveal that the domains of the different chains form layers of antiparallel ß-sheets , including 50-60% of the amino acid residues [2,4] which enclose a predominantly hydrophobic interior. The Fc part also contains carbohydrates which cover part of the hydrophobic interior, thereby creating some distance between the ß-pleated sheets of the two constituent heavy chains.

2.2 IgG adsorption

Like most proteins, IgG molecules tend to accumulate at interfaces between liquid and solid phases. This adsorption is the overall result of various types of interactions between the different components of the system, i.e., the IgG molecules, the sorbent surface, the solvent, and other solutes such as low molecular mass ions. The main interactions considered to be responsible for adsorption are hydrophobic interactions, electrostatic interactions, and structural changes in the protein molecule leading to an increase in conformational entropy [7,8]. Adsorption occurs spontaneously if the sum effect of these interactions is attractive, or, in thermodynamical terminology, if the Gibbs energy of the system decreases. This decrease in the Gibbs energy can be obtained either or both by a decrease in the enthalpy or by an increase in the entropy multiplied by the temperature. A thermodynamic analysis of the different interactions involved in protein adsorption has been described in detail by Norde and Lyklema [9].

2.2.1 Hydrophobic interactions

Proteins and solid surfaces in aqueous solutions are surrounded by water molecules which are somewhat restricted in position and orientation. Upon adsorption, these water molecules are released from the surfaces which results in a gain in entropy. The enthalpy of dehydration from non-polar surfaces is relatively small, the sign changing with temperature, whereas for more polar surfaces the release of water molecules from the surface occurs at the expense of the enthalpy. The non-polar surfaces are generally considered as hydrophobic whereas the polar surfaces are hydrophilic. The importance of hydrophobic interactions is demonstrated by the high affinity of IgG for hydrophobic polystyrene latices regardless of the electrostatic interactions involved [10,11,12]. Furthermore, it is generally found that the amounts adsorbed are higher on hydrophobic surfaces compared to those on hydrophilic surfaces [12,13,14,15,16,17].

Information about the hydrophobicity of IgG molecules has been obtained by judging the protein surface as revealed by X-ray structures of the Fc [2] and Fab [3] fragments of myeloma IgG molecules. For example, the hydrophobicity of the solvent-accessible surface area was calculated as described by Connolly [18,19]. These calculations show that the hydrophobic fraction of the surface area somewhat exceeds the hydrophilic fraction. The Fab fragment is slightly more hydrophobic than the Fc fragment. Furthermore, it is noted that there are no distinct hydrophobic or hydrophilic patches on the protein surface. In contrast to the pronounced effect of the hydrophobicity of the sorbent surface, the influence of the variation in the hydrophobicity of protein surfaces on the adsorption behaviour is considered to be very small [20,21].

2.2.2 Electrostatic interactions

Generally, all proteins and sorbents carry electrostatically charged groups. These charges are balanced by a diffuse and non-diffuse layer of counter charge in the solution. This counter charge consists of an excess of counterions and a deficit of co-ions. Upon adsorption these double layers overlap. Since accumulation of net charge within the adsorbed layer will be opposed strongly by the low dielectric permittivity inside that layer, electrostatic interactions only promote adsorption if charges are neutralised. Ion pair formation between charged groups on the protein and on the sorbent surface is one mechanism of charges neutralisation [22]. A second mechanism is the uptake of low molecular mass ions in the interfacial region [23,24,25,26] which is for example the basis of protein separation by ion-exchange chromatography [27]. The co-adsorption of low

molecular weight ions is essential for explaining the role of electrostatic interactions for IgG adsorption [11]. In addition, for protein adsorption in general there are some indications that low molecular weight ions play a role in bridging negatively charged groups on the sorbent surface and the negatively charged carboxyl groups of the protein. The argument stems from the observation that these carboxyl groups are found to be preferentially located close to the sorbent surfaces [22,28].

Although it is generally found that electrostatic interactions do not play a decisive role in determining the affinity of IgG molecules for sorbent surfaces, they have a pronounced effect on the maximum adsorbed amounts. This is demonstrated by the well-known influence of pH and ionic strength. The adsorbed amount as a function of pH shows a pattern with a maximum around the isoelectric point (i.e.p.) of the IgG [12,29,30]. In most studies, the reduction in adsorbed amount at pH values at both sides of the i.e.p. is ascribed to an expanded structure of the IgG containing a higher net charge density. With increasing ionic strength, the large variation in adsorbed amount with respect to pH diminishes [31]. This is consistent with the observation that the structural stability of IgG molecules increases with increasing ionic strength [32]. The maximum at the i.e.p. of the protein implies that the adsorbed amount is determined by the structure of the IgG molecule rather than to the interactions of IgG with the sorbent surface. However, more recent studies indicate that electrostatic interactions between protein and sorbent have some influence on the amounts adsorbed [10]. Furthermore, using monoclonal IgG it was shown that the maximum amount adsorbed occurs at the i.e.p. of the IgG/sorbent complex [11] rather than at the i.e.p. of the IgG molecule.

2.2.3 Structural rearrangements

Transferring a protein molecule from an aqueous solution to an interface involves a change in its environment, which may lead to structural rearrangements. These structural rearrangements may involve an increase in the conformational entropy of the protein and could be a contribution to the driving force for adsorption. Moreover, the increased flexibility of the protein structure can promote protein-sorbent interactions, such as the above-mentioned hydrophobic and electrostatic interactions. These phenomena have extensively been studied by Norde and co-workers [8,33]. They demonstrated that proteins having a strong internal coherence do not adsorb when they are electrostatically repelled by a hydrophilic surface, whereas proteins having a lower structural stability do adsorb under these conditions. As IgG is adsorbed onto hydrophilic surfaces regardless of

its charge interactions with the sorbent surface [12,29], the IgG molecule is regarded as a protein of relatively low structural stability.

It is believed that structural changes are more pronounced at hydrophobic surfaces because the interactions between the protein and the hydrophobic surface are relatively strong [34]. This was observed for IgG adsorption [16] and it has been suggested that these relatively large structural changes are responsible for a reduced antigen binding capacity [35].

It has furthermore been reported that after the IgG molecule has adsorbed changes in the protein structure continue to occur slowly [16,36,37]. From this observation it has been concluded that the IgG molecules are more tightly bound with increasing adsorption time [38]. These structural changes are more pronounced with increasing charge density on the sorbent surface [39]. Moreover, it has been reported that structural changes are more prominent at a lower degree of surface coverage [16] which is generally observed for proteins having a relatively low structural stability [40,41]. The relatively large structural changes with decreasing coverages of the sorbent surface are reflected in a reduction of the plateau value when the adsorption rate is decreased [42].

2.2.4 Other interactions

In addition to the three main interactions described above it is also possible that Van der Waals interactions are responsible for adsorption, although the contribution is usually considered to be small [21,43] or negligible [44]. Furthermore, it should be noted that hydrodynamic effects can greatly influence the dynamics of the adsorption process [45].

2.2.5 Models for the adsorption process and reversibility aspects

Models of protein adsorption are mainly centred on kinetic aspects [46,47] or on giving a thermodynamic analysis of the overall-adsorption process [9]. A detailed modelling of adsorption is hampered due to the irreversibility of the process. For IgG, it has been found that adsorption is highly irreversible with respect to dilution [10,30], although it has been reported that a small fraction of the adsorbed IgG molecules desorbs, upon replacing the protein solution by pure solvent [37]. The irreversibility of protein adsorption is probably related to adaptation of the protein structure to the sorbent surface in order to optimise its interactions. Nevertheless, a few attempts have been made to model IgG adsorption while ignoring the irreversibility and the possibility of structural changes. Due to these limitations, the model-predictions concerning adsorption are

mainly based the influence of the physical properties of the sorbent surface rather than on the properties of the IgG [21,44,48].

2.2.6 Packing of adsorbed IgG layers

In adsorption studies, the amount adsorbed per unit surface area is an important parameter. It is determined by the spatial distribution, the orientation and conformation of the adsorbed proteins. Adsorption isotherms for IgG generally show well-defined plateau values at higher protein concentrations in solution and these plateau values correspond to densely packed monolayers. The formation of complete monolayers of IgG molecules has experimentally been observed using an Atomic Force Microscope [49,50]. In some rare cases, a stepwise increase in the adsorbed amount (bimodal adsorption) has been reported which was ascribed to a discrete change in the way of packing at higher protein concentrations [51]. As the structure of an IgG molecule is known, it is possible to calculate the dimensions of an IgG molecule in its crystallised conformation. When only minor structural rearrangements take place, the known dimensions allow a more profound evaluation of the adsorbed amounts with respect to the protein orientation. The dimensions as obtained from crystallised Fc [2] and F(ab) [3] fragments are 7.0x6.3x3.1 nm³ and 8.2x5.0x3.8 nm³, respectively. Based on these dimensions, adsorbed amounts can be calculated for some regular orientations of closely packed IgG layers, as shown in Fig. 2.

orientation	A	B	C	D
Γ (mg m^{-2})	5.5	3.7	2.6	2.0

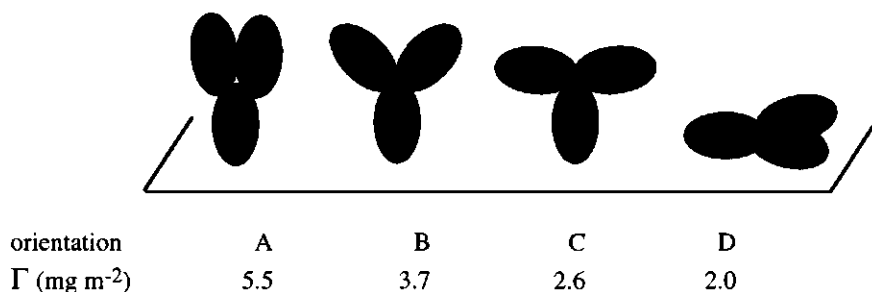*Fig. 2. Schematic drawing and calculated adsorbed amount of some orientations of adsorbed IgG molecules. (A) End-on orientation with contracted F(ab) fragments, (B) and (C) End-on orientation with intermediate and highly repelling F(ab) fragments, respectively, (D) Side-on orientation. The adsorbed amounts are computed using the dimensions of crystallised fragments and assuming closely packed monolayers.*

As the Fab fragments are highly flexible in the hinge region, it is believed that due to electrostatic repulsion the two Fab domains in one IgG molecule elongate when they contain a high net charge density (Figs 2b and 2c) [30,52]. According to the calculation based on the dimensions given above, this effect can result in a decrease in the plateau adsorption by a factor of two. If the IgG adsorbs in a flat orientation the adsorbed amounts will be even lower. A more detailed description of the possible orientations related to adsorbed amounts is given in Chapter 3.

Ellipsometric studies of IgG adsorbed on hydrophobic and hydrophilic surfaces have shown that the layer thickness is about 17-18 nm which corresponds to an end-on orientation of the IgG molecules [13]. In many other studies the end-on orientation for IgG adsorption onto a wide range of surfaces was confirmed from a comparison of the adsorbed amounts and the molecular dimensions of the IgG [30,32]. However, there are also reports that the IgG molecules adsorb in a side-on orientation at hydrophilic surfaces [15]. In addition, a flattened IgG layer has also been observed for IgG adsorption at hydrophobic surfaces when solutions with a low IgG concentration are used [16,50].

2.2.7 Adsorption of the F(ab')₂ and Fc fragments

The IgG molecule consists of two kinds of structural units, viz., the Fc part and the two Fab parts. If these domains differ with respect to their adsorption behaviour, this will certainly affect the preferred orientation of the adsorbed IgG molecules. This is a very important issue, because the orientation of the IgG molecules will have a great impact on the antigen binding capacity.

It has been observed that the general trends for adsorption of F(ab')₂ fragments resemble those for the adsorption of whole IgG molecules [53,54]. Nevertheless, a difference between the two structural units, i.e., the F(ab')₂ and the Fc fragment, was observed in studies of the conformational properties and compactness of IgG molecules and its fragments. It appeared that at low pH values the conformation of the Fc fragment changes whereas the structure of the Fab fragment is not significantly affected [55,56]. This phenomenon was successfully exploited by Van Erp and co-workers who demonstrated that IgG molecules were preferentially adsorbed by their Fc part after the structural stability of the Fc part had been decreased by pre-exposing to pH 2 [57]. It has furthermore been observed that the affinity of the Fc fragment for sorbent surfaces is less sensitive to electrostatic interactions than that of the Fab fragment [58].

Recently, immunological tests have been developed using the F(ab')₂ fragments [59,60,61] or Fab fragments [62]. This development has strongly increased the interest in

the adsorption behaviour of F(ab')$_2$ or Fab fragments. The presence of the Fc fragment is held responsible for anomalous results in immunological tests, caused by for example, non-specific agglutination [58] or undesired interactions with certain components present in serum [59].

2.2.8 Adsorption experiments

In order to determine the role of the various interactions between proteins and sorbent surfaces, various aspects of the adsorption process can be investigated. When the protein is brought into contact with a sorbent surface the proteins will start to adsorb. Fig. 2A shows a typical curve for the time-dependency of protein adsorption. The initial adsorption rate yields information about the energy barrier which must be overcome before the proteins can attach to the sorbent surface. The affinity of proteins for sorbent surfaces is commonly studied by establishing adsorption isotherms, i.e., plots in which the equilibrium adsorbed amount is given as a function of the protein concentration in solution. The initial part of the isotherm reflects the affinity of the protein for the sorbent surface. In Fig. 2b, an example is shown of a high affinity isotherm in which all proteins adsorb when low amounts of protein are supplied.

a) **Adsorption kinetics**

b) **Adsorption isotherm**

→ time

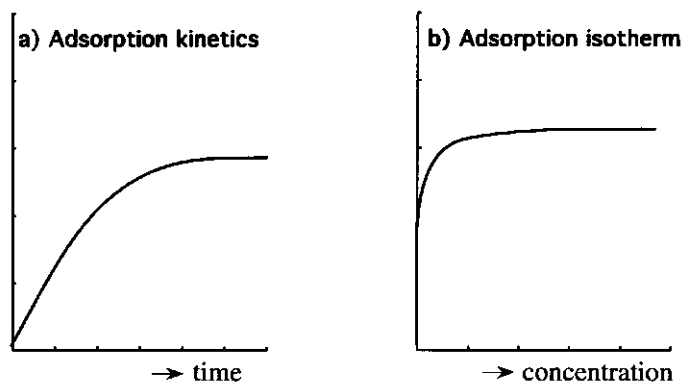→ concentration

Fig. 2. Schematic overview of various adsorption experiments. a) Adsorption as a function of time, b) Adsorption isotherm.

Studies of the adsorbed amount yield a wealth of information about protein-sorbent interactions. Nevertheless, a more detailed determination of the adsorbed state, in particular, the orientation and structure of the protein, requires additional experiments.

This is because the information inferred from the adsorbed amounts is limited to the determination of the area which is effectively occupied by a single IgG molecule on the sorbent surface. This area is affected by the structure of the protein and by a number of other parameters, such as, the orientation of the protein, the repulsion between neighbouring proteins and the spatial distribution. Fortunately, there are some optical methods which can be used to study the structural properties of adsorbed proteins, such as, circular dichroism [41,63], fluorescence spectroscopy [64], and Fourier transform infrared [65,66].

2.3 Fragmentation and characterisation of the IgGs

2.3.1 The IgGs

In the present study monoclonal IgGs directed against the pregnancy hormone human chorionic gonadotropin (hCG) are studied. Immobilised IgG-anti-hCG is widely used in immunoassays in order to diagnose pregnancy [67,68,69,70]. In addition, quantitative serum hCG measurements are also used to monitor the progress of pregnancy, to asses the date of pregnancy, to diagnose the Down syndrome, and to follow the course of trophoblast diseases and testicular cancer [71].

Organon Teknika (Boxtel, The Netherlands) kindly donated two monoclonal immunoglobulins; IgG 1B and IgG 2A from isotype 1. The IgGs were produced in a dialysis module, Na_2SO_4-precipitated and dialysed against 9 g dm^{-3} sodium chloride. The IgGs were stored at -20°C.

2.3.2 Fragmentation of the IgGs

In order to study the adsorption behaviour of the different domains of IgG, both monoclonal IgGs are digested using the cleavage proteins pepsin or papain. Both cleavage proteins can be used to produce F(ab')$_2$ fragments (two covalently linked F(ab') fragments). With papain digestion intact Fc fragments can be obtained, whereas pepsin digests the Fc fragments into smaller pieces [72]

Papain digestion

F(ab')$_2$ and Fc fragments were produced in a controlled way by cleavage with pre-activated papain [73]. Water was purified by reverse osmosis and passed subsequently through a SuperQ system (Millipore). A papain solution of 4.2 g dm^{-3} (Boehringer) was

activated by incubation for 1 hour at 37°C containing 50 mM cysteamine and 2.5 mM EDTA in a 0.1 M sodium acetate buffer pH 5.5. Excess cysteamine was separated from the papain solution by gel filtration on a Sephadex G-25 column (PD-10 column, Pharmacia) equilibrated with 0.15 M sodium chloride. Due to the removal of the reducing reagent cysteamine, the disulphide bonds between the two F(ab) fragments remain intact in this way ensuring that pre-activated papain produces F(ab')$_2$ fragments. Activated papain was added to an IgG solution of 4.2 g dm^{-3} containing 0.1 M sodium acetate and 0.15 M sodium chloride at a papain : IgG weight ratio of 1 : 10. After incubation for 18 hours at 37°C, the reaction was terminated by addition of iodoacetamide to a final concentration of 30 mM. The F(ab')$_2$ fragments were purified using size exclusion chromatography over a Superdex 200 (Pharmacia) gel filtration column equilibrated with 0.15 M sodium chloride. The Fc fraction with a molecular weight of 50 kDa was further purified because it may be contaminated by some Fab fragments. The separation was performed using a specific affinity column for Fc fragments (MAbTrap G, Pharmacia) with 0.02 M sodium phosphate as the binding buffer and 0.1 M glycine/HCl (pH 2.7) as the elution buffer. The eluted fraction was transferred to a 0.15 M sodium chloride solution using a Sephadex G-25 column (Pharmacia) and then concentrated using centricon microconcentrators (Amicon). The digestion resulted in a weight-corrected yield for F(ab')$_2$ 1B and F(ab')$_2$ 2A of 70% and 53%, respectively. For both monoclonals, a weight-corrected yield of 15% was obtained for the Fc fragments.

Pepsin digestion
Pepsin (Sigma) was dissolved in water (0.45 g dm^{-3}) and added to an IgG solution of 4.5 g dm^{-3} containing 0.09 M sodium acetate buffer and 0.15 M sodium chloride to give a pepsin : IgG weight ratio of 1 : 100. The reaction mixture was incubated at 37°C for two hours. The digestion was terminated by changing the pH to 7 by means of a 1 M Tris solution. The F(ab')$_2$ fragments were purified using size exclusion chromatography over a Superdex 200 (Pharmacia) gel filtration column equilibrated with 0.15 M sodium chloride. The digestion resulted in a weight-corrected yield of 83% for F(ab')$_2$ 1B and 53% for F(ab')$_2$ 2A.

2.3.3 Characterisation

The IgGs and their fragments were characterised in terms of their isoelectric point, purity and amino acid composition (Tables 1 and 2). The i.e.p. values of the IgGs and their fragments were determined using isoelectric focusing (IEF) with PhastGel media, pH range 3-9 and silver staining (PhastSystem, Pharmacia).

Table 1. Isoelectric point and purity of the monoclonals IgG 1B and 2A and their F(ab')$_2$ fragments, and the i.e.p. of the Fc fragment.

protein	IgG 1B	F(ab')$_2$ 1B	IgG 2A	F(ab')$_2$ 2A	Fc
i.e.p.	5.6-6.0 (5.8)	5.6-6.1 (5.9)	6.7-7.4 (6.9)	8.2-8.8 (8.5)	5.7-6.3 (6.1)
purity	97%	>99%	87%	98%	-

The Fc parts of different monoclonal IgGs are generally considered to be identical which is reflected in the similar i.e.p. values for the Fc fragments of both monoclonals. In Table 1, the major bands in the respective isoelectric pH regions are given in brackets. The purity of the proteins obtained with high performance size exclusion chromatography (Zorbax, GF-250 Dupont) is given in weight fractions. The impurities in IgG 1B consisted of smaller fragments, but the solutions of IgG and F(ab')$_2$ 2A contained aggregates with total weight fractions of 6% and 2%, respectively.

The molecular mass of the IgGs and the F(ab')$_2$ fragments were 150 kDa and 100 kDa, respectively. For both IgGs, the concentrations were established spectroscopically using an extinction coefficient of 1.45 cm^2 mg^{-1} at 280 nm. This coefficient has been derived for several IgGs directed against hCG by measuring the extinction of an IgG solution and determining the dry weight fraction after evaporation of the solution. The extinction coefficients for the F(ab')$_2$ fragments were determined colorimetrically according to the Folin phenol method of Lowry *et al.* [74] using the corresponding IgGs as the standards. The resulting extinction coefficient were 1.45 cm^2 mg^{-1} for F(ab')$_2$ 1B and 1.48 cm^2 mg^{-1} for F(ab')$_2$ 2A.

Amino acid analysis

The amino acid composition of both IgG 1B and 2A and their corresponding F(ab')$_2$ fragments were determined using amino acid analysis (AAA). Prior to AAA, the protein was hydrolysed in 6 M hydrochloric acid during 16 hours at 105°C. The amino acid composition of the Fc fragment was obtained by subtracting the amino acid composition

of the F(ab')$_2$ fragments from the intact IgG molecules. For the Fc fragments of the two IgGs the average value was taken. The proline, methionine, tyrosine and tryptophan residues were partly or totally degraded during hydrolysis. The number of degraded residues are detected through the amide content. The results of the calculations are shown in Table 2. Although the two monoclonal IgGs differ more than one pH unit in i.e.p., their respective amino acid compositions resemble to a great extent.

Table 2. Amino acid composition in molar fractions for the two monoclonals IgG 1B and IgG 2A and their corresponding F(ab')$_2$ fragments, measured by AAA. The amino acid composition of the Fc fragments is a calculated result. Dissociation constants (pK$_a$) of the ionisable amino acids are given. Due to hydrolysis, Asn and Gln are converted in Asp and Glu, respectively. The corresponding pK$_a$s are those of Asp and Glu.

amino acids	amino acid composition (molar fractions)					pK$_a$
	IgG 1B	IgG 2A	F(ab)$_2$ 1B	F(ab)$_2$ 2A	Fc	
asp/asn*	8.54	8.63	8.21	8.63	10.35	4.5*
thr	8.55	8.50	9.91	10.38	6.13	
ser	9.95	8.62	11.55	10.83	6.32	
glu/gln*	9.43	9.09	8.09	8.16	13.37	4.6*
pro	5.77	6.78	n.m.	n.m.	n.m.	
gly	5.65	5.96	6.61	7.64	3.66	
ala	5.09	5.19	5.89	5.63	4.54	
cys	1.74	1.75	1.50	1.82	2.22	9.3
val	6.53	6.77	7.20	7.33	6.29	
met	0.99	1.98	0.47	0.66	n.m.	
ile	3.36	2.96	2.92	3.02	4.09	
leu	5.87	6.21	6.77	7.86	4.04	
tyr	3.79	3.48	5.63	5.20	n.m.	9.7
phe	3.78	3.51	3.33	2.95	5.41	
lys	6.18	6.01	5.28	6.00	8.11	10.4
NH$_3$	9.53	9.55	13.69	10.40	19.37	
his	1.82	1.94	1.34	1.70	3.01	6.2
arg	2.58	2.57	2.34	2.72	3.09	12
trp	0.86	0.50	n.m.	n.m.	n.m.	

When comparing the amino acid composition of the different domains, the variation in the amounts of most residues is small. Except for the amounts of serine and threonine residues which are relatively higher for the F(ab')$_2$ fragments and the glutamine and/or glutamic acid residues which are dominantly located in the Fc part. As glutamine and/or glutamic acid are more hydrophilic than serine and threonine [75], it makes the F(ab')$_2$ part more hydrophobic than the Fc part.

As it is generally observed that the protein charge influences the adsorption behaviour, the net charges on the proteins are estimated on basis of their amino acid compositions, and the dissociation constants for each class of titratable groups which are also listed in Table 2. The fractions of charged groups are calculated using for each type of dissociable amino acid a dissociation constant which is the average of the corresponding value in a large number of proteins [75]. Because asparagine and glutamine are converted into aspartic and glutamic acid, respectively, the number of carboxyl groups has to be estimated. This is performed by adjusting the number of carboxyl groups in such a way that the calculated isoelectric points coincide with those obtained with isoelectric focusing. Cysteine is excluded from the calculations since many of the cysteine residues are linked in S-bridges and most of the unpaired cysteine residues remain uncharged up to pH 8 which is the highest pH considered in this work. The results of the calculations shown in Fig. 3 are obtained by multiplying the fraction of charged residues with the number of amino acids, which is 1320 for each IgG and 880 for the F(ab')$_2$ fragments.
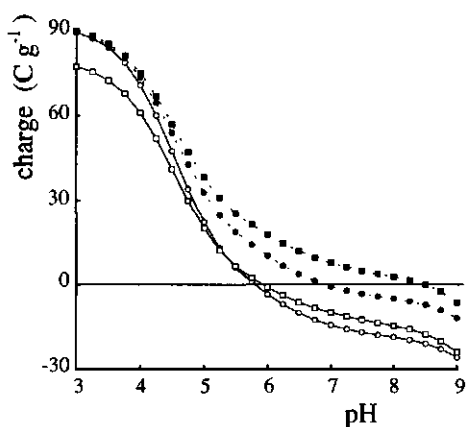

*Fig. 3. Proton charge of the proteins as function of the pH; (*O*) IgG 1B, (*□*) F(ab')$_2$ 1B, (*●*) IgG 2A and (*■*) F(ab')$_2$ 2A, The calculations are based on AAA and pK$_a$ values given in Creighton [75].*

Furthermore, the charges of the C- and N- terminal ends of the four polypeptide chains which have a dissociation constant of 3.9 and 7.4, respectively, are added. In the calculations the influence of electrostatic interactions on proton dissociation is neglected. Nevertheless, Tanford and co-workers [76] showed that at high ionic strength the calculated titration curves agree well with the potentiometrically obtained experimental ones. At low ionic strength the calculations overestimate the absolute values of the net charges but the i.e.p. of the protein is not affected by the ionic strength.

2.4 References

1   J. Yguerabide, H.F. Epstein, and L. Stryer, *J. Mol. Biol.*, **51** (1970) 573.

2   J. Deisenhofer, *Biochemistry*, **20** (1981) 2361.

3   M. Marquart, J. Deisenhofer, R. Huber, and W. Palm, *J. Mol. Biol.*, **141** (1980) 369.

4   R.J. Poljak, L.M. Amzel, B.J. Chen, R.P. Phizackerley, and F. Saul, *Proc. Natl. Acad. Sci. USA*, **71** (1974) 3440.

5   E.W. Silverton, M.A. Navia, and D.R. Davies, *Proc. Natl. Acad. Sci. USA*, **74** (1977) 5140.

6   V.R. Sarma, E.W. Silverton, D.R. Davies, and W.D. Terry, *J. Biol. Chem.*, **246** (1971) 3753.

7   C.A. Haynes, and W. Norde, *Colloids Surfaces B: Biointerfaces*, **2** (1994) 517.

8   W. Norde, and J. Lyklema, *J. Biomater. Sci. Polymer Edn.*, **2** (1991) 183.

9   W. Norde, and J. Lyklema, *J. Colloid Interface Sci.*, **71** (1979) 350.

10   F. Galisteo-González, J. Puig, A. Martín-Rodriguez, and J. Serra-Domènech, *Colloids Surfaces B: Biointerfaces*, **2** (1994) 435.

11   A.V. Elgersma, R.L.J. Zsom, W. Norde, and J. Lyklema, *Colloids Surfaces*, **54** (1991) 89.

12   A. Kondo, S. Oku, and K. Higashitani, *Biothechnol. Bioeng.*, **37** (1990) 537.

13   M. Malmsten, *Colloids Surfaces B: Biointerfaces*, **3** (1995) 297.

14   C.-G. Gölander, Y.-S. Lin, and J.D. Andrade, *Colloids Surfaces*, **49** (1990) 289.

15   M. Okubo, Y. Yamamoto, M. Uno, S. Kamei, and T. Matsumoto, *Colloid Polym. Sci.*, **265** (1987) 1061.

16   U. Jönsson, I. Lundström, and I. Rönnberg, *J. Colloid Interface Sci.*, **117** (1986) 127.

17   T.S. Lebedeva, A.A. Rahnanskaya, V.V. Egorov, and V.S. Pshezhetskii, *J. Colloid Interface Sci.*, **147** (1991) 450.

18   M.L. Connolly, *Science*, **221** (1983) 709.

19   M.L. Connolly, *J. Appl. Cryst.*, **16** (1983) 548.

20   T. Mizutani, *J. Colloid Interface Sci.*, **79** (1981) 284.

21   D.R. Lu, S.J. Lee, and K. Park, *J. Biomater. Sci. Polymer Edn.*, **3** (1991) 127.

22   C.A. Haynes, E. Sliwinsky, and W. Norde, *J. Colloid Interface Sci.*, **164** (1994) 394.

23   T. Arai, and W. Norde, *Colloids Surfaces*, **51** (1990) 1.

24   W. Norde, *Croat. Chem. Acta*, **56** (1983) 705.

25   P. van Dulm, W. Norde, and J. Lyklema, *J. Colloid Interface Sci.*, **82** (1980) 77.

26   J.G.E.M. Fraaije, and J. Lyklema, *Croat. Chem. Acta*, **63** (1990) 517.

27   J. Ståhlberg, B. Jönsson, and C. Horváth, *Anal. Chem.*, **63** (1991) 1867.

28   W. Norde, and J. Lyklema, *J. Colloid Interface Sci.*, **66** (1978) 266.

29   J.E. Johnson, and E. Matijevic, *Colloid Polymer Sci.*, **270** (1992) 353.

30   P. Bagchi, and M. Birnbaum, *J. Colloid Interface Sci.*, **83** (1981) 460.

31   J. Serra, J. Puig, A. Martín, F. Galisteo, M. Gálvez, and R. Hidalgo-Alvarez, *Colloid Polymer Sci.*, **270** (1992) 574.

32   M.E. Soderquist, and A.G. Walton, *J. Colloid Interface Sci.*, **75** (1980) 386.

33   W. Norde, and A.C.I. Anusiem, *Colloids Surfaces*, **66** (1992) 73.

34   B.L. Steadman, K.C. Thompson, C.R. Middaugh, K. Matsuno, S. Vrona, E.Q. Lawson, and R.V. Lewis, *Biothechnol. Bioeng.*, **40** (1991) 8.

35   N.J. Geddes, D.N. Furlong, P. Zientek, K.A. Than, and J.A. Edgar, *J. Colloid Interface Sci.*, **157** (1993) 491.

36   W. van der Vegt, H.C. van der Mei, and H.J. Busscher, *J. Colloid Interface Sci.*, **156** (1992) 129.

37   A.G. Walton, and M.E. Soderquist, *Croat. Chem. Acta*, **53** (1980) 363.

38   A.V. Elgersma, R.L.J. Zsom, J. Lyklema, and W. Norde, *J. Colloid Interface Sci.*, **152** (1992) 410.

39   B.W. Morrissey, L.E. Smith, R.R. Stromberg, and C.A. Fenstermaker, *J. Colloid Interface Sci.*, **56** (1976) 557.

40   W. Norde, and J.P. Favier, *Colloids Surfaces*, **64** (1992) 87.

41   A. Kondo, F. Murakami, and K. Higashitani, *Biothechnol. Bioeng.*, **40** (1992) 889.

42   A.V. Elgersma, R.L.J. Zsom, J. Lyklema, and W. Norde, *Colloids Surfaces*, **65** (1992) 17.

43   C.J. van Oss, R.J. Good, and M.K. Chaudhury, *J. Colloid Interface Sci.*, **111** (1986) 378.

44   J. van Straaten, and N.A. Peppas, *J. Biomater. Sci. Polymer Edn.*, **2** (1991) 91.

45   D. Brune, and S. Kim, *Proc. Natl. Acad. Sci. USA*, **91** (1994) 2930.

46   J.W. Corsel, G.M. Willems, J.M.M. Kop, P.A. Cuypers, and W.T. Hermens, *J. Colloid Interface Sci.*, **111** (1986) 544.

47   D. Kim, C. W, and R.L. Beissinger, *J. Colloid Interface Sci.*, **159** (1993) 1.

48   D.R. Lu, and K. Park, *J. Biomater. Sci. Polymer Edn.*, **1** (1990) 243.

49   J.N. Lin, B. Drake, A.S. Lea, P.K. Hansma, and J.D. Andrade, *Langmuir*, **6** (1990) 509.

50   D.C. Cullen, and C.R. Lowe, *J. Colloid Interface Sci.*, **166** (1994) 102.

51   B.D. Fair, and A.M. Jamieson, *J. Colloid Interface Sci.*, **77** (1980) 525.

52   T. Suzawa, and H. Shirahama, *Adv. Colloid Interface Sci.*, **35** (1991) 139.

53   J.L. Ortega-Vinuesa, and R. Hidalgo-Alvarez, *Colloids Surfaces B: Biointerfaces*, **1** (1993) 365.

54   J.L. Ortega-Vinuesa, and R. Hidalgo-Alvarez, *J. Biomater. Sci. Polymer Edn.*, **6** (1994) 269.

55   L.V. Abaturov, R.S. Nezlin, T.I. Vengerova, and J.M. Varshavsky, *Biochim. Biophys. Acta*, **194** (1969) 386.

56   E. Doi, and B. Jirgensons, *Biochemistry*, **9** (1970) 1066.

57   R. van Erp, Y.E.M. Linders, A.P.G. Van Sommeren, and T.C.J. Gribnau, *J. Immunol. Methods*, **152** (1992) 191.

58   H. Kawaguchi, K. Sakamoto, Y. Ohtsuka, T. Ohtake, H. Sekiguchi, and H. Iri, *Biomaterials*, **10** (1989) 225.

59   A.B. Pereira, A.N. Theofilopoulos, and F.J. Dixon, *J. Immunol.*, **125** (1980) 763.

60   M.L. Yarmush, X. Lu, and D.M. Yarmush, *J. Biochem. Biophys. Methods*, **25** (1992) 285.

61   M. Muratsugu, S. Kurosawa, Y. Mori, and N. Kamo, *Chem. Phar. Bull.*, **40** (1992) 501.

62   F.V. Bright, T.A. Betts, and K.S. Litwiler, *Anal. Chem.*, **62** (1990) 1065.

63   A. Kondo, S. Oku, F. Murakami, and K. Higashitani, *Colloids Surfaces B: Biointerfaces*, **1** (1993) 197.

64   A.G. Walton, and F.C. Maenpa, *J. Colloid Interface Sci.*, **72** (1979) 265.

65   B.W. Morrissey, and R.R. Stromberg, *J. Colloid Interface Sci.*, **46** (1974) 152.

66   D.M. Byler, and H. Susi, *Biopolymers*, **25** (1986) 469.

67   L.A. Cole, D.B. Seifer, A. Kardana, and G.D. Braunstein, *Am. J. Obstet. Gynecol.*, **168** (1993) 1580.

68   B.L.J.C. Konings, E.G.M. Pelssers, A.J.C.M. Verhoeven, and K.M.P. Kamps, *Colloids Surfaces B: Biointerfaces*, **1** (1993) 69.

69   S. Matsuzawa, Y. Itoh, H. Kimura, R. Kobayashi, and C. Miyauchi, *J. Immunol. Methods*, **60** (1983) 189.

70   B. Longhi, B. Chichehian, A. Causse, and J. Caraux, *J. Immunol. Methods*, **92** (1986) 89.

71   L.A. Cole, and A. Kardana, *Clin. Chem.*, **38** (1992) 263.

72   P. Parham, M.J. Androlewicz, F.M. Brodsky, N.J. Holmes, and J.P. Ways, *J. Immunol. Methods*, **53** (1982) 133.

73   R. Kurkela, L. Vuolas, and P. Vihko, *J. Immunol. Methods*, **110** (1988) 229.

74   O.H. Lowry, N.J. Rosebrough, A.L. Farr, and R.J. Randall, *J. Biol. Chem.*, **193** (1951) 265.

75   T.E. Creighton, *Proteins, Structure and Molecular Properties*. New York, Freeman & Co., 1983.

76   C. Tanford, S.A. Swanson, and W.S. Shore, *J. Am. Chem. Soc.*, **77** (1955) 4949.

3 Adsorption of Monoclonal IgGs and their F(ab')$_2$ fragments onto Polymeric Surfaces

The present study deals with the adsorption of monoclonal immunoglobulin G (IgG) and its corresponding F(ab')$_2$ fragment onto three polymer latices. Two of these latices are hydrophobic, one being positively and the other negatively charged; the third latex is a negatively charged hydrophilic latex. Electrostatic and hydrophobic interactions were systematically studied by performing adsorption and electrophoresis experiments as a function of pH and ionic strength, and by using two IgGs which differ in isoelectric point. The affinity of the proteins for the hydrophobic latices was barely influenced by electrostatic interactions. However, at saturation level the adsorbed amounts were dependent on the overall electrostatic interaction, resulting in a maximum adsorbed amount when the protein charge is partly compensated by the sorbent surface charge. For the hydrophilic latex, adsorption was absent when the proteins were electrostatically repelled by the sorbent surface. The trends in the adsorption of IgG and the corresponding F(ab')$_2$ fragments were similar, although there was some evidence that hydrophobic interactions and/or conformational changes were less important for F(ab')$_2$ adsorption. At hydrophobic surfaces the protein molecules adsorbed mainly in an end-on orientation, whereas for a negatively charged hydrophilic latex and high cationic charge densities on the protein, the adsorbed amounts correlated with a close-packed monolayer of side-on oriented proteins.

3.1 Introduction

In various biomedical applications, such as immunological tests and biosensors, immunoglobulin G (IgG) is immobilised on artificial materials. The use of IgG in diagnostics stems from its ability to bind to specific antigens. An IgG molecule consists of three domains; two of them, the so-called Fab parts, contain an antigen-binding site which is located on the top, whereas the third domain, the Fc region, is responsible for

the binding to certain cells. The development of the 'hybridoma technique' for producing monoclonal IgG has led to the production of tests which are highly specific to one single antigenic determinant [1]. Diagnostic tests based on immobilised IgG require an orientation of the adsorbed proteins in which the antigen-binding sites are accessible to the antigens in solution. Moreover, conformational changes resulting in a loss of binding activity must be kept at a minimum. Another unwanted feature is aspecific binding of antigens at the sorbent surface. Since there is evidence that Fc moieties are involved in such aspecific interactions [2], tests have been developed using Fab fragments only [3,4]. The growing interest in this development is reflected in recent studies on the adsorption of Fab fragments [5] and F(ab')$_2$ fragments [6,7]. Adsorption isotherms of IgG and F(ab')$_2$ on polymeric surfaces usually lead to plateau values in the same range as calculated for a close-packed monolayer. The proteins can optimise their interactions with the sorbent surface and with each other by changing their conformation and orientation, which is also reflected in the plateau values of adsorption.

In this study the adsorption behaviour of two monoclonal IgGs, which differ in isoelectric point (i.e.p.), and their corresponding F(ab')$_2$ fragments is investigated. The use of monoclonal IgG offers the advantage of studying the adsorption of proteins with well-defined physical properties. Electrostatic and hydrophobic interactions were systematically studied by adsorption of the proteins onto three polymer latices; two of them are hydrophobic, one having a positive and the other a negative surface charge, and the third is a negatively charged hydrophilic latex. For adsorption at the negatively charged hydrophobic latex, electrostatic interactions are further investigated by performing adsorption experiments at various ionic strengths. Additional information is derived from electrophoretic mobility measurements of the protein-latex complexes.

3.2 Experimental

3.2.1 Materials

Adsorbents
Negatively charged polystyrene latex (PS-) was prepared following the procedure described by Goodwin and co-workers [8], using $K_2S_2O_8$ as the initiator. Both the positive latex (PS+) and the polystyrene latex with a hydrophilic shell (OH-) were supplied by Akzo Nobel (Arnhem, The Netherlands). The hydrophilic latex consists of polystyrene particles covered with a thin hydrogel-like shell. The negative charge was due to sulphate groups on the polystyrene particles and sulphonate groups incorporated in

the hydrogel. None of the latices contained additional emulsifier. Table 1 summarises some of the characteristics. The diameters and the specific surface areas were determined by transmission electron microscopy (TEM). Electron microscopy photographs of all three latices showed that the particles are spherical and homodisperse (data not shown). At least 50 particles of each sample were sized. The specific surface area, s, is obtained from $s=3/\rho r'$, where r' is the volume-surface average radius, given by $\sum n_i r_i^3/\sum n_i r_i^2$ where n_i is the number of particles with radius r_i and ρ is the density. The density of the PS- and PS+ latices is 1.05×10^6 g m^{-3} [9]. The density of the hydrophilic OH- latex was determined by comparing the sizes of the OH- latex particles as measured by light scattering and sedimentation field flow fractionation. The latter technique requires an input of the density. The sizes obtained using these two techniques matched if a density of 1.05×10^6 g m^{-3} was used as input parameter. The number of aggregates present in the latex samples was determined from single particle optical sizing (SPOS) [10], and in Table 1 the fractions of singlets in the original samples are given. Most of the aggregates were doublets and even for PS+, which contained the smallest singlet fraction, the percentage of aggregates larger than triplets was less then 2%. With respect to the hydrophobicity of the surface, it can be mentioned that for tablets of freeze-dried negatively and positively charged polystyrene latices contact angles for a sessile drop of water of ca. 80° have been reported [11]. These latices were comparable to the PS- and PS+ particles. For the hydrophilic latex, it was found that a pressed tablet was completely wetted by water.

Table 1. Charged surface groups, surface charge density (σ_o) as determined by conductometric titration, diameter, specific surface area (s) as determined by TEM, and the fraction of singlets in the various latices as determined by SPOS.

code	charged groups	σ_0 (mC m$^{-2)}$	diameter (nm)	s (m^2 g^{-1})	singlet fraction
PS-	~SO$_4^-$	-32	570±20	10.0	94%
PS+	~C(NH$_2$)$_2$H$^+$	+22	660±60	8.7	84%
OH-	~SO$_3^-$/~SO$_4^-$	-43	330±15	17.5	100%

Proteins

The two monoclonals, IgG 1B and IgG 2A, are both mouse-anti-hCG (human Chorionic Gonadotropin) from isotype IgG-1. F(ab')₂ fragments were produced in a controlled way by cleavage with pre-activated papain, as described in Chapter 2. The IgGs and the fragments were characterised in terms of their i.e.p. and purity. The results

are collected in Table 2. These i.e.p. values of the IgGs and the fragments were determined using isoelectric focusing, with PhastGel media, pH range 3-9 and silver staining (PhastSystem, Pharmacia). In Table 2, the major bands in the respective isoelectric pH regions are given in brackets. For both monoclonals, the Fc fragments have the same i.e.p. of 6.1. The purity of the proteins, obtained with high performance size exclusion chromatography (Zorbax, GF-250 Dupont) is given in weight fractions. The impurities in IgG 1B consisted of smaller fragments, but the solutions of IgG and F(ab')$_2$ 2A contained aggregates with total weight fractions of 6% and 2%, respectively. For both IgGs, the concentrations were established spectroscopically using an extinction coefficient of 1.45 cm^2 mg^{-1} at 280 nm. The extinction coefficients for the F(ab')$_2$ fragments were determined colorimetrically according to the Folin phenol method of Lowry and co-workers [12] using the corresponding IgGs as the standards. This resulted in an extinction coefficient of 1.45 cm^2 mg^{-1} for F(ab')$_2$ 1B and 1.48 cm^2 mg^{-1} for F(ab')$_2$ 2A.

Table 2. Isoelectric points and purity of the monoclonals 1B and 2A and their F(ab')$_2$ fragments.

	IgG 1B	F(ab')$_2$ 1B	IgG 2A	F(ab')$_2$ 2A
i.e.p.	5.6-6.0 (5.8)	5.6-6.1 (5.9)	6.7-7.4 (6.9)	8.2-8.8 (8.5)
purity	97%	>99%	87%	98%

Chemicals

Water was purified by reverse osmosis and subsequently passed through a SuperQ system (Millipore). All other chemicals were of p.a. grade and used without further purification. All experiments were performed in a buffer solution. At pH values below 6 an acetate buffer and for pH values above 5 a phosphate buffer was used. Both buffers were prepared from sodium salts and adjusted to the desired pH with NaOH and HCl. In order to check the influence of the nature of the buffers, both were used for measuring adsorption isotherms at intermediate pH where no significant influence of this nature was observed. The ionic strength was kept low at 5 mM to avoid suppression of electrostatic interactions. Higher ionic strengths which were applied in adsorption experiments with PS-, were obtained by adding NaCl.

3.2.2 Methods

Adsorption isotherms

The protein solutions were desalted, brought to the desired pH and buffer concentration using a Sephadex G-25 column (PD-10 column, Pharmacia), and filtered over a 0.2 μm filter (Acrodisc, Gelman Sciences) in order to remove aggregates. In a 2 cm^3 polystyrene tube (Greiner), 1.4 cm^3 of a protein solution of the desired concentration was added to 0.2 cm^3 of a latex suspension containing latex with a total surface area of about 0.07 m^2. The tubes were gently rotated for about 16 hours. The suspensions were centrifuged for 30 min. at 2×10^4 m s^{-2} (Sarstedt MH2 centrifuge) and 1 cm^3 of the supernatant was sampled to determine the protein concentration. For the PS- latex, the sediment was resuspended and used for electrophoresis experiments. The protein concentration in solution before and after adsorption was determined using a modification of the Lowry method [12], as described by Johnstone and Thorpe [13]. The extinction was measured using a Reader Microelisa system (Organon Teknika, Boxtel). All experiments were performed at 20° C.

Electrophoresis

The electrophoresis measurements were performed with a Zeta Sizer 3 (Malvern Instruments Ltd.). Prior to the measurements the (protein-coated) latex suspension was diluted 1500 times compared to the adsorption experiments in 5 mM buffer solution of the same pH. Desorption of IgG upon dilution with buffer was never found in any system subjected to electrophoresis [14,15]. The measured mobilities were converted into zeta potentials according to the procedure of O'Brien and White [16], which takes into account relaxation and retardation effects but ignores ionic conduction inside the plane of shear.

3.3 Results and discussion

3.3.1 Adsorption onto hydrophobic latices

The adsorption on the two hydrophobic surfaces, PS- and PS+, is discussed first. Adsorption isotherms, in which the adsorbed amount (Γ) is plotted versus the protein concentration in solution after adsorption (cp), are shown in Figs. 1 and 2. These isotherms are well reproducible and the deviation between plateau values for duplicated experiments is always less than 0.2 mg m^{-2}. The slope of the initial part of the isotherm

reflects the affinity of the protein for the surface. At higher protein concentrations, the isotherms reach a saturation level which is determined by the spatial distribution, lateral interaction, conformation, and orientation of the proteins at the sorbent surface. At the hydrophobic PS surfaces, IgG and F(ab')$_2$ fragments adsorb spontaneously, even when the net protein charge and the surface charge repel each other. In most cases the proteins adsorb with high affinity and the isotherms show well-defined plateau values for protein concentrations above 200 g m^{-3}. The adsorption isotherms of IgG 1B and F(ab')$_2$ 1B for the negatively charged PS- latex are shown in Fig. 1. Adsorption isotherms for IgG 2A and F(ab')$_2$ 2A on PS- are not shown, and it is only mentioned here that IgG 2A and F(ab')$_2$ 2A adsorb with high affinity at all pH values. Some of the adsorption isotherms on PS+ are presented in Fig. 2. In this figure, we only show adsorption isotherms around the i.e.p. of the protein, which are high affinity isotherms with well-defined plateau values, and those which deviate from this type. The plateau values of all isotherms are summarised in Fig. 3.
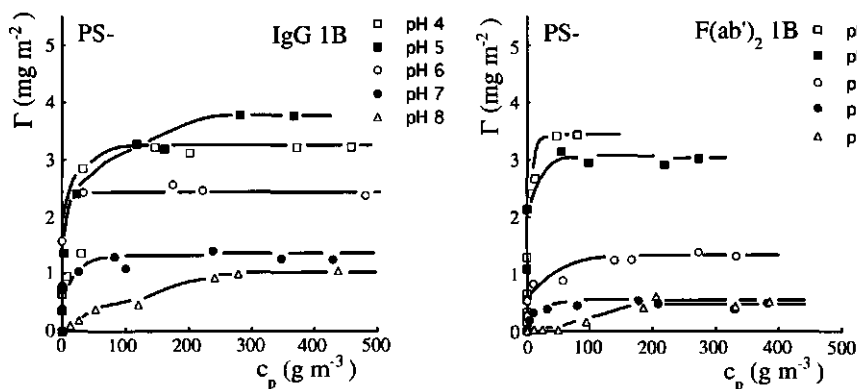
Fig. 1. Adsorption isotherms for IgG 1B and F(ab')$_2$ 1B on the negatively charged hydrophobic PS- surface .

It is generally found that IgG adsorbs with high affinity onto hydrophobic surfaces, which at higher protein concentrations leads to clearly pronounced plateau values [14,17]. However, in some rare cases a decreased affinity was observed under conditions of electrostatic repulsion [17] and a stepwise increase in the plateau values was also reported [18]. When the charge on the protein rises, smaller adsorbed amounts are generally observed, and it is believed that the proteins then occupy a larger surface area. This can be caused by structural changes and by repulsion between the two F(ab) parts

[17,19]. It was found that the adsorption isotherms of polyclonal F(ab')$_2$ fragments on hydrophobic latices resemble those of whole IgG molecules [6]. With respect to the plateau value one should take into account that the molecular weight of an F(ab')$_2$ fragment is two-thirds that of the whole IgG molecule. When the proteins adsorb in an end-on orientation, this implies that the adsorbed amount of F(ab')$_2$ is about one-third lower. However, when the proteins adsorb in a flat orientation, the adsorbed amount is more or less the same for the F(ab')$_2$ fragment as it is for the whole IgG molecule.
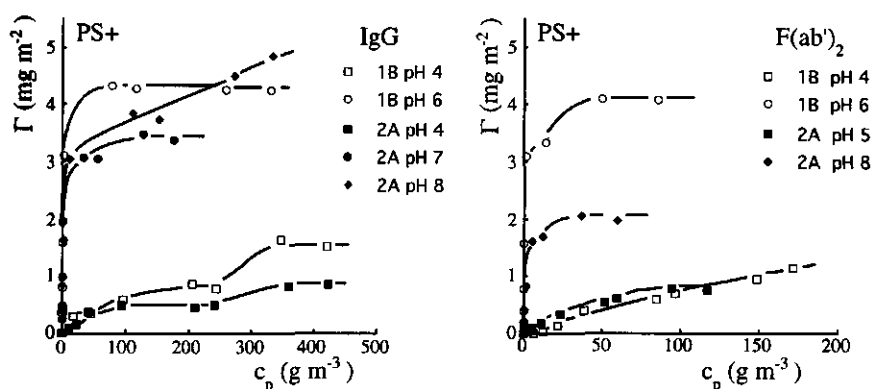

Fig. 2. Adsorption isotherms for IgG 1B, IgG 2A, F(ab')$_2$ 1B, and F(ab')$_2$ 2A on the positively charged hydrophobic PS+ surface.

For most isotherms the affinities, as inferred from the initial slopes, are very high. These affinities can only be reduced by strongly adverse electrostatic protein sorbent interactions. For F(ab')$_2$ 1B on PS- this results in a total absence of adsorption at pH 8 and protein concentrations below 50 g m^{-3}. The general conclusion is that IgG and F(ab')$_2$ adsorption onto the hydrophobic PS- and PS+ latices is dominated by hydrophobic bonding, and that electrostatic interactions have a secondary, but noticeable, influence.

When the proteins are not electrostatically repelled by the surface, most isotherms reach well-defined plateau values below protein concentrations of 100 g m^{-3} (Figs. 1 and 2). However, for IgG 2A adsorbed on PS+ at pH 8, the already high adsorbed amount reached at low protein concentration continues to rise at higher protein concentrations. For IgG 1B adsorbed on PS- at pH 5, this effect is observed to a lesser extent. This indicates that the ongoing adsorption with increasing protein concentration occurs for both IgGs when they are marginally electrostatically attracted by the surface. As most

proteins adsorb with high affinity until lateral interaction inhibits further adsorption, an increase in the adsorbed amount at higher protein concentrations suggests a change in the composition of the adsorbed monolayer, as was earlier reported for IgG adsorption on polystyrene latices [18]. For IgG 2A adsorbed on PS- at pH 7 (see Fig. 3) the adsorbed amount exceeds the maximum calculated for a compact monolayer, as shown in Fig. 8, orientation "A". Therefore, it is not impossible that some aggregation of IgG at the sorbent surface occurs.

In Fig. 3 the plateau values (Γ_{pl}) are given as functions of pH for the two IgGs and their F(ab')$_2$ fragments. For the few isotherms that did not reach a well-defined plateau value, this value was chosen to be equal to the adsorbed amount reached at a protein concentration in the solution of about 200 g m^{-3}. The plateau values depend strongly on the overall electrostatic interactions. The Γ_{pl}(pH)-curves exhibit maxima when the proteins are marginally charged with a sign opposite to that of the surface. When the net charge on the proteins rises, the adsorbed amount decreases. Such a reduction in the adsorbed amount is considerably stronger when the protein charge and surface charge repel each other. This trend is clearly seen when comparing the Γ_{pl}(pH) curves of IgG 1B and F(ab')$_2$ 1B at PS- and PS+ (Fig. 3). These trends are the mirror image of each other with respect to the i.e.p. of the proteins.
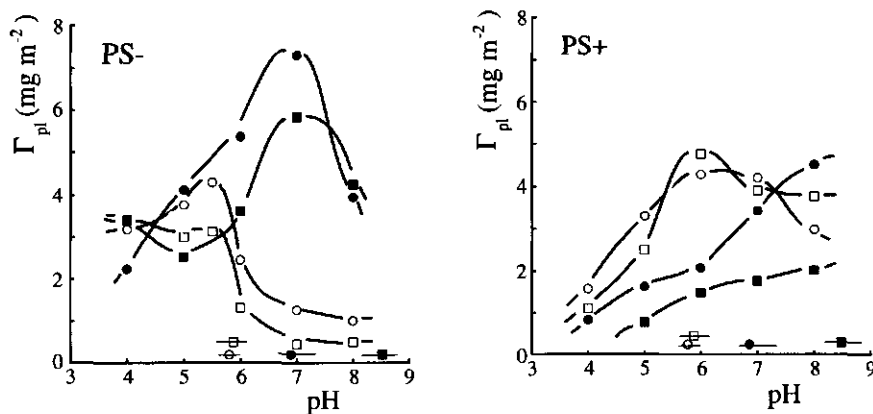

Fig. 3. Plateau adsorption of the two monoclonal IgGs and the F(ab')$_2$ fragments on the hydrophobic PS- (a) and PS+ (b) latices. The proteins are indicated as (○) IgG 1B, (□) F(ab')$_2$ 1B, (●) IgG 2A, and (■) F(ab')$_2$ 2A. The i.e.p. values of the proteins are indicated near the pH-axis using the same symbols.

It is further observed that, when the F(ab')$_2$ fragments contain a relatively high charge opposite to that of the sorbent surface, they exhibit a local minimum in the $\Gamma_{pl}(pH)$- curve. A possible explanation for the increase in adsorbed amount when the charge density on the F(ab')$_2$ fragment rises could be that electrostatic repulsion between the two F(ab') parts of the F(ab')$_2$ fragments causes some of the fragments to adsorb in a stretched or end-on orientation, as shown in Fig. 8, orientation "C". This leads to larger adsorbed amounts for F(ab')$_2$, whereas repulsion between the F(ab') parts of the IgG molecule causes a decrease in adsorption.

The influence of electrostatic interactions on the adsorption behaviour of the proteins on the negatively charged PS- latices is further investigated by considering the results of electrophoresis experiments. In these experiments, a change in the mobility of the latex particles upon adsorption of proteins was obtained. In all electrophoresis experiments in which the proteins were adsorbed on PS- at 5 mM ionic strength, the mobility reduces more or less linearly with the amount of protein adsorbed, except for IgG 2A at pH 6 and 7 where adsorption beyond 3 mg m^{-2} did not further reduce the mobility. The mobilities were converted into zeta potentials according the procedure of O'Brien and White [16]. The zeta potentials corresponding to plateau values for adsorption are plotted in Fig. 4.
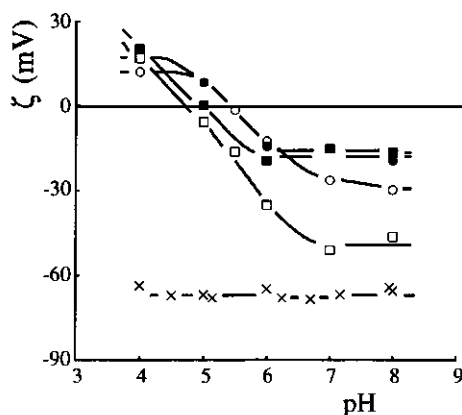

Fig. 4. Zeta potentials of the protein-latex complex, corresponding to plateau values for adsorption of the two monoclonal IgGs and their F(ab')$_2$ fragments on PS-. The proteins are indicated as (○) IgG 1B, (❑) F(ab')$_2$ 1B, (●) IgG 2A, and (■) F(ab')$_2$ 2A. The zeta potential of the bare latex is indicated as x.

The similarity in the pH-dependence of the zeta potential observed for the various protein-covered latex particles is striking, because there are large variations in adsorbed amounts and charges on the proteins. Apparently, upon adsorption the net amount of charges, including a certain amount of low molecular mass ions which can be co-adsorbed [20], remains low to suppress adverse electrostatic interactions. This similarity in ζ(pH) curves, and therefore in the mechanism of charge incorporation into the adsorbed layer, indicates that electrostatic interactions play a role in determining the plateau values of adsorption. It is also seen that for all proteins the zeta potential becomes positive at low pH values, which implies that interactions other than electrostatic are a driving force for adsorption. Comparing the plateau values for adsorption onto PS- (Fig. 3a) with the zeta potentials (Fig. 4), it is seen that the maximum in the adsorbed amount occurs at a pH at which the surface charge of the bare polystyrene latex is not yet fully compensated. Hence, the maximum is neither found at the i.e.p. of the protein (as reported in ref. [17]) nor at the i.e.p of the protein-latex complex (as reported in ref. [14]) but somewhere in between. For $F(ab')_2$ 2A in particular, this effect is clearly illustrated; the deviation of the i.e.p. of the protein (8.5) from the i.e.p. of the protein-latex complex (5.0) is relatively large, whereas the maximum in the adsorbed amount is found at pH 7.

Effect of ionic strength

The role of electrostatic interactions in the adsorption process has been further investigated by determining isotherms at various ionic strengths. This has been done for both IgGs and their corresponding $F(ab')_2$ fragments adsorbed at PS-, at pH 5 and 7. The results are shown in Fig. 5.

At higher ionic strengths, the electrostatic interactions are better screened. Therefore, upon addition of electrolyte the adsorption is enhanced when the electrostatic interactions between protein and sorbent are repulsive, whereas the opposite applies for conditions of attractive electrostatic interactions. Lateral repulsion between proteins is always reduced at higher ionic strengths, resulting in an increased adsorption in the region of higher occupancies of the surface. Therefore, it is expected that under electrostatically repulsive conditions (IgG and $F(ab')_2$ 1B adsorbed at pH 7) salt addition promotes adsorption whereas for attractive conditions (all proteins adsorbed at pH 5) electrolyte inhibits adsorption, at least in the initial parts of the isotherms. These trends are sometimes observed, but there are exceptions pointing to phenomena which need an elaborated explanation.

For IgG 1B adsorbed at pH 5 the plateau value is barely affected by the ionic strength and only at low protein concentration is the adsorption somewhat enhanced, rather than

reduced, by increasing the ionic strength. This indicates that only some lateral repulsion is screened. Adsorption of IgG 1B at pH 7 obeys the above-mentioned rules, which means that screening of electrostatic repulsion gives rise to an increase in the adsorbed amount. In view of the similarity in the i.e.p. values and the adsorption behaviour, the same trend was expected for F(ab')₂ 1B. However, for both pH values a reduction in the adsorbed amount is found at higher ionic strengths.
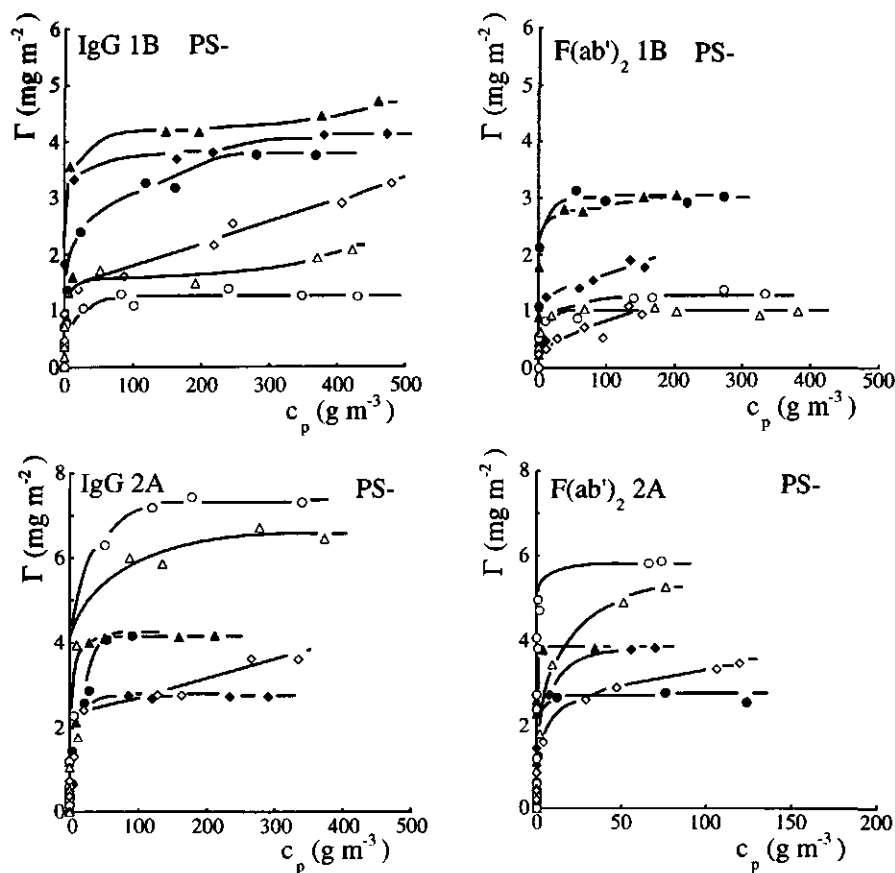

Fig. 5. Adsorption of the two monoclonal IgGs and the F(ab')₂ fragments on PS- at pH 5 (closed symbols) and pH 7 (open symbols). The ionic strengths are indicated as 5 mM (● or ○), 30 mM (▲ or △), and 100 mM (♦ or ◊). The proteins are indicated in the Figure.
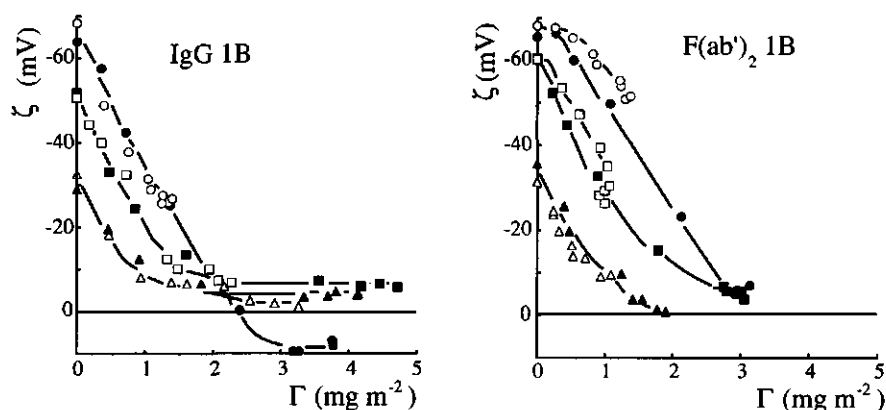
Fig. 6. Zeta-potentials corresponding to the adsorption isotherms IgG 1B and F(ab')₂ 1B on PS- at pH 5 (closed symbols) and pH 7 (open symbols). The ionic strength is indicated as 5 mM (● or ○), 30 mM (▢ or ■), and 100 mM (▲ or △). The proteins are indicated in the Figure.

More information on the effect of ionic strength on the adsorption behaviour is obtained when comparing the zeta potentials corresponding to the isotherms of IgG and F(ab')$_2$ 1B. The results are shown in Fig. 6. The F(ab')$_2$ fragments adsorb until the resulting zeta potentials of the protein-covered latex particles are zero, and the adsorbed amount for which this charge compensation occurs decreases with increasing ionic strength. In contrast, adsorption of the whole IgG molecule may become super equivalent. This is an indication that between proteins and latex, non-electrostatic interactions are more important for adsorption of the whole IgG molecule than for the F(ab')$_2$ fragment. A similar observation has been reported by Kawaguchi and co-workers [5], who showed that for competitive adsorption between the Fc and the Fab fragment, Fc adsorption was less strongly determined by electrostatic interactions. When the influence of the electrolyte concentration on the adsorption behaviour at pH 5 of F(ab')$_2$ 1B is compared to that of F(ab')$_2$ 2A a similar pattern is expected. However, the adsorbed amount of F(ab')$_2$ 2A at pH 5 is not reduced at higher ionic strengths, but increases somewhat. For F(ab')$_2$ 2A, even at 100 mM, the zeta potential of the latex particles could only be reduced to zero by an adsorbed amount as high as 3 mg m^{-2} (data not shown), and therefore the adsorption of F(ab')$_2$ 2A at pH 5 is not reduced by increasing the ionic strength, in contrast to the adsorption of F(ab')$_2$ 1B. From Fig. 5 it could further be observed that for IgG 2A at pH 7 the amount adsorbed at 100 mM is strongly reduced to

a plateau value which is comparable to the maximum adsorption of IgG 1B. At pH 7 the net charge on IgG 2A is zero, indicating that the large adsorbed amounts at low ionic strength were caused by aggregation of the proteins at the surface. This supports our suggestion made earlier in the discussion of the adsorption behaviour at hydrophobic latices.

3.3.2 Adsorption on the hydrophilic latex

Proteins only adsorb onto the hydrophilic OH- latex when the interaction is electrostatically favourable. This is in contradiction with other studies in which IgG was found to adsorb on hydrophilic surfaces even under conditions of electrostatic repulsion [19,21,22]. The nature of the latex used in this study was probably more hydrophilic and/or some steric repulsion was involved. If adsorption does take place, the isotherms show a high affinity and well-defined plateau values. In Fig. 7 the plateau values are plotted against the pH. It is observed that the adsorbed amounts are lower than the corresponding ones on hydrophobic surfaces, also at pH values below the i.e.p. of the protein (compare Fig. 3). The adsorbed amounts vanish completely under electrostatically repelling conditions. It can also be seen that, compared to the negatively charged hydrophobic latex, the pH at which maximum adsorption is found, is more acidic.
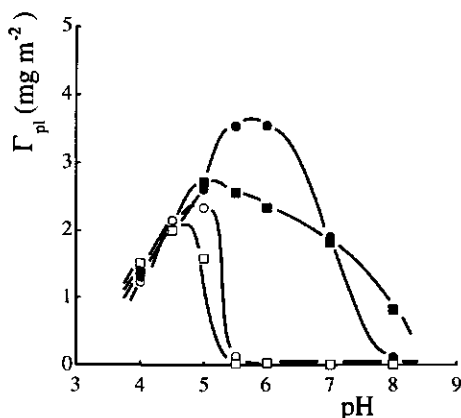

Fig. 7. Plateau adsorption of the two monoclonal IgGs and the F(ab')₂ fragments on OH-. The proteins are indicated as (○) IgG 1B, (❑) F(ab')₂ 1B, (●) IgG 2A, and (■) F(ab')₂ 2A.

These observations indicate that adsorption only occurs if there are enough charges on the protein surface that are attracted by charges on the sorbent surface.

Assuming that the adsorption behaviour is mainly determined by the part of the protein that is in close contact with the surface, it can be concluded that beyond pH 5.5, IgG 2A adsorbs with its F(ab')$_2$ fragment oriented towards the surface. This is inferred from the observation that IgG 2A, unlike IgG 1B, does adsorb in that pH region, whereas the Fc fragments of both monoclonals are the same. However, at pH 8, F(ab')$_2$ fragments do adsorb whereas this is not the case for whole IgG. This might be due to the presence of the Fc part which imposes sterical restrictions on the possible orientations of the F(ab) parts at the sorbent surface.

3.3.3 Orientation of the adsorbed proteins

When only minor structural rearrangements take place, the results of the amounts adsorbed in the plateau region may be interpreted in terms of the orientation of the proteins. As the dimensions of crystallised fragments are known, the surface area per adsorbed protein molecule can be calculated for a complete monolayer of various possible orientations. The dimensions of the proteins are taken from the structures of crystallised Fc fragments [23] and F(ab) fragments [24] and are 7.0x6.3x3.1 nm^3 and 8.2x5.0x3.8 nm^3 for Fc and F(ab), respectively.

	IgG				F(ab')$_2$			
orientation	A	B	C	D	A	B	C	D
Γ (mg m^{-2})	5.5	3.7	2.6	2.0	4.4	3.0	8.7	2.0

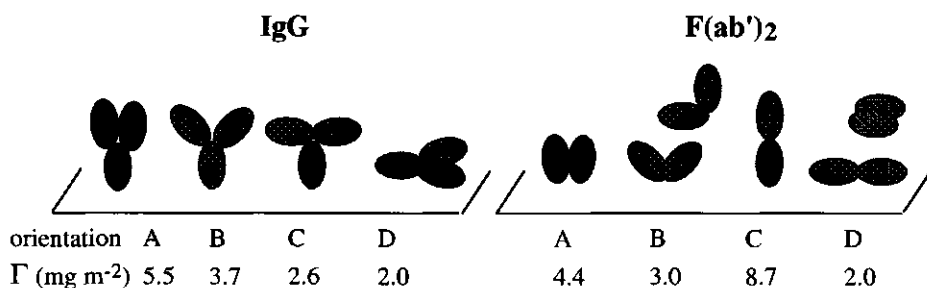*Fig. 8. Schematic drawing and calculated adsorbed amount of some orientations of adsorbed IgG and F(ab')$_2$. (A) End-on orientation with contracted F(ab) fragments, (B) and (C) end-on orientation with intermediate and repelling F(ab) fragments, respectively, (D) Side-on orientation. The adsorbed amounts are computed with the dimensions of crystallised fragments and assuming close-packed monolayers.*

Based on these dimensions the adsorbed amounts are calculated for some regular orientations of the IgG and the F(ab')$_2$ fragments, as shown in Fig. 8. Note, that for IgG adsorbed in orientations A, B and C, turning the molecule upside down does not affect the calculated adsorbed amounts. In orientations "A, B and C" the proteins are adsorbed end-on, whereas for orientations "D" this takes place in a side-on orientation. Because the F(ab')$_2$ fragments are highly flexible in the hinge region it may be expected that, owing to electrostatic interaction, the F(ab') units repel each other at pH values away from the i.e.p.. This could result in a preference for orientation "B" and "C" or something in between. At the i.e.p. the conformation is probably more contracted, resulting in orientation "A". Repulsion or attraction between the F(ab')$_2$ fragments does not affect the calculated adsorbed amounts for orientation "D", although the packing geometry is probably altered in the experimental situation.

If the results of the calculations are compared with the plateau values of adsorption (Fig. 3) it is seen that on hydrophobic latices, maximum adsorption occurs when a large fraction of the proteins is adsorbed in an end-on orientation; see "A". In the literature the maximum in the $\Gamma_{pl}(pH)$-curve for protein adsorption is generally explained by a relatively high conformational stability and/or relatively weak lateral repulsion when the pH is at the i.e.p. of the protein [25]. For IgG and F(ab')$_2$ molecules the decrease in the adsorbed amount at pH values shifted from the i.e.p. is enhanced due to the possibility of repulsion between F(ab) fragments leading to orientation "B" and "C" [13,17,19]. However, the present results indicate that the shape of the $\Gamma_{pl}(pH)$-curve is not only influenced by the charges on the protein and lateral interactions but also depends on the electrostatic protein-sorbent interactions. It is clearly observed that the maximum in the adsorbed amount is located at pH values where the protein is marginally electrostatically attracted by the sorbent surface, and that there is an asymmetry in the decrease of the adsorbed amount at both sides of the i.e.p. of the proteins. These observations can be explained by the electrostatic interactions which are enhanced by a decreased dielectric constant in the contact region between the protein and the sorbent surface. More specifically, it is plausible that adsorbed protein layers will be formed in such a way that the charge density in the inner layer of the protein-latex complex is maximally reduced. As a consequence, large adsorbed amounts are obtained when the proteins and surface marginally oppose each other electrostatically. The interfacial potentials can be further reduced by the uptake of low molecular weight ions into the contact region [20] and by structural or orientational changes of the protein which could result in the asymmetry of the $\Gamma_m(pH)$-curves.

For hydrophilic surfaces, it is observed that the plateau values of adsorption are smaller than those on hydrophobic surfaces and that adsorption only occurs when electrostatic interactions are favourable (Fig. 7). Nevertheless, immunological tests based on hydrophilic surfaces may have the practical advantage that aspecific interactions of the antigen with the sorbent surface are prevented. It is also reported that IgG, adsorbed onto a hydrophilic glass surface, has a higher immunological activity than adsorbed onto polystyrene [26]. With respect to the orientation it can be seen that in the pH range from 4 to 5, the four proteins have similar plateau values around 2 mg m^{-2}. In Chapter 2, Fig. 3, it can be observed that in this pH range all proteins contain a relatively high and similar positive charge. Therefore, it is not unlikely that the proteins increase the electrostatic attraction by adsorbing in a side-on orientation "D". This is supported by the fact that the IgG and F(ab')$_2$ fragments have similar maximally adsorbed amounts, which rules out the possibility that these relative small adsorbed amounts are only caused by lateral repulsion between end-on adsorbed molecules. With respect to the immunological activity this side-on orientation may result in a decreased accessibility for antigens in solution. At higher pH values, the higher adsorbed amount of IgG 2A and F(ab')$_2$ 2A indicate that at least part of the proteins adsorb in an end-on orientation. However, under these conditions it was inferred that IgG 2A adsorbs with its F(ab) domains directed towards the surface which may also lead to a decreased accessibility for antigens in solution.

3.4 Conclusions

As judged from the initial parts of the isotherms, electrostatic interactions are only of minor importance for the adsorption affinity of IgGs and their F(ab')$_2$ fragments onto hydrophobic polystyrene surfaces. However, the plateau values are largely influenced by the overall electrostatic interactions. This results in a maximum in the adsorbed amount at a pH between the i.e.p. values of the protein and the protein-latex complex. The maximally adsorbed amounts correspond to calculated values of the IgG adsorption in an end-on orientation. Adsorption onto the hydrophilic latex is dominated by electrostatic interactions. This results in an absence of adsorption when the protein is electrostatically repelled by the latex surface. When the protein bears a relatively high charge density opposite to that of the surface, electrostatic interactions are maximised by adsorbing in a side-on orientation. A possible consequence of this is that the binding sites are less accessible for antigens. For all surfaces, the adsorption patterns for IgG and the corresponding F(ab')$_2$ fragments are rather similar, although there is some evidence that

hydrophobic interactions and/or conformational changes contribute less to the adsorption of the $F(ab')_2$ fragments.

3.5 Acknowledgements

3.6 References

1   C. Milstein, *Sci. Am.*, **243** (1980) 56.

2   R. Kurkela, L. Vuolas, and P. Vihko, *J. Immunol. Methods*, **110** (1988) 229.

3   F.V. Bright, T.A. Betts, and K.S. Litwiler, *Anal. Chem.*, **62** (1990) 1065.

4   M.L. Yarmush, X. Lu, and D.M. Yarmush, *J. Biochem. Biophys. Methods*, **25** (1992) 285.

5   H. Kawaguchi, K. Sakamoto, and Y. Ohtsuka, *Biomaterials*, **10** (1989) 225.

6   J.L. Ortega-Vinuesa, and R. Hidalgo-Alvarez, *Colloids and Surfaces B: Biointerfaces*, **1** (1993) 365.

7   M. Muratsugu, S. Kurosawa, Y. Mori, and N. Kamo, *Chem. Pharm. Bull.*, **40** (1992) 501.

8   J.W. Goodwin, J. Hearn, C.C. Ho, and R.H. Ottewill, *Colloid Polym. Sci.*, **252** (1974) 464.

9   W. Norde, *Ph.D. thesis*, Agricultural University Wageningen, The Netherlands, 1976.

10   E.G.M. Pelssers, M.A. Cohen Stuart, and G.J. Fleer, *J. Colloid Interface Sci.*, **137** (1990) 350.

11   T. Arai, and W. Norde, *Colloids and Surfaces*, **51** (1990) 1.

12   O.H. Lowry, N.J. Rosebrough, A.L. Farr, and R.J. Randall, *J. Biol. Chem.*, **193** (1951) 265.

13   A. Johnstone, and R. Thorpe, *Immunochemistry in Practice*, 2nd edn., Blackwell Scientific, Oxford, 1987, Chapter 1.

14   A.V. Elgersma, R.L.J. Zsom, W. Norde, and J. Lyklema, *Colloids Surfaces*, **54** (1991) 89.

15   F. Galisteo-González, J. Puig, A. Martín-Rodriquez, J. Serra-Domènech, and R. Hidalgo-Alvarez, *Colloids Surfaces B: Biointerfaces*, **2** (1994) 435.

16   R.W. O'Brien, and L.R. White, *Faraday Trans. 2*, **74** (1978) 1607.

17   P. Bagchi, and M. Birnbaum, J. *Colloid Interface Sci.*, **83** (1981) 460.

18   B.D. Fair, and A.M. Jamieson, *J. Colloid Interface Sci.*, **77** (1980) 525.

19   T. Suzawa, and H. Shirahama, *Adv. Colloid Interface Sci.*, **35** (1991) 139.

20   C.A. Haynes, E. Sliwinsky, and W. Norde, *J. Colloid Interface Sci.*, **164** (1994) 394.

21   A.V. Elgersma, R.L.J. Zsom, W. Norde, and J. Lyklema, *Colloids Surfaces*, **65** (1992) 17.

22   J.E. Johnson, and E. Matijevic, *Colloid Polym. Sci.*, **270** (1992) 353.

23   J. Deisenhofer, *Biochemistry*, **20** (1981) 2361.

24   M. Marquart, J. Deisenhofer, R. Huber, and W. Palm, *J. Mol. Biol.*, **141** (1980) 369.

25   W. Norde, *Adv. Colloid Interface Sci.*, **35** (1986) 267.

26   N.J. Geddes, D.N. Furlong, P. Zientek, K.A. Than, and J.A. Edgar, *J. Colloid Interface Sci.*, **157** (1993) 491.

4 Adsorption Dynamics of IgG and its $F(ab')_2$ and Fc fragments Studied by Reflectometry

The adsorption process of two monoclonal IgGs and their corresponding $F(ab')_2$ and Fc fragments is followed in real-time using reflectometry. The proteins are adsorbed on two surfaces: a hydrophilic silica and a hydrophobic methylated surface. The adsorption experiments are performed at different values for pH and ionic strength. Altogether, these variations enable a systematic study of electrostatic and hydrophobic interactions. At all conditions adsorption is observed. The adsorption of IgG and $F(ab')_2$ on a hydrophilic silica surface is retarded when the proteins are electrostatically repelled by the sorbent surface. This effect is stronger for $F(ab')_2$ fragments than for whole IgG molecules, whereas the adsorption rate of Fc fragments is not significantly affected. On the methylated surface the retardation of the initial adsorption is largely compensated owing to hydrophobic interactions. As a function of pH, both IgGs show maximum adsorption around their isoelectric points. At higher ionic strengths these maxima are less pronounced because of screening of electrostatic interactions. After the protein solution is replaced by a buffer solution the desorbed amount is measured after 15 minutes. These desorbed amounts indicate that the proteins are more tightly bound to methylated surfaces than to silica surfaces. Furthermore, it is observed that, for IgG and Fc adsorbed on silica at low ionic strength, a relatively large fraction desorbs around their i.e.p. whereas this is not the case for $F(ab')_2$.

4.1 Introduction

The physical adsorption of immunoglobulin G (IgG) onto solid surfaces is a process which is commonly applied in biomedicine and food industry where adsorbed IgG molecules are used in detection systems such as immunological tests and biosensors. The desire to control and manipulate protein adsorption in these applications requires a

detailed understanding of the adsorption process. The aim of the present study was to establish a relation between the various physical-chemical properties of the system and the adsorption process. When a protein solution is supplied to a solid surface, five major subprocesses in the adsorption process can be distinguished: 1. transport of proteins towards the surface; 2. actual attachment to the surface; 3. adsorption at higher surface coverages which is hindered due to lateral repulsion between proteins in solution and at the surface; 4. structural and/or orientational rearrangements in the adsorbed proteins; 5. desorption of proteins from the surface. These subprocesses are schematically shown in Fig. 1.
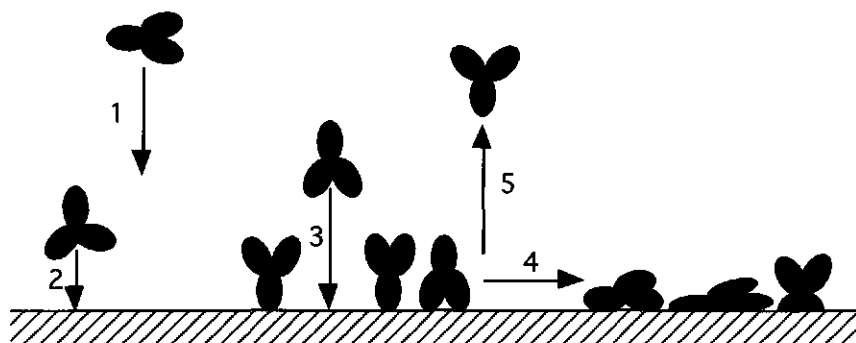
Fig. 1. Schematic representation of the adsorption process of IgG molecules. The arrows represent different subprocesses which can be distinguished in adsorption.

The affinity of proteins for smooth sorbent surfaces is mainly determined by hydrophobic and electrostatic interactions. This affinity may be enhanced by the possibility of structural changes within the protein and is therefore related to the structural stability of the protein [1]. Protein adsorption is generally found to be irreversible or only partially reversible with respect to dilution [2]. This implies that the rates of some subprocesses can influence the final adsorbed state of the proteins. An example is the slow decrease in time of the structural order which has been reported for adsorbed IgG [3,4]. It has also been proven that proteins show a higher tendency to undergo structural changes when the degree of surface coverage is smaller [5,6]. This suggests that structural changes are more likely to occur at relatively low adsorption rates. For IgG and F(ab')$_2$ adsorption at sufficiently high concentrations usually closely-packed monolayers are obtained. Therefore, the final adsorbed amounts are related to the spatial distribution of the proteins which, in turn, is determined by the combined effects of orientation, structure, and lateral interactions between adsorbed protein molecules. The

final adsorbed amounts, however, do not allow for an independent quantification of these effects. Nevertheless, information can be extracted from the development of the adsorbed amount in time exploiting the fact that some subprocesses have different rates.

The influence of the hydrophobicity of the sorbent surface was studied by comparing adsorption on a hydrophobic methylated surface and a hydrophilic silica surface. Electrostatic interactions were varied systematically by adsorbing two monoclonal IgGs, which differ in isoelectric point (i.e.p.), at various pH values and ionic strengths. An IgG molecule consists of three domains; two of them, which are called F(ab) domains, contain an antigen-binding site whereas the third domain, the Fc region, is responsible for the binding to receptors located on cell walls. The orientation of the adsorbed IgG molecule will be influenced by the relative affinity of the different domains for the sorbent surface. In order to study the influence of these domains on the adsorption process, the same set of experiments carried out for IgG was also performed using the corresponding $F(ab')_2$ and Fc fragments. The adsorption behaviour of $F(ab')_2$ is also of great importance because recently immunological tests have been developed by immobilising only the F(ab) fragments [7,8] or $F(ab')_2$ fragments [9].

Various techniques have been used to determine the amount adsorbed as a function of time, including ellipsometry [10,11,12], Fourier transform infrared [13,14], total internal reflection fluorescence [15,16], γ-photon spectroscopy [17] and streaming potential measurements [18]. In the present study we used the optical technique reflectometry which is a simplified version of ellipsometry. Reflectometry is especially suited to study adsorption kinetics because it can rapidly monitor the rates of adsorption using relatively simple and cheap instrumentation. Moreover, no labelling which could alter the adsorption behaviour is required.

4.2 Experimental

4.2.1 Materials

Surfaces

In the present study a hydrophilic silica surface and a hydrophobic methylated surface were used, both based on a silicon wafer (Wacker Chemitronic GmbH). The silicon wafer was oxidised for 1 hour at 1000°C in order to obtain a silica layer of about 100 nm thickness. Such a thickness is essential for obtaining a high sensitivity in reflectometry experiments [19]. The silica wafer was cut into slides of 1 x 5 cm². Prior to each experiment, silica slides were cleaned by placing them for 20 minutes in a chamber with a

constant oxygen flow, while the surface was irradiated by UV-light. In this way organic
contaminants were oxidised and a homogeneous oxide layer was produced with a
minimum of surface damaging [20]. Hydrophobic methylated surfaces were obtained by
immersion of silica slides for 30 minutes in a 0.3 % (v/v) solution of
dichlorodimethylsilane in 1,1,1-trichloroethane. After silanisation the slides were flushed
consecutively with trichloroethane and ethanol. Both the untreated and methylated silica
slides were rinsed with water and dried in a jet of nitrogen gas before placing them in the
reflectometry cell. The contact angles of a sessile drop of water for the methylated and
the silica surface were 90° and 7°, respectively. The silica surface is negatively charged
due to dissociation of hydrolysed silanol groups. It has been reported that the zeta-
potential at an ionic strength of 0.01 M NaCl is around -20 mV at pH 4 and this value
gradually decreases to ca. -55 mV at pH 8 [21]. The methylated silica surface also
contains negative charges due the presence of unsilanised silanol groups. Streaming
potential measurements, performed as described by Norde and Rouwendal [18], showed
that at pH 7 and an ionic strength of 0.01 M the zeta potential of a methylated surface was
-35 mV which is ca. 33% lower than the zeta potential of a silica surface under the same
conditions of pH and ionic strength.

Proteins

Two monoclonal immunoglobulins, IgG 1B and IgG 2A, were studied. They were
kindly donated by Organon Teknika (Boxtel, The Netherlands). Both IgGs were from
isotype 1 and directed against the pregnancy hormone, human chorionic gonadotropin
(hCG). Their respective $F(ab')_2$ and Fc fragments were obtained by papain digestion
under non-reducing conditions as described in Chapter 2.3.2. Some characteristics of the
IgGs and their fragments are listed in Table 1. The isoelectric point (i.e.p.) was
determined using isoelectric focusing (IEF) with PhastGel media, pH range 3-9 and silver
staining (PhastSystem, Pharmacia). The Fc fragments, as obtained after digestion of both
monoclonals, were identical with respect to their i.e.p and molecular weight. In Table 1
the major bands in the respective isoelectric pH regions are given in brackets.

*Table 1. Isoelectric points and purity of the monoclonals IgG 1B and 2A and their
$F(ab')_2$ and Fc fragments.*

protein	IgG 1B	$F(ab')_2$ 1B	IgG 2A	$F(ab')_2$ 2A	Fc
i.e.p.	5.6-6.0 (5.8)	5.6-6.1 (5.9)	6.7-7.4 (6.9)	8.2-8.8 (8.5)	5.7-6.3 (6.1)
purity	97%	>99%	87%	98%	-

The purity of the IgGs and F(ab')$_2$ fragments obtained with high performance size exclusion chromatography (Zorbax, GF-250 Dupont) is given in weight fractions. Impurities in IgG 1B consisted of smaller fragments, but solutions of IgG 2A and F(ab')$_2$ 2A contained aggregates with total weight fractions of 6% and 2%, respectively. The molecular weights of the IgG molecules, the F(ab')$_2$ and the Fc fragments were 150 kDa, 100 kDa, and 50 kDa, respectively. The concentration of both IgGs was established spectroscopically using an extinction coefficient of 1.45 cm^2 mg^{-1} at 280 nm. The extinction coefficients for the F(ab')$_2$ fragments were determined colorimetrically according to the Folin phenol method of Lowry and co-workers [22] using the corresponding IgGs as the standards. This resulted in an extinction coefficient of 1.45 cm^2 mg^{-1} for F(ab')$_2$ 1B and 1.48 cm^2 mg^{-1} for F(ab')$_2$ 2A. Since these extinction coefficients are almost identical to those of the IgGs, an extinction coefficient of 1.45 cm^2 mg^{-1} was assumed for the Fc fragment.

Chemicals

Water was purified by reverse osmosis and passed subsequently through a SuperQ system (Millipore). All other chemicals were of p.a. grade and used without further purification. All experiments were performed in a 5 mM buffer solution. At pH 4 and 5 an acetate buffer, and at pH 6, 7, and 8 a phosphate buffer was used. Both buffers were prepared from sodium salts and adjusted to the desired pH with NaOH and HCl. Ionic strengths higher than 5 mM were obtained by adding NaCl.

4.2.2 Methods

Reflectometry

Reflectometry is an optical technique which continuously monitors the polarisation of a light beam reflected from an interface. Upon adsorption at that interface, the polarisation is altered and this change is measured by determining the ratio between the parallel and perpendicular components of the reflected beam. The reflectometry technique used in the present study was developed by Akzo Research Laboratories Arnhem [23]. The basic principles of the method, the experimental set-up and the calibration procedures are described by Dijt and co-workers [19]. A schematic diagram is shown in Fig. 2. In the reflectometer the solution is impinged perpendicularly to the sorbent surface through a tube drilled in the glass prism (a) and leaves the cell by an overflow system (not shown). A He/Ne laser beam (632.8 nm, 0.5 mW) which is polarised with a minimum polarisation ratio of 500:1 (model 1108P, Uniphase) enters the

cell through the same glass prism. The beam is reflected at the interfaces of the sorbent surface facing the tube exit with an angle of incidence close to the Brewster angle for the water/silicon interface (71°). The reflected beam is splitted in a parallel (p) and perpendicular (s) component relative to the plane of incidence by means of a beamsplitter. Both components of the reflected light are detected by photodiodes and the ratio between the intensity of the parallel, I_p, and the perpendicular, I_s, components is the output signal S ($=I_p/I_s$).
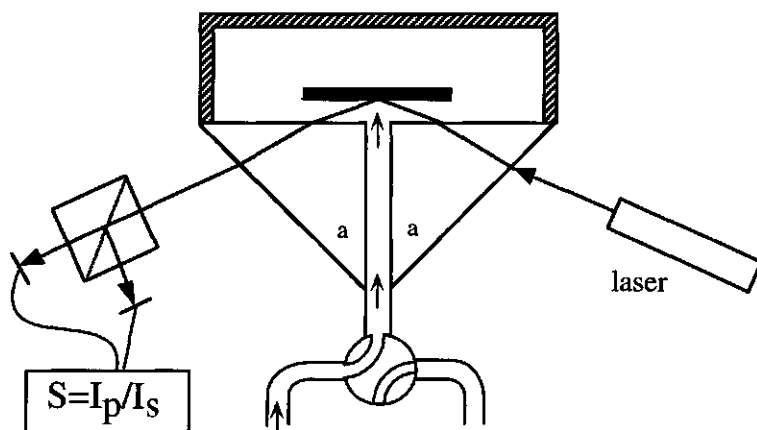
Fig. 2. Schematic diagram of the reflectometer set-up.

For surface concentrations up to 5 mg m^{-2} the change in the signal is linearly related to the adsorbed amount. The following simple expression for the adsorbed amount (Γ) as function of the output signal is derived [19]:

$$\Gamma = Q \frac{\Delta S}{S_0} \tag{1}$$

where the subscript 0 indicates the initial situation at the bare sorbent surface. The change in the signal can be related to the adsorbed amount if the calibration factor Q is known. The factor Q equals the change in the adsorbed amount per relative change in the signal, i.e., it is defined as

$$Q \equiv \frac{d\Gamma}{d(R_p/R_s)/(R_p/R_s)_0} \tag{2}$$

where R_p and R_s are the parallel and perpendicular reflectivity coefficients, respectively. The hydrophilic surface consists of a silicon slide with a high refractive index upon which a thin silica layer is prepared as described before. The hydrophobic methylated surface contains an additional methylsilane layer (see materials section). During the experiment a protein layer is adsorbed on top of the sorbent surface. The Q-factor can be determined if the ratio between the reflectivities of the bare surface $(R_p/R_s)_0$ is known and if a relation between the change in the respective ratios and the adsorbed amount can be established. The ratio between the reflectivities on the bare surface, $(R_p/R_s)_0$, depends on the refractive indices of silicon, silica, and the solution, the thickness of the silica layer, the angle of incidence θ_i and the wavelength of the light. The methylsilane layer on the hydrophobic slides is very thin and therefore it is assumed that the methylsilane layer does not affect the reflectivities. The refractive indices of silicon, silica and water are 3.80, 1.46 and 1.33, respectively. The thickness of the silica layer is found by comparing S_0-values for the wafer under study with wafers having silica layers of known thickness. The angle of incidence is also determined by analysing the S_0 value of a few wafers with known thickness of the silica layer. The only problem left for determining the Q-factor is the expressions for the refractive index and thickness of the protein film. The refractive index for an inhomogeneous layer with an adsorbed amount Γ of average thickness d_p, can be calculated [24] and is given by

$$n_p = n_s + \left(\frac{dn}{dc}\right)\frac{\Gamma}{d_p} \tag{3}$$

where n_s is the refractive index of the buffer solution and dn/dc is the refractive index increment (specific refractivity) of the adsorbed protein layer. For the quotient (Γ/d_p) it was assumed that a thickness of 2.5 nm corresponds to a homogeneous layer of 1 mg m^{-2}. With respect to the properties of the protein layer, the Q-factor is mainly influenced by the specific refractivity (dn/dc); it is highly insensitive to the quotient (Γ/d_p). In the literature, values for the specific refractivities of various globular proteins are reported ranging from 0.182 to 0.188 cm^3 g^{-1} [24,25]. Therefore, a value for the specific refractivity of 0.185 cm^3 g^{-1} was taken. In the calculation of the Q-factor, it is assumed that the specific refractivity remains constant at all surface concentrations. The correctness of this assumption was experimentally validated by De Feijter and co-workers [24]. Substituting these values for the different layers enables the calculation of the Q-factor using the matrix formalism of Abeles, as described by Hanson [26].

4.3 The adsorption process

Transport of proteins towards the surface by stagnation point flow

In the present study the transport of proteins towards the surface (Fig. 1, subprocess 1) is well-controlled by invoking a stagnation point flow. Stagnation point flow results in a constant thickness of the diffusion boundary layer and therefore the protein flux towards the surface is proportional to the protein concentration in solution. The hydrodynamics of the mass flux in a stagnation point flow were described in detail by Dabros and Van de Ven [27]. For dilute protein solutions an analytical expression for the protein flux, J_0 (g m^{-2} s^{-1}), can be obtained if the protein concentration near the sorbent surface equals zero (denoted by the subscript 0)

$$J_0 = 0.53 \left(D^2 \alpha \varphi R^{-4}\right)^{1/3} c_p = k c_p \tag{4}$$

Here, D is the diffusion coefficient (m^2 s^{-1}), α a dimensionless flow intensity parameter which is constant for a certain cell geometry and flow rate, φ the flow rate (m^3 s^{-1}), R the radius of the circular hole through which the solution enters the cell and c_p the protein concentration in solution (g m^{-3}). Hence, for a given cell the protein flux is equal to the protein concentration in solution, multiplied by a constant which we call the transport coefficient k. The transport coefficient k can be established since in the present study all parameters are known. The flow rate is determined from the weight of solution that passes through the flow system in 10 minutes and amounts to 1.8 10^{-8} m^3 s^{-1}. The diffusion coefficient for IgG is 4.0 10^{-11} m^2 s^{-1} [16,28], the radius of the inlet tube is 0.9 10^{-3} m and the flow intensity parameter which is related to the geometry of the cell and the flow rate [27] is estimated to be 3.5. These values result in a transport coefficient of 2.8 10^{-6} m s^{-1}. For IgG concentrations of 7.5 g m^{-3} were used in all experiments and this results in a theoretical protein flux of 1.3 mg m^{-2} min^{-1}.

Initial stage of the adsorption process.

If the protein reaches the surface, it may experience an energy barrier which prevents a fraction of the arriving protein from adsorption (Fig. 1, subprocess 2). This energy barrier could for instance be caused by an energetically unfavourable overlap of the electrical double layers or by hydrodynamic effects [29]. This means that the adsorption rate (dΓ/dt) expressed in mg m^{-2} s^{-1} may be retarded and can formally be written as

$$(d\Gamma/dt)_{t\to0} = \beta J_0 \tag{5}$$

where the subscript $t\to0$ indicates the initial stage of the process. The retardation factor ß can easily be found from the experimental results by dividing the initial adsorption rate by the theoretical protein flux towards the surface. The factor ß is related to the magnitude of the Gibbs energy of the barrier, G, by ß = exp(-G/RT) where R is the gas constant and T the temperature.

Adsorption at higher surface coverages

When part of the surface is occupied with adsorbed proteins less space is left for adsorption and, consequently, the adsorption rate decreases. A fraction of the protein flux encounters inaccessible parts on the surface and the effective adsorption rate is then expressed as

$$d\Gamma/dt = \beta J_0 \left[1 - \int_0^t AJ(\tau)d\tau\right] \tag{6}$$

where A is the area occupied by one unit mass of protein. The factor A equals the inverse of the adsorbed amount in a closely-packed monolayer. If the factors ßJ and A remain constant during the whole process, an equation for the adsorbed amount as a function of time can be obtained by rewriting Eq. 6 using Laplace transformations.

$$\Gamma(t) = A^{-1}(1 - e^{-\beta J_0 At}) \tag{7}$$

Examples of adsorption curves according to Eq. 7 with different values for the retardation factor ß and the factor A are shown in Fig. 3. From this figure it can be seen that for the chosen conditions the adsorption should reach well-defined plateau values within 30 minutes.

However, in practice the adsorption process is much more complicated. When the surface does not accommodate all proteins that diffuse towards it, the diffusion-limited conditions ($c_p=0$ at interface) no longer apply, thereby affecting the protein flux J_0. Another aspect which will influence the adsorption process is the electrostatic repulsion between adsorbed proteins and newly arriving proteins because the distance over which this repulsion is effective may exceed the dimension of the protein molecule.
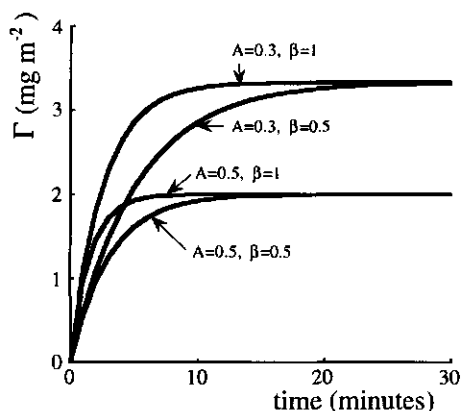
Fig. 3. The adsorbed amount as a function of time, calculated from Eq. 7. The values for the parameters A and β are indicated in the figure and for the protein flux J_0 1.3 mg m^{-2} min^{-1} is taken, which is close to the value applied in our experiments.

Furthermore, at larger surface coverages the adsorption rate may be reduced by the formation of small adsorption sites which require a specific orientation of newly arriving protein molecules to become attached to the surface. These processes of electrostatic or steric repulsion between adsorbed proteins and proteins in solution (Fig. 1, subprocess 3) will increase the effective surface area (A) blocked by the adsorbed proteins. Consequently, the reduction in the adsorption rate, as calculated by Eq. 6 will be underestimated.

Structural rearrangements of adsorbed proteins

Attainment of adsorption saturation, which is reflected in the development of a plateau value for $\Gamma(t)$ is influenced by the effective area occupied by a protein molecule. Upon adsorption proteins may undergo structural rearrangements which is, for instance, inferred from the fact that the attachment of IgG molecules to solid surfaces is stronger after longer incubation time [3,4]. These structural changes are enhanced due to intramolecular electrostatic repulsion when proteins contain more net charges [30] or when the charge contrast between the protein and sorbent is increased [5,6]. It has also been reported that at higher surface coverages reorientation of the adsorbed proteins occur [31]. In these processes (Fig. 1, subprocess 4) often a change in the occupied surface area is involved which will be reflected in the shape of the $\Gamma(t)$ curves. It should

be mentioned that proteins may as well undergo structural changes before attachment in order to subdue an existing energy barrier [1,32].

Desorption

Although protein adsorption is generally considered to be irreversible with respect to dilution [33,34], it has been reported that upon replacing the protein solution by pure solvent a small fraction of the adsorbed proteins may desorb, the desorbed amount depending on history [35,36]. The extent of desorption may give information on the strength of the interactions between the protein and the sorbent surface.

4.4 Results and discussion

4.4.1 General aspects of adsorption kinetics

All reflectometry experiments were performed at protein concentrations of 7.5 g m^{-3} for the IgG and F(ab')₂ and 5 g m^{-3} for Fc. The ionic strength was 5 mM or 0.1 M. A typical set of adsorption curves is shown in Fig. 4 in which adsorption of IgG 1B on methylated silica (4a) and silica (4b), at pH 4, 6 and 8 and an ionic strength of 5 mM is followed in time.
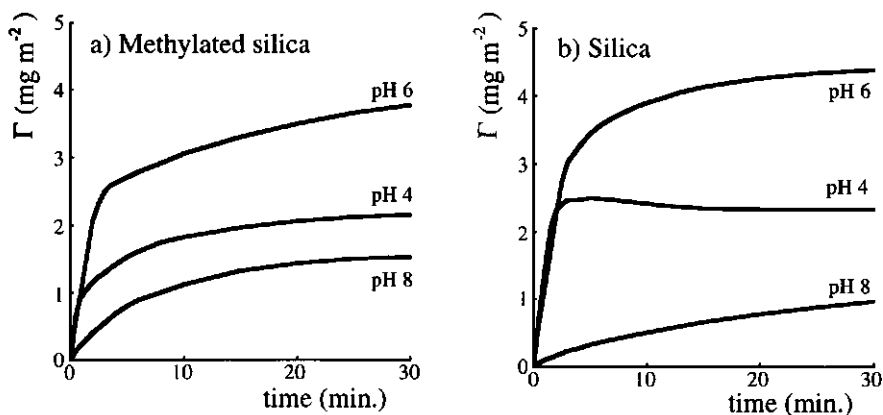

Fig. 4. The adsorption process of IgG 1B on methylated silica (a) and silica (b) at different pH values. The IgG concentration was 7.5 g m^{-3} in a 5 mM buffer solution.

The initial adsorption rates at pH 4 and 6 are more or less equal for both surfaces whereas at pH 8 the initial adsorption is retarded. Since the i.e.p. of IgG 1B is 5.8, these results imply that the initial adsorption is retarded when the protein is electrostatically repelled by the sorbent surface. At pH 8 the retardation is stronger for adsorption on the hydrophilic silica surface than for adsorption on the hydrophobic methylated surface. For adsorption under non-repelling electrostatic conditions (pH 4 and 6) the adsorbed amounts rise linearly in time till the $\Gamma(t)$-curves start to bend off. At this point the proteins in solution are repelled by the already adsorbed proteins. When comparing the adsorption curves on methylsilane at pH 4 and at pH 6 it can be observed that the $\Gamma(t)$-curve at pH 4 starts to deviate from the initial slope at much smaller adsorbed amounts. In this case, the range over which electrostatic repulsion is effective exceeds the dimensions of the protein molecule itself which could result in a relatively strong electrostatic repulsion between adsorbed proteins and proteins in solution. Furthermore, it is possible that at pH 4 the IgG molecules adsorb in a more expanded structure, thereby occupying a larger surface area.

When comparing the curves in Fig. 4 with those calculated in Fig. 2 one major difference can be noticed. Namely, in Fig. 2 all curves reach saturation adsorption within 30 minutes, whereas this was not found in the experiments. This difference can be ascribed to the repulsion between adsorbed proteins and proteins in solution. Another striking observation is the overshoot effect occurring upon adsorption on silica at pH 4. This overshoot can be explained assuming that a rapid initial adsorption is followed by slower structural and/or orientational changes which cause the IgG molecules to occupy a larger surface area thereby displacing pre-adsorbed molecules.

The adsorption of both IgGs, their corresponding $F(ab')_2$ and Fc fragments will be discussed more systematically below by considering subsequently the initial adsorption rates, the development of the curves towards saturation adsorption and the degree of desorption that occurs after replacement of the protein solution by a buffer solution.

4.4.2 Initial adsorption rate

The initial adsorption rates, $(d\Gamma/dt)_{t\to 0}$ for both IgGs and their $F(ab')_2$ fragments are shown in Fig. 5, whereas the initial adsorption rates for Fc are shown in Fig. 6. The plotted values of IgG and $F(ab')_2$ are averages ($N \geq 2$). The deviation from the average of one individual measurement never exceeded 0.2 mg m^{-2} min^{-1}. The initial adsorption rates for Fc were not duplicated.

The initial adsorption rate may be determined by two of the five subprocesses of the adsorption process depicted in Fig. 1, i.e., the protein flux towards the surface and/or the actual attachment. The transport of protein towards the surface is described by Eq. 4, which shows that the protein flux equals the protein concentration multiplied by a transport coefficient k. For IgG, the flux towards the surface was estimated to be 1.3 mg m^{-2} min^{-1}. The value of 1.3 mg m^{-2} min^{-1} corresponds to the maximum values of the initial adsorption rates found for IgG adsorption, as indeed observed, see Fig. 5. It strongly indicates that under conditions of maximum adsorption rate, i.e., electrostatic attraction irrespective of the type of sorbent surface and ionic strength, all protein molecules arriving at the sorbent surface do adsorb on it.
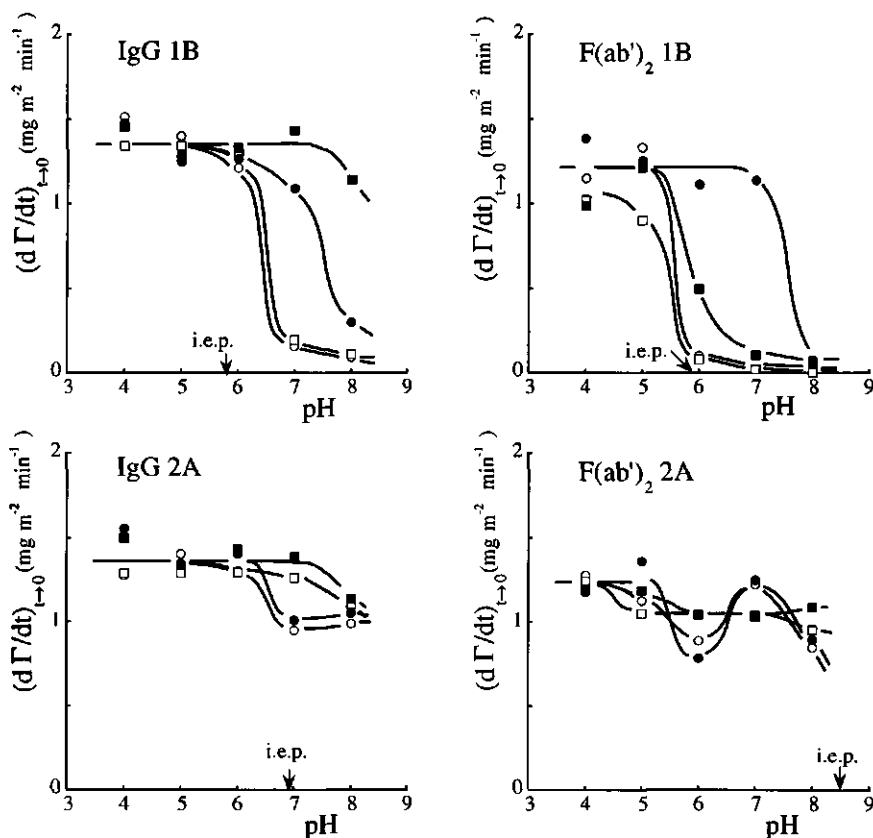

Fig. 5. Initial adsorption rates for IgG 1B and IgG 2A and their respective F(ab')2 fragments, adsorbed on methylated silica (closed symbols) and silica (open symbols) at ionic strength of 5 mM (● or ○) and 0.1 M (■ or ❑).

Hence, the adsorption rates under these conditions are limited by the diffusion of the proteins.

Under conditions of electrostatic repulsion, which prevail for IgG 1B and F(ab')$_2$ 1B beyond pH 6, a large reduction in the initial adsorption rate is observed in most cases. For IgG 2A, only a relatively small reduction in the initial adsorption rate is observed at pH values beyond the i.e.p. of 6.9. The modest retardation of the adsorption rate of IgG 2A can be ascribed to the presence of its F(ab')$_2$ part (i.e.p. = 8.5) which is still electrostatically attracted by the sorbent surface at these pH values.

The reduction in the initial adsorption rate is much stronger for adsorption on silica than on methylated silica. This suggests that electrostatic repulsion is compensated for by hydrophobic interactions. It is generally believed that hydrophobic interactions are short-ranged, which implies that the proteins have to be very close to the surface before hydrophobic interactions become effective. Therefore, the initial adsorption rates should be regarded as sticking probabilities.

The retardation factor of the adsorption rate (ß), introduced in Eq. 5, can be expressed in terms of an activation Gibbs energy for the deposition of proteins at the sorbent surface. For IgG 1B and F(ab')$_2$ 1B, these values are shown in Table 2. To compute these Gibbs energies, it was assumed that in the absence of an energy barrier, the initial adsorption rates for IgG and F(ab')$_2$ 1B equal the average of the adsorption rates at pH 4 and 5, viz., 1.40 and 1.15 mg m^{-2} min^{-1}, respectively. The values for the Gibbs energy of the barrier given in Table 2 are in the same range as those obtained for the adsorption of human plasma albumin at polystyrene surfaces under conditions of electrostatic repulsion [37].

In Table 2 it can be seen that at pH 7 and 8 the F(ab')$_2$ fragments experience Gibbs energy barriers which are about twice as high as those for the whole IgG molecule.

Table 2. The molar Gibbs energies (kJ mol^{-1}) of the deposition barriers as experienced by IgG and F(ab')$_2$ molecules arriving at the silica and the methylated surfaces, for different values of pH and ionic strength.

	silica				methylsilane			
	IgG 1B		F(ab')$_2$ 1B		IgG 1B		F(ab')$_2$ 1B	
	5 mM	0.1 M	5 mM	0.1 M	5 mM	0.1 M	5 mM	0.1 M
pH 6	0	0	5.9	6.6	0	0	0	2.0
pH 7	5.4	4.8	9.4	9.6	0.6	0	0	5.8
pH 8	6.7	6.2	11.7	14.9	3.8	0.5	6.6	7.1

At pH 6 the difference is even larger because at this pH the adsorption of IgG is essentially diffusion limited whereas the adsorption of the F(ab')$_2$ fragment is strongly retarded by electrostatic repulsion. This observation indicates that for IgG adsorption an additional driving force must exist which is related to the presence of the Fc part. This conclusion is supported by the initial adsorption rates of the Fc fragment, presented in Fig. 6. It is shown that these rates are barely affected by the hydrophobicity of the sorbent surface or the ionic strength.
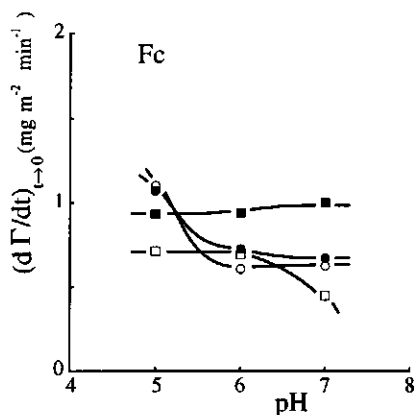

Fig. 6. Initial adsorption rates of Fc fragments, adsorbed on methylated (closed symbols) and silica (open symbols) surfaces at ionic strength of 5 mM (● or ○) and 0.1 M (■ or □). Note that the flux of Fc fragments towards the surface is lower than that of the IgG or F(ab')$_2$ due to the lower protein concentration in solution.

Even at pH 7 adsorption is not significantly retarded although the Fc fragment is electrostatically repelled by the surface. It is therefore concluded that all Fc fragment arriving at the sorbent surface attach. A similar difference between adsorption of Fab and Fc fragments was observed by Kawaguchi and co-workers [38] who reported that adsorption of Fc was less strongly influenced by electrostatic interactions than that of Fab. It is generally observed that proteins having a lower structural stability can adsorb onto hydrophilic surface under conditions of electrostatic repulsion whereas this is not the case for proteins with a higher structural stability [1]. Therefore, it is possible that the high adsorption rates of the Fc fragment under these conditions are caused by its relatively low structural stability.

Another result in Table 2 is that the ionic strength has no significant influence on the magnitude of the energy barrier for IgG adsorption on silica surfaces. At higher ionic strengths the electrostatic interactions are better screened. Therefore, it is expected that under conditions of electrostatic repulsion the adsorption rate would increase with increasing ionic strengths as is observed for adsorption of IgG 1B on the methylated surface. The ionic strength-independent adsorption on silica indicates that the adsorption rate is retarded due to the mere presence of charged groups on the surface and not by the long-range over which electrostatic interactions are effective.

Summarising we can say that adsorption in the initial stage is reduced if the IgG or F(ab')$_2$ fragments are electrostatically repelled from the surface. This repulsion is stronger for F(ab')$_2$ than for whole IgG molecule whereas the initial adsorption rate of the Fc fragment is not affected by electrostatic interactions. At methylated surfaces, the retardation is not strongly felt because adsorption is promoted by the contribution from hydrophobic interactions. The relatively strong repulsion experienced by the F(ab')$_2$ domain of the IgG molecule if adsorbed onto an electrostatically repelling hydrophilic surface could imply that an IgG molecule is preferentially adsorbed with its Fc domain onto the sorbent surface and that the Fab parts are pointed towards the solution. This is in line with suggestions made in the literature that IgG adsorption preferentially takes place by its Fc part [39,40,41].

4.4.3 Structural and/or orientational rearrangements of adsorbed proteins

Upon further adsorption a larger surface area becomes occupied and proteins closely approaching the surface experience a repulsion caused by interaction with already adsorbed proteins. In most cases, surfaces are filled gradually until plateau values are reached. However, in some experiments a reduction in the adsorbed amount was observed after longer adsorption times. This overshoot effect for protein adsorption was already reported by De Feijter and co-workers [24]. The overshoot was observed for adsorption of IgG 1B onto silica surfaces at pH values of 4 and 5, i.e., under conditions of electrostatic attraction. These adsorption curves are shown in Fig. 7a. At an ionic strength of 5 mM, the overshoot effects are clearly present, whereas at 0.1 M a combination of an overshoot effect followed by a slow increase in the adsorbed amount is observed. The latter results in an inflection point in the $\Gamma(t)$-curve. The overshoot suggests that proteins are squeezed out of the solid/liquid interface by neighbouring proteins which are optimising the interactions with the sorbent surface thereby increasing their occupied surface area. This means that IgG 1B molecules, adsorbing onto hydrophilic silica under

conditions of electrostatic attraction, change their orientation and/or structure in order to optimise their interaction with the sorbent surface. In Chapter 3 it is suggested that IgG molecules which are strongly electrostatically attracted by a hydrophilic sorbent surface can optimise their interaction by adapting a side-on orientation. It is also possible that the overshoot is the result of structural changes. However, the overshoot effect would then be expected to occur within a larger range of experimental conditions, for example, also at hydrophobic surfaces which are supposed to have a relatively large effect on the structure of the adsorbed proteins.
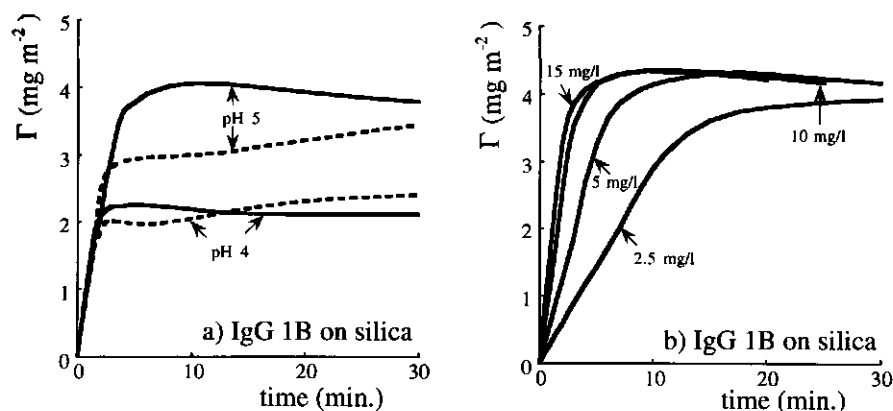

Fig. 7. Adsorption curves for which overshoot effects were observed. a) adsorption of IgG 1B on silica at different pH values at 5 mM (solid lines) and 0.1 M (dotted lines). b) overshoot effect for adsorption of IgG 1B on silica at pH 5 and 5 mM ionic strength as function of protein concentration.

Overshoot can only occur if the attachment process is faster than the rate at which orientational and/or structural rearrangements take place. The time-dependence of these processes is clearly demonstrated in Fig. 7b, in which adsorption curves of IgG 1B adsorbed on silica at pH 5 are shown as function of the protein flux towards the surface. The protein flux has been varied by changing the protein concentration (see Eq. 4). At high protein concentrations the surface is rapidly filled and a relatively strong overshoot effect is observed whereas at low protein concentrations (2.5 g m^{-3}) the overshoot is absent. Overshoot is not observed on methylated surfaces, apparently because on hydrophobic substrates reconformations take place fast as compared to the rate of supply.

The ongoing adsorption beyond the inflection point (Fig. 7a, dotted lines) implies that proteins continue to be squeezed out and that at the same time unoccupied surface area is

available for newly arriving proteins. It indicates that the protein molecules are not homogeneously distributed over the sorbent surface. This is consistent with atomic force microscopy studies of IgG adsorption, in which it was found that adsorbed IgG molecules display nucleation at a number of sites which, upon further adsorption, results in a homogeneous distribution [36,42]. When such an adsorption mechanism is followed it would be expected that the adsorption rate is enhanced after the first patches of adsorbed proteins are produced. Experimentally, this should be reflected in a sigmoidal shape of the $\Gamma(t)$-curve. As sigmoidal curves are not observed, it is concluded that if nucleation of proteins at the surface occurs, these nuclei do not enhance the adsorption rate.

4.4.4 Plateau values of adsorption

For both IgGs and their F(ab')$_2$ fragments, the amounts adsorbed after 30 minutes on the methylated and silica surfaces at ionic strengths of 5 mM and 0.1 M are shown in Fig. 8; the data for the Fc fragments are plotted in Fig. 9. Since only a limited amount of Fc fragments was available, Fc adsorption is followed for a period of only 10 minutes. Although in most experiments half of the surface is occupied within the first 5 minutes of the adsorption process, it often took at least 30 minutes to reach plateau values. This implies that in most cases the presented "plateau" values do not represent complete adsorption saturation.

For protein adsorption it is generally observed that maximum adsorption takes place around the i.e.p. of the protein [43]. This effect is related to the low net charge on the protein which results in a high structural stability and therefore in a relatively small area occupied per molecule. The structural stability of the protein decreases when the net charge on the protein rises. For IgG and F(ab')$_2$ adsorption this effect is enhanced owing to the increased distance between the two F(ab) parts [40,44]. In addition, there is a third factor of kinetic nature. When the proteins attain a relatively high charge density, the adsorption is retarded because of electrostatic repulsion between adsorbed proteins and proteins in solution. Because structural changes occur more easily at lower surface coverages, a slower adsorption process enhances the probability of larger structural changes.

The plateau values for the adsorption of IgG 1B are consistent with the trends that are normally observed for IgG adsorption. The maximum adsorbed amount is found at the i.e.p. of the IgG molecule. The plateau values are lower at both sides of the i.e.p. and this reduction is stronger under conditions of electrostatic repulsion between the protein and the sorbent. Furthermore, it can be noticed that the pH dependency of the plateau values

is much stronger at an ionic strength of 5 mM than at 0.1 M. The hydrophobicity of the surface only affects the plateau values beyond the i.e.p. of the proteins. Apparently, electrostatic repulsion between protein and sorbent is at least partly compensated for by hydrophobic interactions. The above mentioned observations indicate that the maxima arises due to interactions of electrostatic nature.
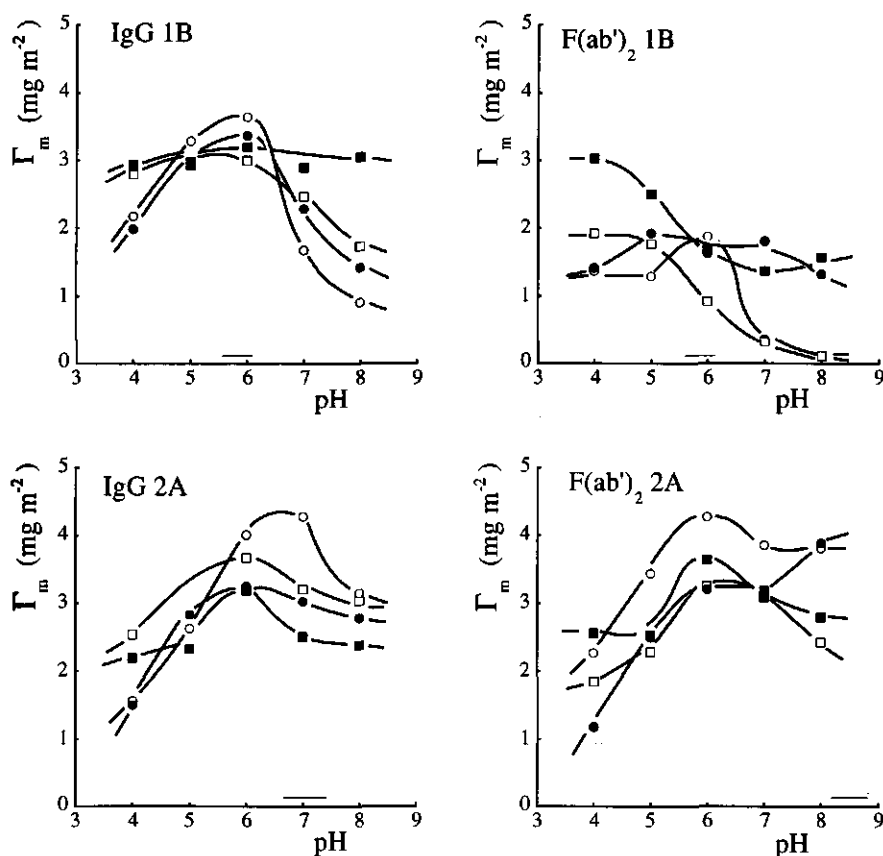

Fig. 8. Amounts of IgG 1B and IgG 2A and their respective F(ab')₂ fragments adsorbed after 30 minutes of incubation on methylated (closed symbols) and silica (open symbols) surfaces at ionic strength of 5 mM (● or ○) and 0.1 M (■ or □). The range of the i.e.p. values of the proteins are indicated by solid lines near the pH-axis of the respective figures.

For the plateau values of IgG 2A, similar observations are made although the pH region in which maximum adsorption is found has been broadened. The broadness of this peak is probably caused by the relatively large difference between the i.e.p. of the Fc part (6.0) and that of the Fab parts (8.5). The plateau values for adsorption of the F(ab')$_2$ 1B at low ionic strength also show maxima around the i.e.p. of the protein. At ionic strengths of 0.1 M a completely different pattern is observed. In this case, below the i.e.p. the plateau values increase when the pH decreases. The relatively large adsorbed amounts of F(ab')$_2$ 1B fragments at pH 4 may be related to configurational options that are not possible for whole IgG molecules. For example, it is possible that due to the high charge density the two Fab parts repel each other which results in a "cigar" shaped F(ab')$_2$ molecule. If some of these F(ab')$_2$ molecules adsorb in an end-on orientation, large adsorbed amounts would result.

The amounts of Fc adsorbed after 10 minutes, as shown in Fig. 9, are all around 2.2 mg m^{-2} except for Fc adsorbed on silica at pH 7 and 5 mM. The constant plateau-adsorption indicates that the adsorbed state is not much affected by the different protein-sorbent interactions, which is in agreement with earlier conclusions inferred from the initial adsorption rates.
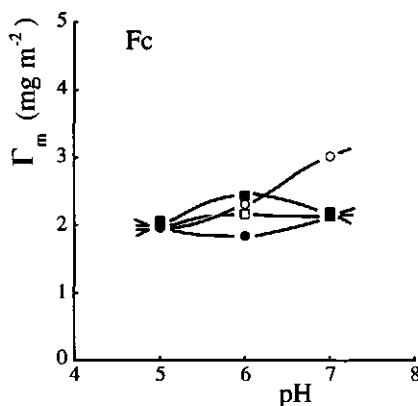
Fig. 9. Amounts of Fc fragments adsorbed after 10 minutes of incubation on methylated (closed symbols) and silica (open symbols) surfaces at ionic strength of 5 mM (● or ○) and 0.1 M (■ or □).

4.4.5 Desorption

After completing the adsorption, a buffer solution of the same pH and ionic strength was supplied to the sorbent surface, maintaining a constant flow. The amounts of IgG and F(ab')₂ fragments desorbed after 15 minutes are plotted in Fig. 10 and those of the Fc fragments in Fig. 11. The desorption after 15 minutes may be related to the average strength of the protein-sorbent interactions and/or to the presence of a fraction which is less strongly adsorbed.

Fig. 10. Desorption of IgG 1B, IgG 2A and their respective F(ab')₂ fragments after 15 minutes of buffer flow through the cell. The prote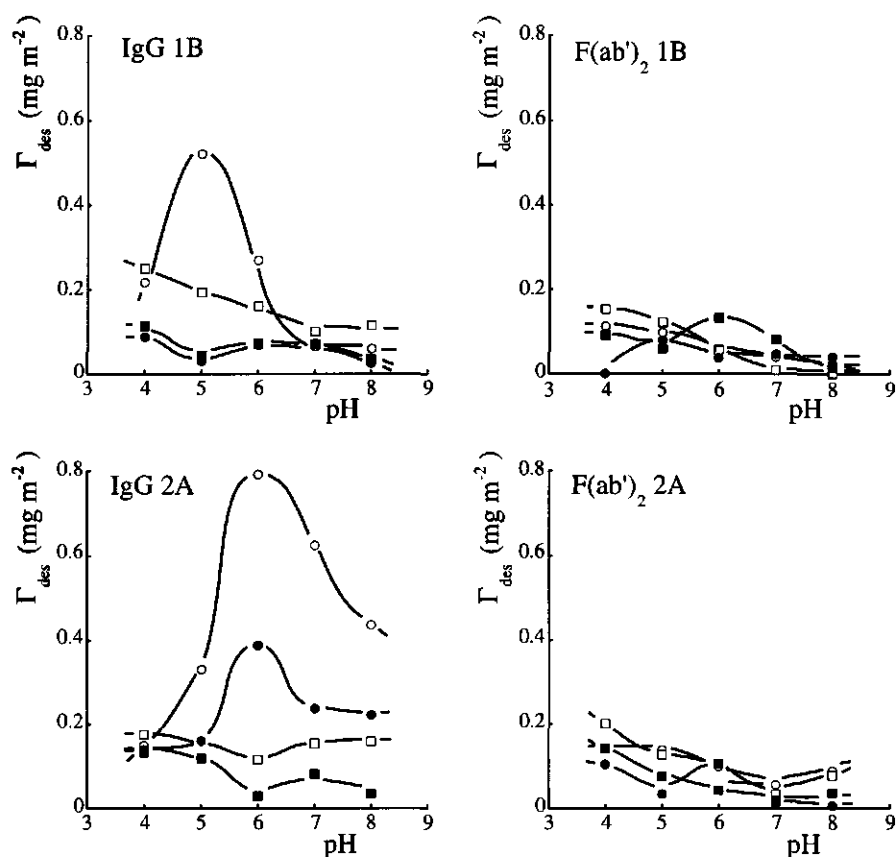ins were adsorbed on methylated (closed symbols) and silica (open symbols) surfaces at ionic strengths of 5 mM (● or ○) and 0.1 M (■ or ❑).

It is seen that under all conditions some desorption occurs which is in contrast to the often reported total irreversibility of IgG adsorption, as mentioned in the discussion of the adsorption process. The trend is that desorption from methylated surfaces is smaller than from silica surfaces, indicating that the proteins are more tightly bound to hydrophobic surfaces. In most of the cases, desorption remains below 0.1-0.2 mg m^{-2}, which is less than 10% of the amount originally adsorbed. A significant exception are the two IgGs adsorbed on silica at low ionic strength around their i.e.p. values. As such large desorptions were totally absent for the F(ab')$_2$ fragments, a weak bonding via the Fc fragment for part of the adsorbed molecules may be held responsible for the large IgG desorption. This is supported by the high extent of Fc desorption at identical experimental conditions (Fig. 11). For both IgGs, these relatively large desorbed amounts correspond to conditions in which also relatively large adsorbed amounts were reached (Fig. 8). This suggest that part of these high adsorbed amounts were attained because a fraction of the IgG molecules could be weakly bound by their Fc fragments. Furthermore, as a general trend, it is observed that desorption of F(ab')$_2$ decreases at higher pH values. Apart from the large desorbed amounts around the i.e.p. values of both IgGs, the same decrease in desorption at increasing pH can be observed for the IgGs. Since this effect does not show any relation with the i.e.p. values of the IgGs or F(ab')$_2$ fragments, it is inferred that this is related to the charge of the sorbent surface which increases at higher pH values. This might be an indication that the proteins are more strongly attached at a sorbent surface of higher charge densities.
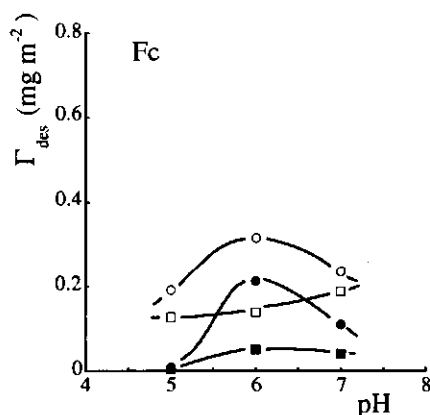

Fig. 11. Desorption of Fc fragments after 15 minutes of buffer flow through the cell. Fc fragments were adsorbed on methylated (closed symbols) and silica (open symbols) surfaces at ionic strengths of 5 mM (● or ○) and 0.1 M (■ or □).

4.5 Conclusions

As inferred from the initial adsorption rates, IgG molecules and their $F(ab')_2$ fragments experience a Gibbs energy barrier when adsorbing under conditions of electrostatic repulsion to a hydrophilic silica surface. Such a barrier is barely felt at the hydrophobic methylated surfaces. The magnitude of the Gibbs energy barrier is about twice as high for the $F(ab')_2$ fragments than for the whole IgG molecule, whereas Fc adsorption is not noticeably influenced by variation in protein-sorbent interactions. The conclusion that the $F(ab')_2$ part is repelled by the sorbent surface, suggests that the whole IgG molecule is preferentially adsorbed by its Fc fragment. A practical consequence is that these adsorption conditions allow the Fab parts to be directed towards the solution where they are accessible for antigen binding. Maximum adsorption for IgGs is found around their i.e.p. values. These maxima are less strongly pronounced at higher ionic strengths and/or at increasing hydrophobicity of the sorbent surface, indicating that they are determined by interactions of electrostatic nature. As judged from desorption studies, proteins are more tightly bound to hydrophobic methylated surfaces than to hydrophilic silica surfaces. Furthermore, it is inferred that at silica surfaces, under conditions of low ionic strength, relatively large adsorbed amounts of IgG are obtained around their i.e.p. because a fraction of the IgG molecules is able to attach weakly to the sorbent surface by their Fc fragments.

4.6 References

1   W. Norde, and J. Lyklema, *J. Biomater. Sci. Polym. Edn.*, **2** (1991) 183.

2   C.A. Haynes, and W. Norde, *Colloids Surfaces B: Biointerfaces*, **2** (1994) 517.

3   M.E. Soderquist, and A.G. Walton, *J. Colloid Interface Sci.*, **75** (1980) 386.

4   A.V. Elgersma, R.L.J. Zsom, J. Lyklema, and W. Norde, *J. Colloid Interface Sci.*, **152** (1992) 410.

5   A. Kondo, F. Murakami, and K. Higashitani, *Biothechnol. Bioeng.*, **40** (1992) 889.

6   W. Norde, and J.P. Favier, *Colloids Surfaces*, **64** (1992) 87.

7   F.V. Bright, T.A. Betts, and K.S. Litwiler, *Anal. Chem.*, **62** (1990) 1065.

8   M.L. Yarmush, X. Lu, and D.M. Yarmush, *J. Biochem. Biophys. Methods*, **25** (1992) 285.

9   A.B. Pereira, A.N. Theofilopoulos, and F.J. Dixon, *J. Immunol.*, **25** (1980) 763.

10   J.W. Corsel, G.M. Willems, J.M.M. Kop, P.A. Cuypers, and W.Th Hermens, *J. Colloid Interface Sci.*, **111** (1986) 544.

11   M. Malmsten, *Colloids Surfaces B: Biointerfaces*, **3** (1995) 297.

12   B.W. Morrissey, L.E. Smith, R.R. Stromberg, and C.A. Fenstermaker, *J. Colloid Interface Sci.*, **56** (1976) 557.

13   L. van Straaten, and N.A. Peppas, *J. Biomater. Sci. Polym. Edn.*, **2** (1991) 113.

14   F.-N. Fu, M.P. Fuller, and B.R. Singh, *Appl. Spectroscopy*, **47** (1993) 98.

15   C-G. Gölander, Y-S. Lin, V. Hlady, and J.D. Andrade, *Colloids Surfaces*, **49** (1990) 289.

16   D. Kim, W. Cha, and R.L. Beissinger, *J. Colloid Interface Sci.*, **159** (1993) 1.

17   P. van Dulm, and W. Norde, *J. Colloid Interface Sci.*, **91** (1983) 248.

18   W. Norde, and E. Rouwendal, J. *Colloid Interface Sci.*, **139** (1990) 169.

19   J.C. Dijt, M.A. Cohen Stuart, and G.J. Fleer, *Adv. Colloid Interface Sci.*, **50** (1994) 79.

20   P. Frantz, and S. Granick, *Langmuir*, **8** (1992) 1176.

21   L. Bousse, S. Mostarshed, B. van der Shoot, N.F. de Rooij, P. Gimmel, and W. Göpel, *J. Colloid Interface Sci.*, **147** (1991) 22.

22   O.H. Lowry, N.J. Rosebrough, A.L. Farr, and R.J. Randall, *J. Biol. Chem.*, **193** (1951) 265.

23   AKZO, Eur. Patent Application No. 88200230.6.

24   J.A. de Feijter, J. Benjamins, and F.A. Veer, *Biopolymers*, **17** (1978) 1759.

25   G.E. Perlmann, and L.G. Longsworth, *J. Am. Chem. Soc.*, **70** (1948) 2719.

26   W.N. Hanson, J. *Optical Soc. Am.*, **58** (1968) 380.

27   T. Dabros, and T.G.M. van de Ven, *Colloid Polym. Sci.*, **261** (1983) 694.

28   H. Nygren, and M. Stenberg, *J. Colloid Interface Sci.*, **107** (1985) 560.

29   D. Brune, and S. Kim, *Proc. Natl. Acad. Sci. USA*, **91** (1994) 2930.

30   W. Norde, F. MacRitchie, G. Nowicka, and J. Lyklema, *J. Colloid Interface Sci.*, **112** (1985) 447.

31   B.D. Fair, and A.M. Jamieson, *J. Colloid Interface Sci.*, **77** (1980) 525.

32   W. Norde, and A.C.I. Anusiem, *Colloids Surfaces*, **66** (1992) 73.

33   F. Galisteo-González, J. Puig, A. Martín-Rodriguez, and J. Serra-Domènech, *Colloids Surfaces B: Biointerfaces*, **2** (1994) 435.

34   A.V. Elgersma, R.L.J. Zsom, W. Norde, and J. Lyklema, *Colloids Surfaces*, **54** (1991) 89.

35   S. Oscarsson, *J. Colloid Interface Sci.*, **165** (1994) 402.

36   J.N. Lin, B. Drake, A.S. Lea, P.K. Hansma, and J.D. Andrade, *Langmuir*, **6** (1990) 509.

37   W. Norde, *Croat. Chim. Acta*, **56** (1983) 705.

38   H. Kawaguchi, K. Sakamoto, and Y. Ohtsuka, *Biomaterials*, **10** (1989) 225.

39   J. Serra, J. Puig, A. Martín, F. Galisteo, MaJ. Gálvez, and R. Hidalgo-Alvarez, *Colloid Polym. Sci.*, **270** (1992) 574.

40   T. Suzawa, and H. Shirahama, *Adv. Colloid Interface Sci.*, **35** (1991) 139.

41   I. Vikholm, and O. Teleman, *J. Colloid Interface Sci.*, **168** (1994) 125.

42   D.A. Cullen, and C.R. Lowe, *J. Colloid Interface Sci.*, **166** (1994) 102.

43   W. Norde, *Adv. Colloid Interface Sci.*, **35** (1986) 267.

44   P. Bagchi, and M. Birnbaum, *J. Colloid Interface Sci.*, **83** (1981) 460.

5 Changes in the Secondary Structure of Adsorbed IgG and F(ab')$_2$ Studied by FTIR Spectroscopy

The purpose of the present study is to find a quantitative relationship between the adsorption behaviour and the secondary structure of proteins. The adsorption of two monoclonal IgGs which differ in isoelectric point and their corresponding F(ab')$_2$ fragments is followed in time. The proteins are adsorbed on hydrophilic silica and on hydrophobic methylated surfaces at different values of pH and ionic strength. The adsorption behaviour is studied by measuring FTIR spectra of the adsorbed proteins. The adsorbed amount is related to the integrated area of the amide II region of the spectrum. The secondary structure of the adsorbed proteins is evaluated by analysing the second derivatives of the amide I region. Quantitative information on the secondary structure is obtained by applying a fitting procedure which assumes the absorption bands for the different structural components to be Lorentzian shaped. The results show that for IgG the adsorbed amounts decrease with an increasing net charge density on the protein. This decrease is correlated to a reduction in the β-sheet content which suggests that IgG molecules adsorb in a less compact conformation. The adsorption-induced reduction in the β-sheet content is larger at hydrophobic methylated surfaces than at hydrophilic silica surfaces. The dependence of the amount of structural elements on the pH diminishes at higher ionic strength. F(ab')$_2$ fragments contain a higher fraction of β-sheet than whole IgG molecules and these fractions are less strongly influenced by the adsorption conditions. Therefore, it can be concluded that the F(ab')$_2$ fragments have a higher structural stability towards adsorption than whole IgG molecules.

5.1 Introduction

Adsorption of immunoglobulin G (IgG) to solid surfaces is of great interest for biomedical applications, such as immunoassays and biosensors. The desire to control and manipulate protein adsorption in these applications requires a detailed understanding of

the mechanism of adsorption. One important aspect of adsorption is the change in the environment of the protein which may result in conformational changes [1,2,3] and, in turn, may induce an alteration in the biological activity. It has also been reported that adsorbed IgG molecules become more tightly bound as the contact time with the sorbent surface increases. This observation was ascribed to slow structural rearrangements within the IgG molecules in order to optimise interactions with the sorbent surface [2,4,5]. These structural changes were more pronounced at lower surface coverages [1,6]. The purpose of the present study is to relate the secondary structures of adsorbed IgGs and their $F(ab')_2$ fragments to the adsorption behaviour under various conditions of pH, hydrophobicity of the surface, ionic strength, and incubation time. Adsorption of $F(ab')_2$ is investigated in order to obtain information about the influence of these domains of the IgG molecule on the adsorption process. This is of practical importance since the Fab parts contain the antigen binding sites. Consequently, in immunological tests the Fab parts of the adsorbed IgG molecules should retain their biological activity to bind antigens and the Fab parts should be oriented in such a way as to be accessible to antigens.

The secondary structure of proteins may be studied using infrared spectroscopy. Spectra of adsorbed protein layers can accurately be obtained by using the high sensitivity of the Fourier Tranform Infrared (FTIR) method in combination with attenuated total reflectance (ATR). The ATR/FTIR technique has proven its value in the quantitative analysis of secondary structure elements of adsorbed proteins. Examples include studies in which the secondary structure of proteins were subjected to different sorbents [7], various solvents [8], and temperature variations [9]. Other techniques for studying the protein structures in solution or at interfaces are NMR, circular dichroism (CD) and time-resolved fluorescence. Unfortunately, NMR is rather time-consuming and only suitable for studying small proteins.

Table 1. The amounts of the structural components of several IgGs and the Fab fragments as determined by different methods.

protein	method	ß-sheet	unordered	bends/turns	α-helices	reference
Fc	X-ray*	45%	26%	21%	7%	[10]
Fab	X-ray*	47%	23%	28%	2%	[11]
Fab	X-ray	50-60%				[12]
IgG	FTIR	76%			9%	[13]

* As calculated by using the DSSP program described by Kabsch and Sander [14].

Fluorescence spectroscopy is very sensitive to structural changes, however the information obtained is restricted to the micro-environment of the chromophores. CD studies of adsorbed proteins require a high protein/sorbent ratio in order to obtain the same sensitivity as with FTIR [15]. More detailed information on the secondary structure of proteins may be obtained by X-ray crystallography, but the inherent crystallised state of the proteins does not allow for a study of environmentally induced structural changes. In Table 1, the fractions of structural elements as obtained by various methods are summarised and it can be concluded that IgG largely consists of ß-sheet structures whereas the α-helix content is relatively small.

In the present study the amide I and amide II absorption regions are evaluated. The two absorption regions arise from two chemical groups of the protein backbone. Part of a typical infrared spectrum of IgG is shown in Fig. 1. The amide I band primarily represents the C=O stretching vibrations of the peptide bonds groups (coupled to the in-plane NH bending and C-N stretching modes). The frequency of this vibration depends on the nature of the hydrogen bonding in which the C=O group is involved. This, in turn, is highly sensitive to the secondary structure adopted by the polypeptide chain, e.g. α-helices, ß-sheets, turns and disordered structures [16]. Hence, structural analyses are obtained from the amide I region. In principle, it is also possible to utilise the amide II and amide III regions for structural analysis. However, the sensitivity of the amide II region for the polypeptide conformation is small. Therefore, the area of this region is only used to quantify the adsorbed amount.
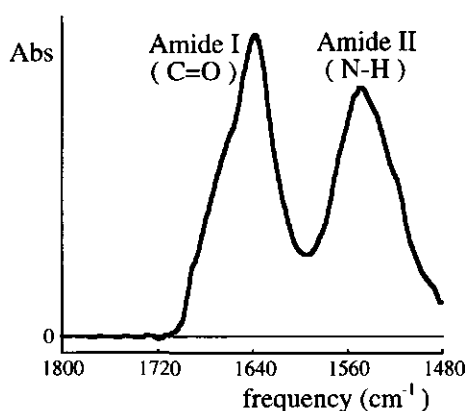

Fig. 1. Infrared absorption spectrum of the amide I and II region of IgG 1B adsorbed at silica, measured after one hour, pH 5, ionic strength 5 mM.

The use of the amide III region (1100-1500 cm^{-1}) for determination of secondary structure is troublesome because these bands are rather weak. Moreover, in our study a silicon crystal was used which is opaque in the amide III region.

The structural analysis is complicated because the absorption bands of the different structural components almost coincide in the amide I region. Therefore, it is necessary to improve the resolution of the spectra. Unfortunately, this cannot be accomplished by increasing the instrumental resolution because resolving overlapping bands is limited by the natural bandwidth. However, mathematical procedures are available which improve the discrimination between the individual bands. Options for resolution enhancement are Fourier self-deconvolution and second derivative calculations [17]. Both methods have successfully been applied in quantitative analyses of the secondary structure of several proteins [13,18]. It should be emphasised that the resolution of the spectra is enhanced at the expense of a decreased signal to noise ratio. In the present study, the secondary structure is evaluated by analysing the second derivatives of the amide I absorption band.

5.2 Materials and methods

Proteins

The two monoclonal immunoglobulins G, IgG 1B and IgG 2A, were both mouse-anti-hCG (human Chorionic Gonadotropin) from isotype IgG-1. These IgGs, which were kindly donated by Organon Teknika (Boxtel, the Netherlands). F(ab')$_2$ fragments were produced by cleavage with pepsin, as described in Chapter 2.3.2. The isoelectric point (i.e.p.) of both IgGs and their fragments were determined using isoelectric focusing (IEF), using PhastGel media, pH range 3-9 and silver staining (PhastSystem, Pharmacia). In Table 2, the major bands in the respective isoelectric pH-regions are given in brackets. The Fc fragments of both monoclonals have an i.e.p. of 6.1. For both IgGs concentrations were established spectroscopically using an extinction coefficient of 1.45 cm^2 mg^{-1} at 280 nm.

Table 2. Isoelectric points of the monoclonals IgG 1B and IgG 2A and their F(ab')$_2$ fragments.

protein	IgG 1B	F(ab')$_2$ 1B	IgG 2A	F(ab')$_2$ 2A
i.e.p.	5.6-6.0 (5.8)	5.6-6.1 (5.9)	6.7-7.4 (6.9)	8.2-8.8 (8.5)

The extinction coefficients for the $F(ab')_2$ fragments were determined colorimetrically according to the Folin-phenol method of Lowry and co-workers [19] using the corresponding IgGs as the standards. This resulted in an extinction coefficient of 1.45 cm^2 mg^{-1} for $F(ab')_2$ 1B and 1.48 cm^2 mg^{-1} for $F(ab')_2$ 2A.

Surfaces

In the present study a hydrophilic silica surface and a hydrophobic methylated surface were used, both based on a cylindrical internal reflectance (CIRcle) crystal made of silicon (Spectra-Tech Inc.). This crystal has a silica surface layer. Prior to each experiment, the crystal was cleaned by placing it in a chamber with a constant oxygen flow, while the surface was irradiated by UV-light for 40 minutes. In this way organic contaminants were oxidised and a homogeneous oxide layer was produced with a minimum of surface damaging [20]. Hydrophobic methylated surfaces were obtained by immersion of the crystal in 0.3 % (v/v) dichlorodimethylsilane in 1,1,1-trichloroethane for 30 minutes. After silanisation the crystal was flushed consecutively with trichloroethane and ethanol. The contact angles of a sessile drop of water for the methylated and the silica surface were 90° and 7°, respectively. The silica surface is negatively charged due to the hydrolysed silanol groups. It has been reported that the zeta-potential at an ionic strength of 0.01 M NaCl is around -20 mV at pH 4 and that this value gradually decreases to ca. -55 mV at pH 8 [21]. The methylated surface also contains some negative charges due the presence of unsilanised silanol groups. Streaming potential measurements, performed as described by Norde and Rouwendal [22], showed that at pH 7 and an ionic strength of 0.01 M the zeta potential of a methylated surface was -35 mV which is less than 33% lower than the zeta potential of a silica surface under the same conditions of pH and ionic strength.

FTIR-measurements

Spectra are collected with a model 1725X FTIR spectrometer (Perkin-Elmer). The protein spectra are detected with a nitrogen cooled mercury cadmium telluride (MCT) detector at a resolution of 2 cm^{-1}, using a normal Norton-Beer apodisation function. The FTIR spectrometer is continuously purged with air which was freed from water and carbon dioxide vapour. Both the untreated and methylated crystal were rinsed with water and dried in a jet of nitrogen gas before placing them in a flow cell (Spectra-Tech Inc.) with cell loading tubes outside the compartment. The solutions are injected in the flow cell using the pump of an FPLC-system (Pharmacia). After the crystal has been placed in the flow cell, the cell is filled with a buffer solution and aligned. Two hours after the sample compartment is closed, a background spectrum is measured which is the average

of 500 scans. During this time a buffer solution flows through the cell. The adsorption experiment starts after the flow cell has quickly been filled with a protein solution by means of a protein flow of 1 ml min^{-1} for five minutes. In such an experiment, the adsorption is monitored during six hours at 16 different points in time. Each point in time consists of the average of 300 scans and requires about nine minutes. During the first two hours, a spectrum is recorded every ten minutes and over the next four hours one spectrum is taken every hour. During the experiment, the protein concentrations remain constant due to a constant flow (0.1 ml min^{-1}) of the protein solution. All experiments are performed in a 5 mM buffer solution. At pH 4 and 5 an acetate buffer, and at pH 6, 7, and 8 a phosphate buffer is used. Both buffers are prepared from sodium salts and adjusted to the desired pH with NaOH and HCl. Ionic strengths higher than 5 mM are obtained by adding NaCl. Water is purified by reverse osmosis and subsequently passed through a SuperQ system (Millipore). All chemicals are of p.a. grade and used without further purification. Unless otherwise stated, the experiments are performed using protein concentrations of 50 g m^{-3} and ionic strengths of 5 mM.

The amounts adsorbed are quantified by applying the method as described by Sperline and co-workers. [23] which is based on the relative absorption intensities of the proteins in solution and adsorbed at the interface. This method requires an input of the penetration depth of the evanescent wave, which in turn is determined by the wavelength of light, the angle of incidence, and the refractive indices of the silicon crystal and the solution. The angle of incidence and the number of reflections are determined as described by Sperline and co-workers [24] and resulted in values of 41° and 6.68, respectively. The refractive indices of silicon and the solution are 3.80 and 1.33, respectively. The calculation of the penetration depth at the maximum of the amide II band at a wavenumber of 1545 cm^{-1} resulted in a value of 4.87 10^{-5} cm.

5.3 Second derivatives and band fitting

Second derivative spectra

The resolution-enhanced infrared spectra allow identification of the various secondary structures present in the adsorbed proteins. Assuming a Lorentzian shape of line broadening, the intensity of an infrared absorption peak $A(\upsilon)$ can be expressed as

$$A(\upsilon) = A_0\gamma^2 \Big/ \Big[\gamma^2 + (\upsilon - \upsilon_0)^2\Big]$$

(1)

where A_0 is the maximum absorbance of the band, υ_0 is the frequency of the maximum, and γ is the half-width at half-height. An example of a Lorentz curve and its second derivative is shown in Fig 2. In this Figure it can be seen that the maximum frequency position of an individual band in the original absorption spectrum is located at the position of a minimum in the second derivative. Second derivative spectroscopy has proven to be a valuable tool for accurate determination of the frequency of the different absorption bands [18,25,26]. In addition to the frequency position, information on the width and the maximum absorption intensity of the individual bands can be obtained from the second derivative as is shown in Fig. 2b.
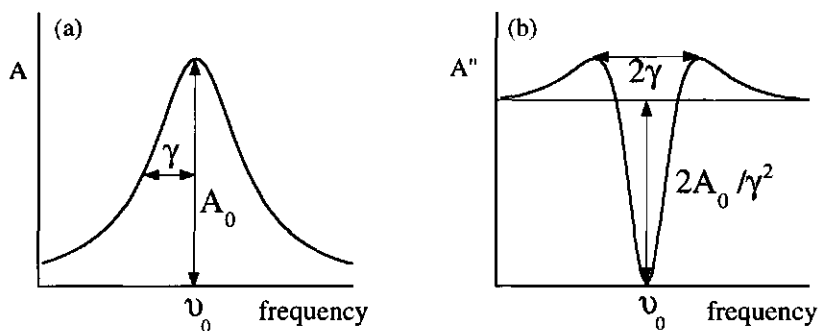

Fig. 2. A Lorentz curve (a) and its second derivative (b). The parameters describing the shapes of the curves (Absorption intensity A, intensity at the maximum A_0, bandwidth 2γ, and frequency position υ_0) are depicted in the figures.

Thus, all three parameters (υ_0, γ and A_0) describing a Lorentz curve can be extracted from the second derivative. However, accurate determination of the bandwidths (2γ) from the maxima in the second derivative is complicated due to the presence of neighbouring peaks. Consequently, the determination of the absorption intensity (A_0) from the magnitude of the minimum is even less accurate because of its proportionality to the square of the bandwidth. Despite the above mentioned inaccuracies, the obtained parameters (υ_0, γ, A_0) can successfully be used as input parameters for a fitting procedure which fits the summation of the absorption bands of the individual structural components to the original infrared spectrum. Prior to this procedure, some adjustments to the absorption spectrum have to be made. First, a problem inherent in measuring proteins in aqueous solutions is the strong and broad water absorption band around 1640 cm^{-1}. In practise, the intense absorption band of the solution is largely accounted for by

subtracting the protein absorption spectra with a background spectrum of the buffer solution. A scaling factor was used in such a way that the spectral region from 1800 to 1720 was flat. Second, traces of water vapour are present in the cell compartment which result in sharp absorption peaks. Water vapour peaks are removed in a similar fashion by subtracting water vapour spectra which are obtained in blank experiments. The scaling factor for this subtraction was based on the intensity of the water vapour absorption peaks at 1844, 1792 and 1772 cm^{-1}. Third, the overlap between the amide I and amide II bands has to be resolved. As the analysis is based on the amide I region, the small part of absorption due to the NH groups in the amide I region is subtracted, assuming a Lorentzian shape for the amide II band. After eliminating the interfering absorption due to water and the NH-band, an absorption band of the amide I region remains. Before calculating a second derivative, noise must be suppressed because small fluctuations in absorption intensity are magnified in the derivatives. Most noise originates from inadequate elimination of water vapour. The noise is suppressed by performing a Gaussian filtering (smoothing algorithm) over a frequency range of 35 cm^{-1} [27].

Fitting procedure

Most of the peak positions (v_0) were easily found in the second derivative spectra and the respective bandwidths (γ) and maximum absorption intensities (A_0) could be calculated. However, the peak positions of the ß-structure (~1636 cm^{-1}) and the random structure (~1645 cm^{-1}) were sometimes difficult to distinguish. This difficulty arose when either one of the two peaks was relatively large so that the other peak showed up as a shoulder instead of a separate peak in the second derivative. As both ß-sheet and random structures should be present, a peak for the ß-sheet or the random structure was added if one of these peaks was represented by a shoulder instead of a separate peak. The shape of the additional Lorentz peak was then based on earlier results; v_0 was set at 1634 cm^{-1} or 1645 cm^{-1} for the ß-sheet or random structure, respectively. In either case the bandwidth (2γ) was set to 16 cm^{-1}, which was close to the average value of the bandwidths normally found for these absorption peaks. A_0 was chosen to be smaller than the lowest obtained intensities, relative to the total absorption intensity.

In general, bandwidths of the structural components are in the range of 8-28 cm^{-1} [13,28]. In some second derivative spectra, peaks appeared with very small bandwidths ($2\gamma < 7$ cm^{-1}). It was assumed that these small fluctuations originated from noise. To avoid assignment of absorption peaks to these physical anomalies, peaks with bandwidths smaller than 7 cm^{-1} are ignored and incorporated in the nearest absorption peak.
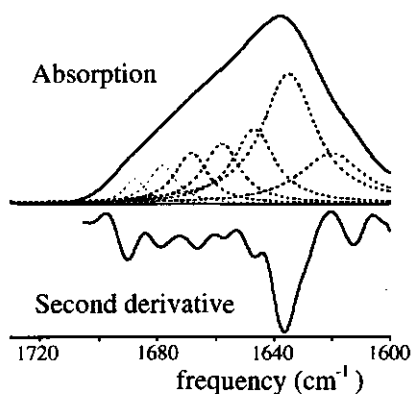
Fig. 3. Absorption spectrum of the amide I region of IgG 1B adsorbed at pH 5 after one hour of adsorption and its second derivative. The calculated individual absorption bands of the structural components are shown in dashed lines.

Before starting the fitting procedure, the obtained depths of the minima in the second derivative spectrum and, subsequently, the calculated maximum intensities were corrected for the interference of all neighbouring peaks. The curve fitting is performed by stepwise iterative adjustment towards a minimum root-mean-square error of the different parameters determining the shape and position of the absorption peaks. The following procedure was followed: (1) The calculated maximum intensities were iterated first because these were the least accurate. (2) Secondly, the intensities and frequency positions were fixed and the bandwidths were iterated. (3) Then, only the frequency position remained fixed and all other parameters were iterated. (4) Finally, all variables were iterated. An example of an original spectrum, its second derivative, and the individual absorption peaks obtained in this way are shown in Fig. 3.

Peak assignment to structural elements

The second derivatives of the spectra reveal that the amide I band consists of 6 major components which were found in all spectra. In some spectra one or two additional peaks were found, one around 1655 cm⁻¹ and the other in the low frequency region around 1612 cm⁻¹. The corresponding frequencies are listed in the head-row of Table 3. Although the peaks showed some variation in characteristic frequency, the deviation from the average value was in most cases less than 2 cm⁻¹. The assignment of the absorption peaks to secondary structure elements was partly based on other studies in which infrared spectra were analysed for proteins of known secondary structure and partly based on more

fundamental information about the frequency positions as obtained from theoretical calculations of the normal vibration frequencies for ß-sheets and α-helices. In Table 3 the absorption frequencies as found in our analyses are given, followed by a short summary of assignments to comparable frequencies reported in the literature.

The amide I components associated with ß-strands are located in the low frequency range between 1620 and 1640 cm^{-1}. In the analysed spectra one major peak was found at 1636 cm^{-1} together with a smaller component in the lower frequency region around 1623 cm^{-1}. The major peak of 1636 cm^{-1} is generally ascribed to anti-parallel ß-sheets and it has a bandwidth of ca. 22 cm^{-1}. The smaller component at 1623 cm^{-1} is relatively broad with a bandwidth of ca. 28 cm^{-1}. This peak may originate from subtle differences in hydrogen bonding patterns in the anti-parallel ß-strands or from parallel ß-sheets [18,28]. In some spectra a small peak is found at even lower frequencies, visualised around 1612 cm^{-1}. This peak is ascribed to absorption by the side-chains of tyrosine and arginine [29] and therefore ignored in further quantification of the different structural components. In most FTIR studies the spectra show a band close to 1645 cm^{-1} which is generally assigned to "unordered" segments. In the present study this component is located around 1646 cm^{-1} with a bandwidth of ca. 18 cm^{-1}. A component around 1654 cm^{-1} is frequently observed and associated with α-helices. For IgG this structural element is not significantly present as demonstrated in other studies (see Table 1). Accordingly, this peak is absent in some of the measured spectra. As absorption peaks of turns are located in the high frequency region [30], the peaks located at 1664 and 1688 cm^{-1} are assigned to turns. As indicated in Table 3, a high frequency component around 1676 cm^{-1} has been assigned to ß-sheet structure although this assignment has not unequivocally been established.

Table 3. Assignments of the amide I frequencies to secondary structure elements. Comparison with other FTIR studies of IgG and theoretical calculations. The structural elements are abbreviated as U = unordered, ß = ß-sheets, α = α-helices and T = turns.

	1623±2	1636±1	1646±3	1654±2	1664±2	1676±2	1688±2
IgG (D$_2$O)[13]	ß (1624)	ß (1637)	U (1645)	α (1651)		ß (1672)/ T (1670)	T (1683, 1688, 1694)
IgG (H$_2$O)[26]		ß (1637)			U/T (1665)		U/T (1685)
IgG (on Ge)[8]	ß (1629)	ß (1639)	U (1651)		U (1663)	ß/T (1674)	T (1690)
calculated[31]		ß (1630)		α (1655±2)			ß (1695, weak)

This assignment was based on the relation of the magnitude of the 1676 cm^{-1} peak with the ß-sheet content [18]. However, in our study no correlation was found between the integrated area of the low frequency ß-sheet peaks and the 1676 cm^{-1} peak which was low (ca. 7 % of the total amide I intensity) and constant. Therefore, this band was assigned to turns rather than to ß-sheets.

The structural components were quantified by the integrated areas of the respective peaks. This implies that the effective absorbtivities were assumed to be equal. This assumption was validated in an extensive study using 21 proteins in which a remarkably good correlation was found between estimates for secondary structures as obtained from infrared analysis and X-ray data, respectively [13]. In the present study the secondary structure of adsorbed IgG and F(ab')₂ is mainly focused on the amount of ß-sheet structure. This because the ß-sheet structure is predominantly present in IgG molecules and the assignment of ß-sheet structure is univocally related to the absorption band at 1636 and 1623 cm^{-1}.

5.4 Results and discussion

5.4.1 General trends in the adsorption behaviour

Adsorbed amounts

First some general trends for the adsorption kinetics, (Γ(t)) will be discussed for a typical set of adsorption curves of IgG 1B and F(ab')₂ 1B on silica and methylated surfaces, as shown in Fig. 4. The results for IgG 1B adsorbed on silica are averages of duplicated measurements and the deviation from the average value may amount to ca. 10%. The reproducibility in the adsorbed amounts is poor due to the inaccuracies of the alignment which has to be adjusted before each measurement. A small variation in alignment will lead to a difference in pathlength. Changes in temperature can also cause slight changes in pathlength [32].

The adsorption curves in Fig. 4 show a similar pattern to those obtained with reflectometry (Chapter 4), although the adsorption rates as measured with FTIR are lower. This is caused by the difference in which the proteins are supplied to the sorbent surface. It is seen that for IgG 1B and F(ab')₂ 1B adsorbed at the hydrophilic silica surface the initial adsorption rates are low at pH 7 and 8. This is in agreement with the observation, made in Chapter 4, that adsorption at hydrophilic surfaces is retarded under conditions of electrostatic repulsion. The adsorption retardation is smaller for proteins with a lower structural stability because they are able to compensate electrostatic repulsion by

structural changes [33]. These structural changes promote adsorption because a loss in secondary structure results in a gain in conformational entropy of the protein. Furthermore, the higher flexibility in the protein structure may lead to an optimisation of the interactions between the proteins and the sorbent surface. In Fig. 4, it can be observed that under conditions of electrostatic repulsion the adsorption rate of F(ab')$_2$ 1B is lower than that of whole IgG although the i.e.p. values of both proteins are around pH 6. Accordingly, this might be caused by a stronger structural stability of the F(ab')$_2$ fragments compared to that of the whole IgG molecules.
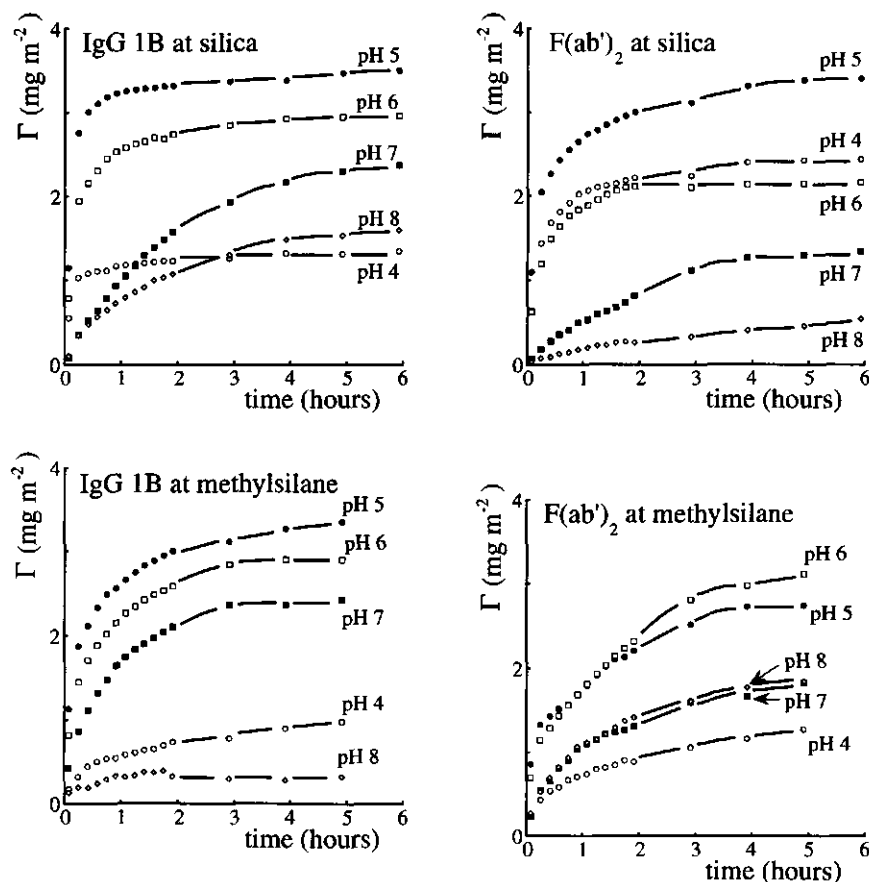

Fig. 4. Adsorption of IgG 1B and F(ab')$_2$ 1B on silica and methylated surfaces at different pH values as depicted in the figures.

On the hydrophobic methylated surfaces it is expected that adsorption is promoted due to hydrophobic interactions. For $F(ab')_2$ 1B adsorbed under conditions of electrostatic repulsion (pH > 6) this leads to higher adsorbed amounts on methylated surfaces than on silica. The opposite is observed for IgG 1B where the adsorbed amount at pH 8 is lower on methylsilane than on silica. At this pH value, IgG 1B and $F(ab')_2$ 1B contain high net charge densities which might result in large structural changes in the proteins due to intramolecular electrostatic repulsion. Furthermore, it is generally believed that the structural changes are stronger at hydrophobic surfaces. Therefore, it might be possible that at methylated surfaces the proteins containing a high net charge density are after a certain time more smeared out over the sorbent surface, thereby reducing the remaining area on which adsorption can take place. Since these relatively low adsorbed amounts under these conditions are mainly observed for IgG 1B, it could be an indication that $F(ab')_2$ 1B has a lower tendency to undergo structural rearrangements.

The results of the adsorbed amounts will further be discussed on the basis of the plateau values which in most cases are reached within 6 hours. For the various adsorption experiments these plateau values are presented in Figs. 6, 7, 9, and 10.

Structural analysis

The amide I region of all FTIR-spectra were analysed for the secondary structure. If not carefully executed, the mathematical procedure of resolution enhancement may lead to erroneous results. For example, some authors assume that some of the peaks have a Gauss instead of Lorentz distribution [26,34]. Another source of inaccuracy is related to fluctuations in the IR spectrum caused by changes in the physical properties other than the numbers of absorbing groups such as refractive indices of the different layers, or simply by inadequate removal of "noise". These effects can alter the number or the location of the peak positions. However, the results of the analysis show that in all spectra six or seven peaks are found and that the variation in the peak position is relatively small (see Table 3). Since, the position of the peaks and bandwidths were not fixed in the fitting procedure, small deviations from the actual peak position or bandwidth may occur, leading to uncertainties in the integrated intensities of the individual bands. Nevertheless, the obtained results are in good agreement with other studies, as reported in Table 1. Furthermore, the relative changes in the amounts of the various structural components due to the different adsorption conditions are in line with the expectations as inferred from the general trends for IgG adsorption. Hence, we conclude that our analysis gives reliable results.

A few examples of the obtained ß-sheet content for IgG and F(ab')$_2$ adsorbed on silica at an ionic strength of 5 mM are shown in Fig. 5. In Fig. 5a, the resulted amounts of ß-sheet are shown for two independent measurements of IgG 1B adsorbed at pH 5. In this figure, it is observed that during the first two hours the difference between duplicate measurements is small, however, the difference increases at later times. This is probably an artefact, caused by small alterations in the actual background, whereas all spectra are corrected for the same background spectrum as measured before the start of the adsorption experiment. Variations in the background can originate from slight changes in the temperature, water vapour content, and from a decreased cooling of the MCT detector. Nevertheless, as a general trend, it was observed that the amounts of ß-sheet slowly decrease in time. This observation is in line with previous data from which it has been concluded that IgG molecules are more tightly bound after longer adsorption times, thereby undergoing further structural changes [2,4].
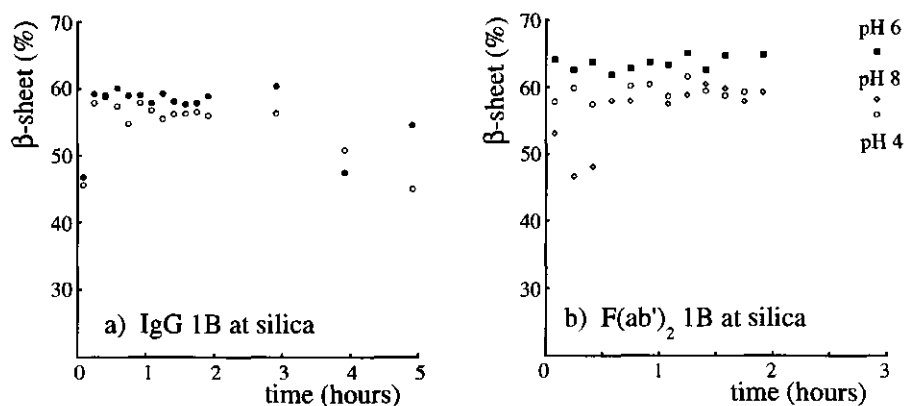

Fig. 5. a) The percentage of β-sheet followed in time for two identical measurement of IgG 1B adsorption at pH 5. b) The percentage of β-sheet for adsorbed F(ab')$_2$ 1B at pH 4, 6 and 8. Both proteins were adsorbed on silica at an ionic strength of 5 mM.

The obtained fractions of the structural components showed a larger deviation between two successively measured spectra in one experiment if there was no dominating structural element. This inaccuracy is caused by the applied fitting procedure. If two or three individual peaks of equal intensity are located next to each other, a relatively larger variation in peak position and bandwidth occurs in the fitting procedure. This implies that one peak could increase its integrated absorption area at the expense of the magnitude of

the neighbouring peaks. The deviations in the results of the fractions of structural elements were also larger when the adsorbed amount, i.e., the absorption intensity, was lower. For the above-mentioned reasons, the discussion of the results is mainly concentrated on the average fractions of the structural elements. In order to minimise time effects, the average was taken of the results obtained from measurements between the first half and two hours. The resulting ß-sheets fractions, together with the standard deviations are presented in Figs. 6, 7, 9, and 10. The fractions of the structural elements in the high frequency region (1676 and 1688 cm^{-1}) were hardly affected by changes in pH and amounted to ca. 10 %. This implies that the fractions of the sum of unordered and α-helical structure equals the total integrated intensity (100 %) minus the reported percentages of ß-sheets and the 10 % of the turns and bends.

From Fig. 5a, it can been seen that the fractions of ß-sheet as obtained in the first 10 minutes of the adsorption process were lower than the ß-sheet contents measured at later time intervals. This trend is found in most experiments and suggests that relatively large changes in the secondary structure occur in the initial stage of the adsorption process and that the structure is stabilised after it is adsorbed. Unfortunately, FTIR is unable to accurately detect fast processes.

5.4.2 Adsorption on silica

The results for adsorption on silica are summarised in Fig. 6. The plateau values are shown in Fig. 6a and the average fractions of ß-sheet structures are plotted in Fig. 6b. It is clearly seen that a maximum in the adsorbed amount arises at a pH at which the protein is marginally electrostatically attracted by the sorbent surface. Furthermore, it is remarkable that the plateau values for IgG 2A and F(ab')₂ 2A are considerably higher than those for IgG 1B and F(ab')₂ 1B. This observation suggests that the 2A proteins adsorb in a different orientation or in a more densely packed monolayer compared to that of the 1B proteins. A similar observation was made in Chapter 3 for adsorption onto negatively charged polystyrene latices. In that Chapter it was indicated that the relatively large adsorbed amount arises due to aggregation of IgG 2A at the sorbent surface.

From Fig. 6b, it can be seen that for both IgG 1B and IgG 2A the ß-sheet contents decrease at pH values shifted away from their i.e.p. values. This reduction in the ß-sheet content is a strong indication that increased structural rearrangements of the IgG molecules result in an adsorbed state in which the proteins become somewhat smeared out over the surface, thus leading to a decreased adsorbed amount. This effect is generally held responsible for the influence of the pH on the adsorption of proteins, including IgGs

[35,36,37]. The F(ab')$_2$ fragments show a totally different pattern. The ß-sheet content in the fragments is hardly influenced by the pH and in all cases the fraction of ß-sheet for F(ab')$_2$ was higher than that of its corresponding IgG. Hence, the secondary structure of F(ab')$_2$ is more stable than that of IgG with respect to adsorption. From the results of the adsorption kinetics (see Fig. 4), it was already concluded that adsorption of F(ab')$_2$ was not so strongly driven by other than electrostatic interactions compared to that of IgG. From these results it can be concluded that at hydrophilic surfaces under conditions of electrostatic repulsion F(ab')$_2$ adsorption is stronger opposed than that of whole IgG molecules because F(ab')$_2$ is less able to rearrange its structure.
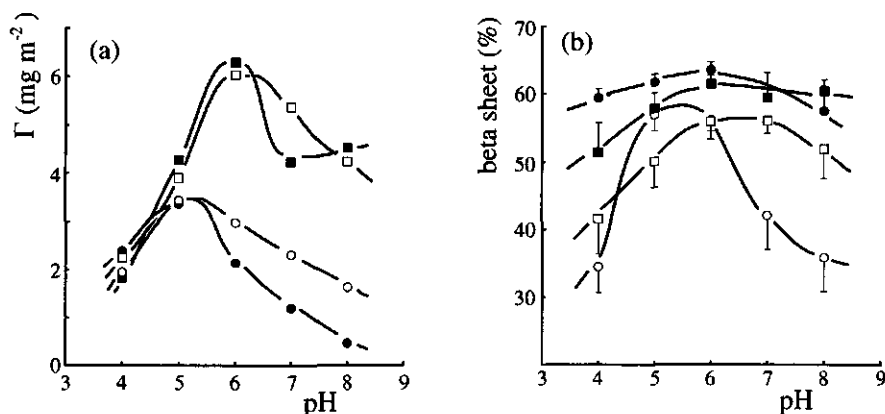

Fig. 6. Adsorption of the different proteins on silica as function of pH: a) plateau values and b) the fractions of β-sheet structure and standard deviation. The proteins are indicated as (O) IgG 1B, (●) F(ab')$_2$ 1B, (❑) IgG 2A, and (■) F(ab')$_2$ 2A.

In the literature, it is generally found or suggested that IgG adsorption preferentially takes place with the Fc domain [36,38,39,40,41,42]. These authors suggest that this phenomenon is related to the more hydrophobic nature of the Fc part. However, in Chapter 2 it was concluded that the F(ab')$_2$ domain is somewhat more hydrophobic than the Fc domain. Furthermore, the present results indicate that adsorption of the Fc part is preferred due to its low structural stability compared to that of the F(ab')$_2$ fragment. This finding is supported by the observation that Fc fragments show a higher tendency to undergo structural changes with respect to acid denaturation than Fab fragments [43,44]. Moreover, in the production of immunoassays it has been found that, after exposing IgG

to a solution of pH 2, the IgG molecules mainly adsorb with their Fc fragments which resulted in an enhanced antigen binding capacity [45].

5.4.3 Adsorption on methylated silica

The results of adsorption on methylated silica are shown in Fig. 7. The plateau values for the adsorbed amounts show a maximum around the i.e.p. of the proteins. Compared to adsorption on the silica surfaces these maxima are somewhat shifted towards higher pH values. Under conditions of electrostatic repulsion the adsorbed amounts for F(ab')₂ 1B at methylated surfaces are higher than those for the silica surface which is probably caused by the compensation of electrostatic repulsion by hydrophobic interactions. For both IgGs the final adsorbed amounts strongly decrease when the net charge on the protein rises.

With respect to the fractions of ß-sheet structures it is expected and observed that structural rearrangements are larger with increasing hydrophobicity of the sorbent surface. This effect is related to the enhanced possibility of exposing hydrophobic residues, located at the interior of the protein, to the sorbent surface. In general, in this study the results are in line with this expectation; and ß-sheet contents for the adsorbed proteins at methylated surfaces were found to be lower compared to those at silica. More specifically, the ß-sheet content for F(ab')₂ fragments is marginally reduced whereas the reduction in ß-sheets is much larger for IgG 2A at pH values shifted from the i.e.p of IgG 2A.
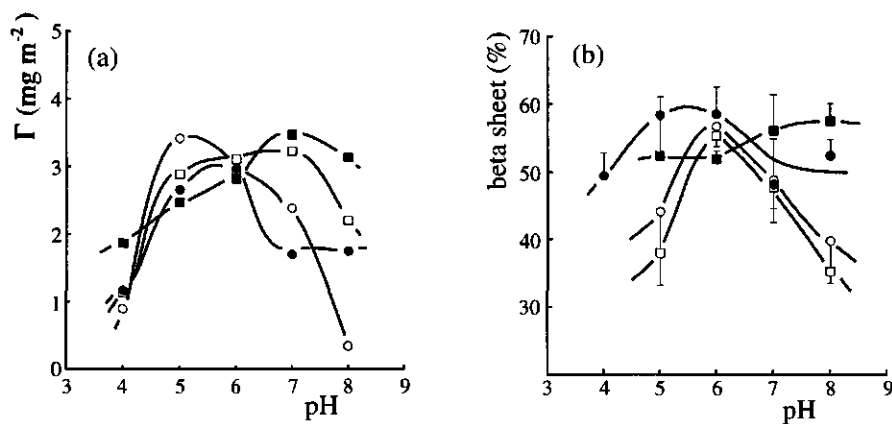

Fig. 7. Adsorption on methylated silica as function pH; a) plateau values and b) the fractions of β-sheet structures and the standard deviation. The proteins are indicated as (O) IgG 1B, (●) F(ab')₂ 1B, (▢) IgG 2A, and (■) F(ab')₂ 2A.

This again indicates that the structure of F(ab')₂ is less sensitive to adsorption. For IgG 1B it was observed that the ß-sheet content at methylsilane under conditions of electrostatic repulsion was higher than that at silica surfaces. The explanation could be that under these conditions, adsorption of IgG 1B at silica was enhanced due to its ability to undergo structural rearrangements.

It is remarkable that for adsorption at the hydrophobic surfaces a relative large peak around 1654 cm⁻¹ was found. Such a peak is generally assigned to α-helix structures. For both IgGs and their F(ab')₂ fragments the fractions of α-helices in the pH range from 4 to 8 were about 20 % and 14 %, respectively. These values are higher than those presented in Table 1 and also exceed the values for adsorption at the hydrophilic silica surface, which were totally absent or, at maximum, below 10 %.
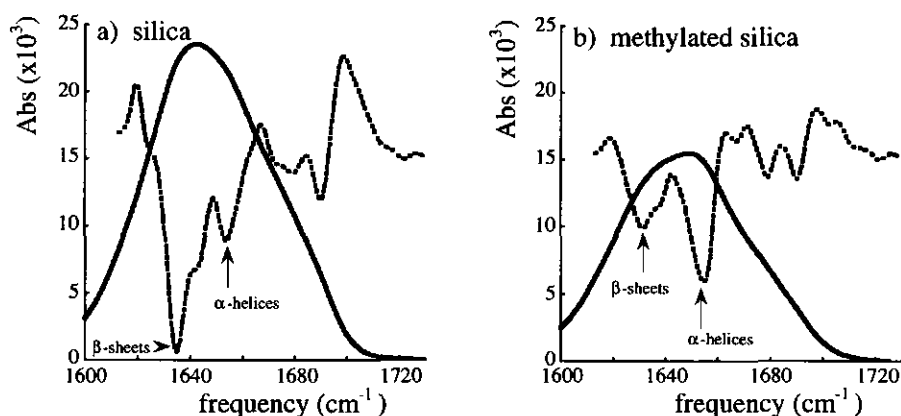
Fig. 8. The smoothed amide I absorption band and its second derivative for adsorbed IgG 2A at silica (a) and methylsilane (b). The spectrum is measured after ca. 1.5 hour of adsorption from a 50 mg dm⁻³ IgG solution, pH 5 and an ionic strength of 5 mM.

An example of the increase in α-helix structure is shown in Fig. 8 in which the original spectrum and the second derivative for adsorption of IgG 2A on silica and methylated silica at pH 5 are compared. From this figure it can be observed that the shape of both absorption bands differ and from the second derivative it can be seen that the ß-sheet peak located at 1636 cm⁻¹ is reduced at the methylated surface whereas the α-helix peak increases. Since the α-helix peak (1654 cm⁻¹) was located close to the unordered peaks (1646 and 1654 cm⁻¹) the obtained fractions for the amounts of α-helices were not sufficiently accurate to give an overall quantitative picture for the presence of α-helices

under the various adsorption conditions. However, the trend clearly suggest that the α-helix content increases upon adsorption on hydrophobic surfaces.

5.4.4 Effect of the adsorption rate

It has been reported that structural changes in adsorbed proteins tend to be larger when the degree of surface coverage is smaller [1,6]. It is therefore expected that the extent of structural rearrangements increases with decreasing rate of adsorption. The adsorption rate is varied by changing the supplied protein concentration from 50 g m^{-3} to 10 g m^{-3} for IgG 1B adsorption on silica. The shapes of the $\Gamma(t)$ curves show similar patterns when corrected for the lower adsorption rates although the saturation adsorption after 6 hours is altered as shown in Fig. 9a.
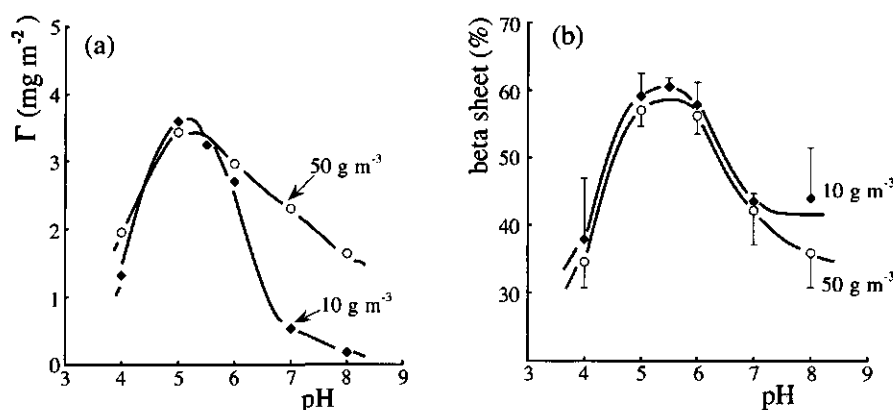
Fig. 9. Effect of IgG 1B concentration on adsorption on silica at 5 mM ionic strength. a) adsorbed amounts b) the fractions of β-sheet structures. The proteins concentrations are indicated as (O) 50 g m⁻³ and (◆) 10 g m⁻³ and the standard deviation in the fraction of the β-sheet content is depicted by vertical lines.

The variation in the adsorption rate hardly affects the maximum of the $\Gamma(pH)$-curve. On the other hand, when the net charge on the protein rises, the adsorbed amounts obtained at lower adsorption rates were reduced, especially when the protein is electrostatically repelled by the sorbent surface. A possible explanation is that at lower adsorption rates the protein molecules have more time to adjust their conformation and/or orientation to the surface before neighbouring molecules arrive. This may lead to a larger surface area per adsorbed protein molecule. The structural changes upon adsorption would likely be

reflected in an alteration of the secondary structure. However, as shown in Fig. 9b, no significant differences in secondary structure are observed. The logical conclusion is that the decreased adsorbed amounts at lower protein concentrations are caused by changes in the orientation and/or in the two-dimensional ordering of the IgG molecules on the surface, rather than by progressed perturbation of the protein structure. These observations contradict the before-mentioned increased structural rearrangements at lower surface coverages. It could be that the adsorption rates at 50 g m^{-3} are already sufficiently low to allow for maximum structural rearrangements.

5.4.5 Effect of ionic strength

It has been reported that at higher ionic strength the conformational stability of adsorbed IgG is greatly enhanced [2]. This effect is related to the screening of electrostatic interactions. Therefore it is expected that at high ionic strength the plateau values and the fractions of structural elements are less sensitive to variations in pH. This effect is studied by comparing the adsorption of both IgGs at silica and methylated silica in the pH-range from 5 to 8, at two ionic strengths, 5 mM and 0.1 M. From the plateau values of adsorption as shown in Fig. 10a, it can be seen that the variation as a function of pH is less compared to that at an ionic strength of 5 mM (Figs. 6a and 7a).
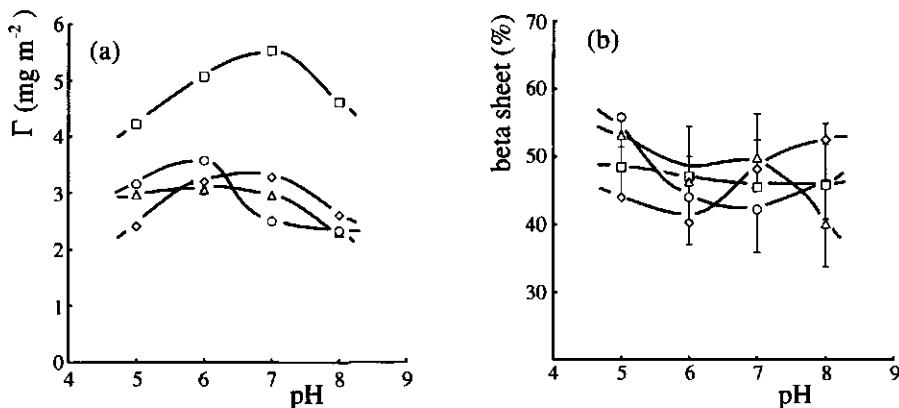

Fig. 10. Adsorption of IgG 1B and IgG 2A at an ionic strength of 0.1 M at silica and at methylated surfaces; a) plateau values and b) the fractions of β-sheet structures and the respective standard deviations. The proteins and sorbent surfaces are indicated as (O) IgG 1B at silica, (△) IgG 1B at methylated silica, (❑) IgG 2A at silica, and (◊) IgG 2A at methylated silica.

The variation in the ß-sheet content is also reduced when the ionic strength is increased. These results confirm the expected influence of ionic strength on the variation of the plateau values and the extent of structural perturbation with pH. However, most values for the amount of ß-sheet are lower than those observed for adsorption at 5 mM ionic strength. This ionic strength-induced decrease in structural stability for IgG adsorption at pH values close to the i.e.p. was earlier indicated by Serra and co-workers [36]. It might be possible that at higher ionic strength more low molecular weight ions are incorporated in the adsorbed layer. These low molecular weight ions can screen electrostatic repulsion between negatively charged groups on the protein and sorbent surface or even produce ion-pairs between these charged groups. Indication for ion-pair formation between carboxyl groups on the protein and negatively charged groups on the sorbent surface have been inferred from titration studies [46,47]. The formation of ion-pairs between protein and sorbent surface can induce distortion of the protein structure resulting in a decrease of the amount of ordered segments.

5.5 Conclusions

It is demonstrated that the ATR/FTIR technique and the applied fitting procedure using second derivative spectra are valuable tools to study secondary structure elements in adsorbed proteins. From the analysed IR spectra it is inferred that at higher net charge densities of the IgG molecule, the plateau value of IgG adsorption reduces as does the fraction ß-sheet structure. The reduction in the ß-sheet content is stronger at methylated surfaces than at silica indicating that larger structural changes are induced upon adsorption on hydrophobic sorbent surfaces. Furthermore, an increase in the amount of α-helices is found that at the hydrophobic methylated surface. At higher ionic strengths the influence of the pH-dependent electrostatic interaction on the adsorption is suppressed. As inferred from the adsorption kinetics as well as from the results of the structural analysis, it is concluded that the F(ab')2 fragment is structurally more stable than the whole IgG molecule. These results may imply that the Fc part has a stronger affinity for sorbent surfaces because it gains more conformational entropy upon adsorption. Accordingly, IgG molecules may be preferentially adsorbed with their Fc parts attached on the sorbent surface and their, relatively unperturbed, Fab parts pointing towards the solution.

5.6 References

1   W. Norde, and J.P. Favier, *Colloids and Surfaces,* **64** (1992) 87.

2   M. E. Soderquist, and A.G. Walton, *J. Colloid Interface Sci.,* **75** (1980) 386.

3   A. Kondo, S. Oku, F. Murakami, and K. Higashitani, *Colloids and Surfaces B: Biointerfaces,* **1** (1993) 197.

4   A.V. Elgersma, R.L.J. Zsom, W. Norde, and J. Lyklema, *J. Colloid Interface Sci.,* **152** (1992) 410.

5   W. van der Vegt, H.C. van der Mei, and H.J. Busscher, *J. Colloid Interface Sci.,* **156** (1993) 129.

6   A. Kondo, F. Murakami, and K. Higastani, *Biotechnol. Bioeng.,* **40** (1992) 889.

7   J.S. Jeon, R.P. Sperline, and S. Raghavan, *Appl. Spectroscopy,* **46** (1992) 1644.

8   F.M. Wasacz, J.M. Olinger, and R.J. Jakobsen, *Biochemistry,* **26** (1987) 1464.

9   J.L. Kirsch, and J.L. Koenig, *Appl. Spectroscopy,* **43** (1989) 445.

10   J. Deisenhofer, *Biochemistry,* **20** (1981) 2361.

11   M. Marquart, J. Deisenhofer, R. Huber, and W. Palm, *J. Mol. Biol.,* **141** (1980) 369.

12   R.J. Poljak, L.M. Amzel, B.L. Chen, R.P. Phizackerley, and F. Saul, *Proc. Natl. Acad. Sci. USA,* **71** (1974) 3440.

13   D.M. Byler, and H. Susi, *Biopolymers,* **25** (1986) 469.

14   W. Kabsch, and C. Sander, *Biopolymers,* **22** (1983) 2577.

15   B.R. Singh, and M.P. Fuller, *Appl. Spectroscopy,* **45** (1991) 1017.

16   M. Levitt, and J. Greer, *J. Mol. Biol.,* **114** (1977) 181.

17   J.K. Kauppinnen, D.J. Moffatt, H.H. Mantsch, and D.G. Cameron, *Anal. Chem.,* **53** (1981) 1454.

18   H. Susi, and D.M. Byler, *Biochem. Biophys. Res. Commun.,* **115** (1983) 391.

19   O.H. Lowry, N.J. Rosebrough, A.L. Farr, and R.J. Randall, *J. Biol. Chem.,* **193** (1951) 265.

20   P. Frantz, and S. Granick, *Langmuir,* **8** (1992) 1176.

21   L. Bousse, S. Mostarshed, B. van der Shoot, N.F. de Rooij, P. Gimmel, and W. Göpel, *J. Colloid Interface Sci.,* **147** (1991) 22.

22   W. Norde, and E. Rouwendal, *J. Colloid Interface Sci.,* **139** (1990) 169.

23   R.P. Sperline, S. Muralidharan, and H. Freiser, *Langmuir,* **3** (1987) 198.

24   R.P. Sperline, S. Muralidharan, and H. Freiser, *Appl. Spectroscopy,* **40** (1986) 1019.

25   D.C. Lee, J.A. Hayward, C.J. Restall, and D. Chapman, *Biochemistry,* **24** (1985) 4364.

26   B.R. Singh, M.P. Fuller, and G. Schiavo, *Biophys. Chem.,* **46** (1990) 155.

27   P. Marchand, and L. Marmet, *Rev. Sci. Instrum.,* **54** (1983) 1034.

28   W.K. Surewicz, and H.H. Mantsch, *Biochim. Biophys. Acta,* **952** (1988) 115.

29   Y.N. Chirgadze, O.V. Fedorov, and N.P. Trushina, *Biopolymers,* **14** (1975) 679.

30   S. Krimm, and J. Bandekar, *Biopolymers,* **19** (1980) 1.

31   A.M. Dwivedi, and S. Krimm, *J. Phys. Chem.,* **88** (1984) 620.

32   R.J. Jakobsen, and S.W. Strand, *Internal Reflection Spectroscopy,* Ed. F.M. Mirabella, Practical Spectroscopy Series Vol. 15, Marcel Dekker Inc. NY, (1992) pp 107-140.

33   T. Arai, and W. Norde, *Colloids Surfaces,* **51** (1990) 1.

34   N. Kossovsky, A. Nguyen, K. Sukiassians, A. Festekjian, A. Gelman, and E. Sponsler, *J. Colloid Interface Sci.,* **166** (1994) 350.

35   F. Galisteo-González, J. Puig, A. Martín-Rodriguez, J. Serra-Domènech, and R. Hidalgo-Alvarez, *Colloids Surfaces B: Biointerfaces*, **2** (1994) 435.

36   J. Serra, J. Puig, A. Martín, F. Galisteo, MaJ. Gálvez, and R. Hidalgo-Alvarez, *Colloid Polym. Sci.*, **270** (1992) 574.

37   A.V. Elgersma, R.L.J. Zsom, W. Norde, and J. Lyklema, *Colloids Surfaces*, **54** (1991) 89.

38   H. Kawaguchi, K. Sakamoto, Y. Ohtsuka, T. Ohtake, H. Sekiguchi, and H. Iri, *Biomaterials*, **10** (1989) 225.

39   T. Suzawa, and H. Shirahama, *Adv. Colloid Interface Sci.*, **35** (1991) 139.

40   I. Vikholm, and O. Teleman, *J. Colloid Interface Sci.*, **168** (1994) 125.

41   P. Bagchi, and S.M. Birnbaum, *J. Colloid Interface Sci.*, **83** (1981) 460.

42   D.C. Cullen, and C.R. Lowe, *J. Colloid Interface Sci.*, **166** (1994) 102.

43   L.V. Abaturov, R.S. Nezlin, T.I. Vengerova, and Ja.M. Varshavsky, *Biochim. Biophys. Acta*, **194** (1969) 386.

44   E. Doi, and B. Jirgensons, *Biochemistry*, **9** (1970) 1066.

45   R. van Erp R., Y.E.M. Linders, A.P.G. van Sommeren, and T.C.J. Gribnau, *J. Immunol. Methods*, **152** (1992) 191.

46   W. Norde, *Croat. Chem. Acta*, **56** (1983) 705.

47   C.A. Haynes, E. Sliwinsky, and W. Norde, *J. Colloid Interface Sci.*, **164** (1994) 394.

6

The effect of Adsorption on the Antigen Binding by IgG and its F(ab')$_2$ fragments

The adsorption of two monoclonal IgGs and their F(ab')$_2$ fragments is studied in relation to the binding of antigen to the adsorbed proteins using reflectometry. Adsorption and antigen binding experiments are performed under various conditions such as, hydrophobicity of the surface, pH, and ionic strength. In this way, a relation between the various interactions involved in the adsorption process and its effect on the antigen binding efficiency is obtained. From adsorption experiments and from infrared spectroscopy measurements it is inferred that the Fc part of an IgG molecule is structurally less stable than the F(ab')$_2$ part. This lower structural stability promotes adsorption of the IgG molecules with their Fc parts to the sorbent surface, directing the Fab parts towards the solution. Indeed, it is found that the antigen binding ratios are higher under adsorption conditions at which the affinity of F(ab')$_2$ fragments for the sorbent surface is relatively low. Furthermore, it is observed that the orientation of an adsorbed IgG molecule with an uneven charge distribution can strongly be influenced by electrostatic interactions. This resulted in a total absence of immunological activity under conditions in which the Fab parts are strongly electrostatically attracted by the sorbent surface.

6.1 Introduction

The production of immunological tests and biosensors commonly involves a step in which immunoglobulin G (IgG) is adsorbed onto solid surfaces. For example, in an enzyme-linked immuno-sorbent assay (ELISA), IgG is immobilised on the walls of a plastic microtiter plate. The function of immuno-assay techniques depends on the capability of the immobilised IgG to bind antigens. An IgG molecule consists of three domains which are grouped together in a "Y"-shaped form. The antigen binding sites are located on the far ends on two of these three domains. These two domains are identical

and are called the Fab regions. The biological function of the third domain, the Fc region, is to specifically bind to receptors. Upon adsorption, an IgG molecule can partly, or even completely, loose its ability to bind antigens. This adsorption-induced reduction in the effective immunological activity can be caused by changes in the protein structure and/or by an unfavourable orientation of the antigen binding sites at the sorbent surface which makes them inaccessible for the antigen.

The purpose of the present study is to find a relationship between protein-sorbent interactions and the antigen binding efficiency of adsorbed IgG and $F(ab')_2$ fragments. Protein-sorbent interactions are varied by adsorbing the proteins on both hydrophilic silica and hydrophobic methylated silica surfaces. Furthermore, electrostatic interactions are studied by performing experiments at various values for the pH and ionic strength. The experiments are carried out with two monoclonal IgGs, which differ in their isoelectric point (i.e.p.), and the composition of their respective $F(ab')_2$ fragments. Both IgGs are directed against the pregnancy hormone, human chorionic gonadotropin (hCG). The orientation of the adsorbed IgG molecule will be influenced by the relative affinity of the different domains for the sorbent surface. In order to study this influence, experiments are performed using the single $F(ab')_2$ and Fc fragments. Information concerning the antigen binding efficiency by $F(ab')_2$ fragments is of particular interest for the new development of immuno-assays based on $F(ab)$ or $F(ab')_2$ fragments instead of the whole IgG molecule [1,2]. Immobilisation of the Fab domains only, avoids anomalous results in immunological tests which are caused by the presence of the Fc fragments [3,4].

The antigen binding efficiency is studied by supplying the antigen, hCG, to adsorbed layers of IgG or $F(ab')_2$ and monitoring the amount of hCG which is bound. In order to avoid adsorption of hCG to unoccupied sites on the sorbent surface, the surface is post-coated with BSA; this method is generally applied in immunological tests [5,6]. It should be mentioned that BSA coating itself may affect the orientation or the spatial distribution of the adsorbed IgG or $F(ab')_2$ layer. This makes the interpretation of hCG binding in terms of the adsorbed behaviour of IgG or $F(ab')_2$ molecules somewhat ambiguous. Furthermore, the possibility exists that BSA displaces the already adsorbed IgG or $F(ab')_2$ molecules.

The adsorption process of IgG or $F(ab')_2$ fragments and subsequent binding of hCG is measured by the optical technique reflectometry. Using reflectometry, the amount of proteins immobilised on the sorbent surface can be monitored *in situ* as a function of time.

6.2 Experimental

6.2.1 Materials

Surfaces

In the present study, a hydrophilic silica surface and a hydrophobic methylated surface were used, both based on a silicon wafer (Wacker Chemitronic GmbH). The silicon wafer was oxidised for 1 hour at 1000°C to obtain a silica layer of about 100 nm thickness. Such a thickness is essential for obtaining a high sensitivity in reflectometry experiments [7]. The silica wafer was cut into slides of 1 x 5 cm². Prior to each experiment silica slides were cleaned by placing them for 20 minutes in a chamber with a constant oxygen flow during which the surface was irradiated by UV-light. In this way, organic contaminants were oxidised and a homogeneous oxide layer was produced with a minimum of surface damage [8]. Hydrophobic methylated surfaces were obtained by immersion of silica slides for 30 minutes in 0.3 % (v/v) dichlorodimethylsilane in 1,1,1-trichloroethane. After silanisation the slides were consecutively flushed with trichloroethane and ethanol. Both the untreated and methylated silica slides were rinsed with water and dried in a jet of nitrogen gas before placing them in the reflectometry cell. The contact angles of a sessile drop of water for the methylated and the silica surface were 90° and 7°, respectively. The silica surface is negatively charged due to the hydrolysed silanol groups. It has been reported that its zeta-potential at an ionic strength of 0.01 M NaCl is around -20 mV at pH 4 and that this value gradually decreases to ca. -55 mV at pH 8 [9]. The methylated surface also contains some negative charges due the presence of unsilanised silanol groups. Streaming potential measurements, performed as described by Norde and Rouwendal [10] showed that the zeta potential of a methylated surface at pH 7 and an ionic strength of 0.01 M was -35 mV, which is less than 33% lower than the zeta potential of a silica surface under the same conditions of pH and ionic strength.

Proteins

Two monoclonal immunoglobulins, IgG 1B and IgG 2A, were studied. They were kindly donated by Organon Teknika (Boxtel, The Netherlands). Both IgGs were from isotype 1 and directed against hCG. Their respective F(ab')₂ and Fc fragments were obtained by papain digestion under non-reducing conditions, as described in Chapter 2.3.2 Some characteristics of the IgGs, their F(ab')₂ and Fc fragments, BSA and hCG are listed in Table 1. The isoelectric points of the IgGs and the fragments were determined using isoelectric focusing (IEF) with PhastGel media, pH range 3-9 and silver staining

(PhastSystem, Pharmacia). In Table 1 the major bands in the respective isoelectric pH-regions are given in brackets. The purity of the IgGs and F(ab')$_2$ fragments obtained with high performance size exclusion chromatography (Zorbax, GF-250 Dupont) is given in weight fractions. Impurities in IgG 1B consisted of smaller fragments only. Besides small fragments, solutions of IgG 2A and F(ab')$_2$ 2A contained aggregates with total weight fractions of 6% and 2%, respectively. For both IgGs concentrations were established spectroscopically using an extinction coefficient of 1.45 cm^2 mg^{-1} at 280 nm. This coefficient has been derived for several IgGs directed against hCG by measuring the extinction of an IgG solution and determining the protein fraction after evaporation of the solvent. The extinction coefficients for the F(ab')$_2$ fragments were determined colorimetrically according to the Folin phenol method of Lowry and co-workers [11] using the corresponding IgGs as the standards. This resulted in an extinction coefficient of 1.45 cm^2 mg^{-1} for F(ab')$_2$ 1B and 1.48 cm^2 mg^{-1} for F(ab')$_2$ 2A. The adsorbed layer of IgG or F(ab')$_2$ is post-coated with bovine serum albumin (BSA). (Sigma Chemical Co., Cohn fraction V). The antigen hCG was obtained in sealed flasks, containing 550 IU (ca. 8000 IU/mg), from Diosynth (Oss, The Netherlands).

Table 1. Isoelectric points, molecular weight, and purity of IgG 1B and 2A, their fragments, hCG, and BSA.

Proteins	isoelectric point	MW (kDa)	purity
IgG 1B	5.6-6.0 (5.8)	150	97%
F(ab')$_2$ 1B	5.6-6.1 (5.9)	100	>99%
IgG 2A	6.7-7.4 (6.9)	150	87%
F(ab')$_2$ 2A	8.2-8.8 (8.5)	100	98%
Fc	5.7-6.4 (6.1)	50	-
hCG	5.4	38	-
BSA	4.8	66	-

Chemicals

Water was purified by reverse osmosis and passed subsequently through a SuperQ system (Millipore). All chemicals were of p.a. grade and used without further purification. Experiments were performed with protein solutions containing 5 mM buffer. At pH 4 and 5 an acetate buffer was used, and at pH 6, 7, and 8 a phosphate buffer. Both buffers were prepared from sodium salts and adjusted to the desired pH with NaOH and HCl. Ionic strengths higher than 5 mM were obtained by adding NaCl.

6.2.2 Methods

Reflectometry

Reflectometry is an optical technique in which the polarisation of a light beam, after reflection on a flat sorbent surface, is continuously monitored. Upon adsorption on this surface, the polarisation of the reflected beam changes and the extent of this alteration can be related to the adsorbed amount. The basic principles of the method, the experimental set-up and the calibration procedures have been described in detail by Dijt and co-workers [7] and in Chapter 4. In the same Chapter, the parameters used for calculating the adsorbed amounts are given. The solutions are applied to the sorbent surface by an impinging jet system which produces a stagnation point flow. This stagnation point is positioned at the place where the beam is reflected. The stagnation point flow offers the advantage of having a well-controlled protein flux towards the surface [12]. This protein flux is proportional to the protein concentration in solution and to the two-third power of the diffusion coefficient of the proteins. Furthermore, the stagnation point flow provides an easy and quick method of replacing solutions. All solutions approach the sorbent surface at a rate of ca. 1 cm^3 per minute.

Immunological activity

The determination of the immunological activity of the adsorbed proteins consists of a few steps in which the different proteins are applied to the sorbent surface and in which the amounts of immobilised proteins are measured using reflectometry. A typical reflectometry pattern is shown in Fig. 1. First, a layer of IgG or F(ab')₂ is adsorbed at the sorbent surface by impinging an IgG or F(ab')₂ solution of 7.5 g m^{-3} towards the surface for 30 minutes. Second, the surface is post-coated with BSA to cover the remaining unoccupied surface area. The BSA is applied to the surface by circulating a 30 g m^{-3} BSA solution through the cell for 15 minutes. Finally, the immunological activity is measured by streaming a hCG solution (1 g m^{-3}) over the surface. Between each step-wise addition of the different proteins, the cell is flushed during 15 minutes with buffer solution.

Adsorption of IgG and F(ab')₂ on silica and methylated surfaces is studied as a function of pH and ionic strength. For this purpose, it is preferable that the pH and ionic strength remain constant during the whole experiment. Therefore, BSA post-coating and hCG binding are performed under the same conditions (pH and ionic strength) as adsorption of IgG or F(ab')₂. The effect of pH and ionic strength on hCG binding and BSA post-coating along with the influence of BSA coating on the adsorbed IgG or F(ab')₂ layer will be discussed in more detail below.
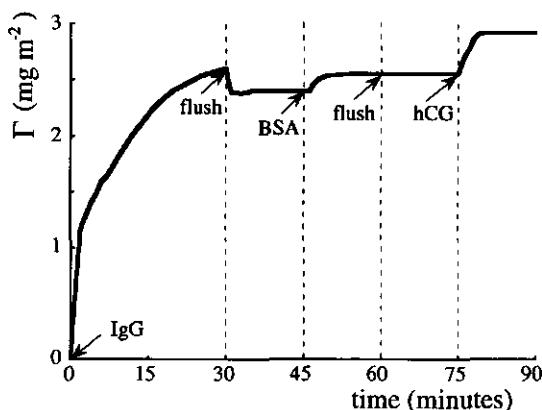
Fig. 1. Adsorption of IgG 1B (7.5 g m^{-3}, pH 5), post-coating with BSA (30 g m^{-3}) and binding of hCG binding (1 g m^{-3}) at a methylated surface. The experiment was performed at 0.1 M ionic strength.

Post-coating with BSA

The step of BSA post-coating is inherent to activity measurements. The necessity of BSA post-coating stems from the affinity of the hCG molecule for the sorbent surfaces under all experimental conditions. Thus, post-coating with BSA prevents non-specific binding of hCG to the sorbent surface. Unfortunately, in all experiments, post-coated BSA molecules may interact with the pre-adsorbed IgG or F(ab')$_2$ fragments thereby affecting the orientation and/or conformation of these proteins. Another problem related to the sequential adsorption of BSA is the displacement of pre-adsorbed IgG or F(ab')$_2$ by BSA. Displacement of adsorbed IgG by sequential adsorption of BSA has extensively been studied and no displacement of IgG occurs when the amount of IgG adsorbed at polystyrene latices is less then 3 mg m^{-2}. However, at higher adsorbed amounts BSA might displace some IgG molecules implying that BSA can displace up to 10 % of the adsorbed IgG molecules for the conditions applied in the present study [13]. Furthermore, it has been found that HSA, which shows a similar adsorption behaviour as BSA [14,15], did not displace IgG adsorbed at silica [16]. In Chapter 5, it was concluded from desorption measurements that the F(ab')$_2$ fragments are, in general, more tightly bound to sorbent surfaces than the whole IgG molecules. Therefore, it is expected that the extent of displacement of F(ab')$_2$ by BSA is relatively small. Since the displacement of IgG or F(ab')$_2$ is not accounted for in this study, the reported hCG binding ratios may be somewhat underestimated.

hCG binding

The affinity of both monoclonals for hCG, expressed as the association constant for the IgG-hCG binding, is relatively strong and amounts to $2x10^9$-10^{10} dm^3 mol^{-1} [17]. The IgG-hCG binding step is investigated with hCG concentrations of $1.1x10^{-8}$ mol dm^{-3} implying that at least 95% of the available binding sites of the IgG molecules should be occupied. Indeed the results of a few hCG binding experiments at a three times higher hCG concentration ($3.3x10^{-8}$ mol dm^{-3}) showed that these higher hCG concentrations did not significantly increase the fraction of bound hCG. Note that the reported association constants [17] were measured under physiological conditions (pH 7.3, 0.15 M), whereas the experiments discussed here are performed at various pH values and ionic strengths. The effects of the pH and ionic strength on the hCG binding are investigated by performing an ELISA test using the following procedure. First, IgG 1B and IgG 2A are added to a microtiter plate coated with sheep-anti-mouse (S-a-M) IgG. In a second incubation step, hCG was added in a concentration of $2x10^{-9}$ mol dm^{-3} (which was 8 times lower than the concentration used in the presented reflectometry experiments) and dissolved in solutions of various pH values (5, 6, 7, and 8) and ionic strengths (5 and 100 mM). As a third step, the amount of bound hCG was detected by adding consecutively M-a-hCG/hRP and tetramethylbenzidine which results into a coloured product that is detected using a Reader Microelisa System (Organon Teknika, Boxtel). After each incubation, the microtiter plate was rinsed three times with a standard PBS/Tween solution. The results showed that the degree of hCG binding was not significantly affected by the pH and the ionic strength over the range used in this study. With respect to sequential adsorption of hCG, it is not likely that a small protein like hCG is able to displace IgG or BSA from the surface [18]. In most experiments a well-defined plateau for hCG binding was reached within a few minutes after the hCG had been added. However, in some experiments the quick initial increase of the amount of hCG at the sorbent surface was followed by an additional slow increase which is probably caused by adsorption of hCG at the sorbent surface. This is not surprising because hCG showed affinity for the sorbent surface under all experimental conditions. Moreover, hCG molecules are relatively small and they may become accommodated at uncovered sorbent areas between the larger IgG and BSA molecules. Nevertheless, the antigen binding by the IgG or F(ab')2 fragments can be distinguished from non-specific hCG adsorption because antigen-antibody binding is a much faster process than adsorption. In order to suppress the influence of hCG adsorption, the hCG binding ratio was established within six minutes after application of the hCG solution.

6.3 Results and discussion

6.3.1 General aspects of the adsorption behaviour

Since the purpose of the present study is to relate the antigen binding efficiency to the adsorption behaviour of IgG or $F(ab')_2$, some aspects of the adsorption behaviour will be discussed first. A more elaborated description of the adsorption process of both IgGs and their $F(ab')_2$ fragments on silica and methylated silica is given in Chapter 4. Furthermore, general trends of IgG and $F(ab')_2$ adsorption are reported in Chapters 3 and 5. Here, a succinct discussion of the adsorbed amounts after 30 minutes as shown in Fig. 2 is given. For the adsorption of IgG and $F(ab')_2$ densely packed monolayers are generally obtained in which the proteins are in most cases adsorbed in an end-on orientation (see Chapter 3). The maxima in the adsorbed amounts occur around the i.e.p. values of the proteins or, more precisely, when the proteins are marginally electrostatically attracted by the sorbent surface. When the net charge on the proteins rises the adsorbed amounts decrease and this decrease is generally stronger at low ionic strength. From FTIR studies, as described in Chapter 5, it was inferred that for IgG molecules this last-mentioned effect was at least partly caused by a reduction in the structural stability at high net charge densities on the protein molecules. This low structural stability may result in conformations in which the proteins are smeared out over the surface, thereby occupying a higher surface area per molecule. As described in Chapter 3 and in other IgG adsorption studies [19,20], the reduction in the adsorbed amounts at both sides of the i.e.p. was enhanced by lateral repulsion between the Fab parts of the IgG or $F(ab')_2$ molecules. At higher ionic strength these effects of electrostatic repulsion are screened. This is reflected in the adsorption of both IgGs at pH 4, which is significant larger at a higher ionic strength on both the silica and the methylated surfaces.

The silica surface contains a negative surface charge density which increases with increasing pH. This implies that a protein is electrostatically repelled by the surface at a pH beyond its i.e.p. value. This results in a relatively strong reduction in the adsorbed amounts, as can be seen for IgG and $F(ab')_2$ 1B adsorbed at silica at pH > 6.
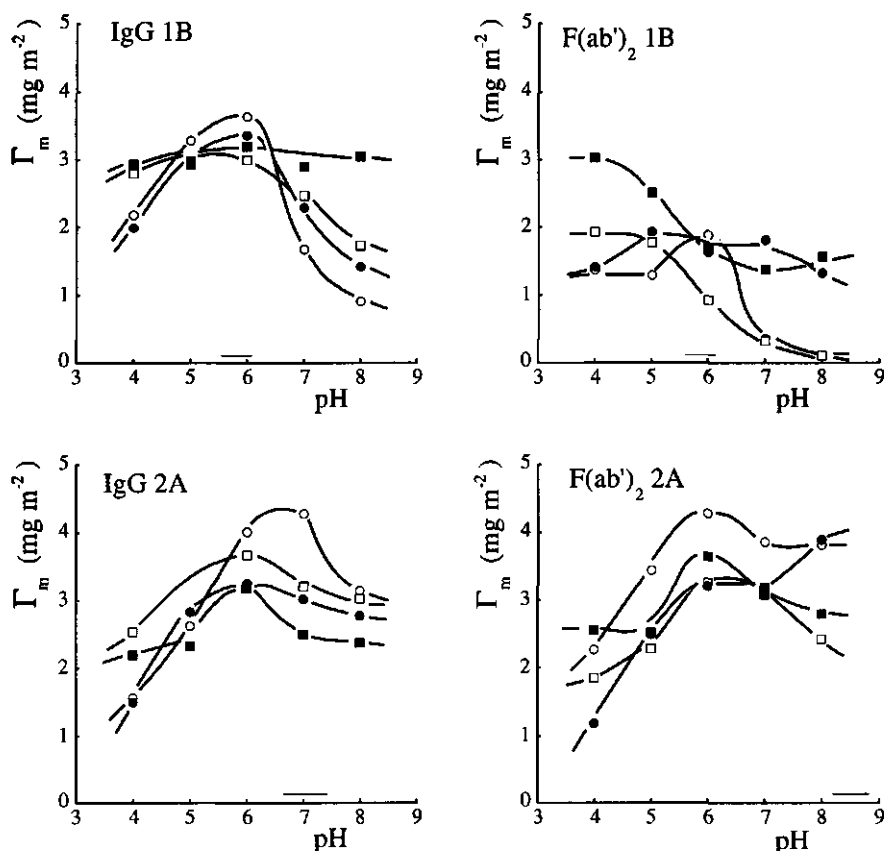
Fig. 2. Adsorbed amount of IgG 1B and IgG 2A and their F(ab')₂ fragments after 30 minutes of adsorption on silica (open symbols) and methylated (closed symbols) surfaces at ionic strengths of 5 mM (● or ○) and 0.1 M (■ or □). The i.e.p. values of the proteins are indicated by solid lines near the pH-axis.

At hydrophobic surfaces the influence of electrostatic repulsion between proteins and the sorbent surface is reduced. The reason is that the number of free hydroxyl groups, responsible for the negative charges at the silica surface, will be reduced due to the silanisation process. In addition, electrostatic repulsion is compensated for by hydrophobic interactions. Experimentally this is demonstrated by the adsorbed amounts under conditions of electrostatic repulsion which for IgG 1B and F(ab')₂ 1B are higher on the methylated surface than on silica.

6.3.2 hCG binding efficiency

Binding of hCG by IgG and F(ab')$_2$ adsorbed on silica or methylated surfaces is studied at ionic strengths of 5 mM and 0.1 M and in a pH range around the i.e.p. values of the respective proteins, i.e., for IgG 1B and F(ab')$_2$ 1B at pH 5, 6, and 7 and for IgG 2A and F(ab')$_2$ 2A at pH 6, 7, and 8. The antigen binding capacities of IgG and F(ab')$_2$ fragments are calculated by dividing the molar amount of bound antigen by the molar amount of adsorbed IgG or F(ab')$_2$. As both the IgG molecule and the F(ab')$_2$ fragment contain two antigen binding sites, this number is the theoretical maximum binding ratio. Most of the immunological activity measurements were duplicated and the reproducibility in the hCG/IgG or hCG/F(ab')$_2$ binding ratio was better than 0.1. In the Figs. 3 and 5 the hCG binding ratios are plotted as a function of pH for IgG 1B and IgG 2A, respectively. The hCG binding ratios for both F(ab')$_2$ fragments are shown in Fig. 6. It is noted that in none of the systems the binding ratio exceeds unity. This implies that never more than 50% of the potentially available binding sites for hCG are occupied.
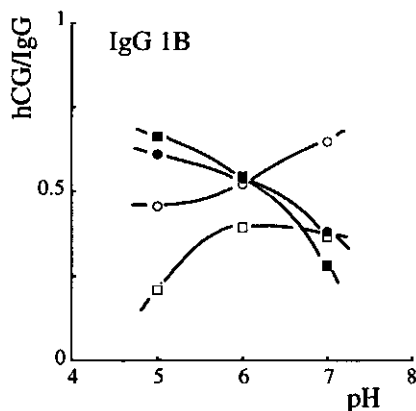

Fig. 3. hCG binding efficiency of IgG 1B adsorbed on silica (open symbols) and methylated (closed symbols) surfaces at ionic strengths of 5 mM (● or ○) and 0.1 M (■ or ❑).

For IgG 1B adsorbed on the methylated surface, it is observed that the hCG binding ratio decreases when the pH increases, suggesting that this trend is related to electrostatic interactions. With respect to adsorption, however, in Chapter 3 it was inferred from the initial adsorption rates that the IgG molecule does not experience an energy barrier before adsorption takes place. Furthermore, the i.e.p. values of the Fc and Fab part are almost

identical. For the above-mentioned reasons it is expected that the decrease in hCG binding with increasing pH does not reflect an electrostatically induced orientation of the IgG molecule due to preferential adsorption of either the Fc or the Fab domain. A feasible explanation for the relatively low hCG binding capacity at pH 7 might be that it is opposed by electrostatic repulsion between the hCG (i.e.p. = 5.4) and the Fab part (i.e.p. = 5.9).

For IgG 1B adsorption on silica at low ionic strength, the hCG binding ratios increase with increasing pH. This effect can be explained by the differences in the adsorption behaviour of the Fc part and the Fab part at hydrophilic surfaces under conditions of electrostatic repulsion. The electromobility measurements discussed in Chapter 3 indicate that non-electrostatic interactions are more important for whole IgG molecules than for the $F(ab')_2$ fragments. This was reflected in a lower adsorption rates of $F(ab')_2$ than for IgG or, even more so for Fc, if these proteins were adsorbed on silica surfaces under conditions of electrostatic repulsion (Figs. 5 and 6, Chapter 4). The adsorption for the different proteins under these conditions are shown in Fig. 4. In Chapter 5 it was concluded that the enhanced adsorption of the Fc part results from its relatively low structural stability in a 5 mM ionic strength solution. This low structural stability enhances adsorption because it enables an increase in conformational entropy of the protein and, in addition, the higher flexibility of the protein allows an optimisation of the protein-sorbent interactions such as electrostatic and hydrophobic interactions.
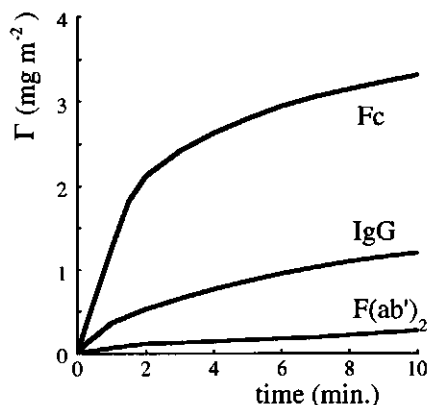

Fig. 4. Adsorption of IgG 1B and its F(ab')₂ and Fc fragments at silica surfaces, pH 7 and 5 mM ionic strength. The applied protein concentrations were 7.5 g m⁻³ for IgG and F(ab')₂ respectively, and 5 g m⁻³ for Fc.

Consequently, a larger fraction of the Fab parts are expected to be directed towards the solution and, hence, accessible for antigen binding. Preferential adsorption of IgG through its Fc part is most pronounced under adverse adsorption conditions. Therefore, it is expected that a relatively high antigen binding efficiency is obtained for IgG adsorption on silica at pH 7 and low ionic strength. Experimental data show that indeed a relatively high hCG binding ratio is observed under these conditions, although this ratio is still in the same range as found for other adsorption conditions. At methylated surfaces, the orientation of the IgG molecules is expected to be more random. Therefore, the effect of increasing hCG binding ratios at higher pH values for IgG on silica is more pronounced if these ratios are compared to those at the methylated surface. A similar effect of an increased antigen binding ratio caused by preferential adsorption of the structurally less stable Fc part has been reported for the production of immunoassays after acid treatment of the IgG molecules [21].

For IgG 2A, adsorbed on silica at pH 6 and 7 and an ionic strength of 5 mM, the addition of hCG did not result in hCG binding but in desorption of the IgG molecules (see Fig. 5). Normally it is not expected that a small protein like hCG is able to replace a large IgG molecule [18]. However, in Chapter 4 it was already reported that under these conditions relatively large amounts of IgG 2A desorb if a pure buffer solution is applied after the adsorption step. The desorption was attributed to a fraction of the IgG molecules which was only weakly attached to the sorbent surface.
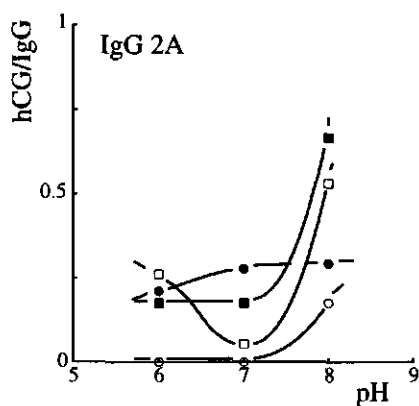

Fig. 5. hCG binding efficiency of IgG 2A adsorbed on silica (open symbols) and methylated (closed symbols) surfaces at ionic strengths of 5 mM (● or ○) and 0.1 M (■ or □).

The absence of hCG binding indicates that the binding sites are not accessible. At pH 6 and 7 the Fab part is positively charged and thus electrostatically attracted by the negative charges on the sorbent surface, whereas the Fc part is electrostatically repelled. Hence, it appears that under these conditions, electrostatic interactions are strong enough to induce a specific orientation of the IgG molecules with its Fab parts towards the sorbent surface thus rendering the Fab parts inaccessible for antigen binding. In Chapter 3, an indication of such an orientation was already found for IgG 2A adsorbed on hydrophilic latex particles under similar conditions for pH and ionic strength. The absence or relative low hCG binding is less pronounced at higher ionic strengths and at hydrophobic surfaces which supports the suggestion that the low hCG binding capacity is caused by interactions of electrostatic nature. The alternative interpretation that the low hCG binding ratios at pH 6 and 7 would result from a decreased structural stability, and hence, in a reduction of the biological activity of the Fab part is unlikely. In chapter 5 it was shown that the secondary structure of the F(ab')₂ fragment was hardly affected by the pH in the range between pH 6 and 8. Furthermore, the reduction in structural order was larger for adsorption on methylated silica than for adsorption on silica.

At pH 8 the net charge of the Fab part of IgG 2A is lower than that at pH 6 or 7. It is therefore assumed that the IgG molecules are less strongly oriented when they adsorb at pH 8. In the discussion of the hCG binding ratios of IgG and F(ab')₂ 1B it was concluded that the Fc part shows a high affinity for sorbent surfaces due to its low structural stability even under conditions of electrostatic repulsion. Consequently, at pH 8 part of the IgG molecules should adsorb with its Fc domain, thereby increasing the hCG binding ratio. This explanation is supported by the observation that at pH 8 the hCG binding ratios are higher when the electrostatic interactions are better screened by an increase in ionic strength.

In Fig. 6a, the hCG binding ratios are shown for F(ab')₂ 1B. The binding ratios for adsorption on silica at pH 7 were excluded from the measurements because at these values relatively low adsorbed amount of F(ab')₂ are obtained and even after coating with BSA the possibility remains that hCG adsorbs onto unoccupied areas on the sorbent surface. The hCG binding ratios for F(ab')₂ 1B are in the same order, or even somewhat higher, than for IgG 1B. For adsorption at low ionic strength a decrease in the hCG binding ratio is observed with increasing pH. This decrease is similar to that observed for the whole IgG 1B molecules adsorbed on methylated surfaces, which were expected to be randomly oriented (Fig. 3). At pH 5 it is seen that the hCG binding ratios are lower than those at high ionic strength. Comparing the data in the Figs. 6a and 2 reveals that these lower binding ratios correspond to relatively high adsorbed amounts of the F(ab')₂

fragments. In Chapter 4, it was suggested that these relatively large adsorbed amounts are caused by the configuration of the adsorbed F(ab')₂ fragments which differs from that at low ionic strength. Apparently, the configuration at high ionic strength results in a relatively low antigen binding capacity.
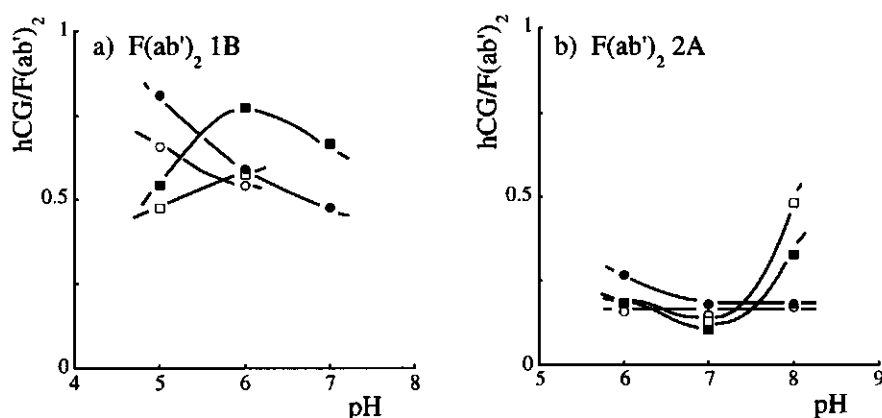

Fig. 6. hCG binding efficiency of a) F(ab')₂ 1B and b) F(ab')₂ 2A adsorbed on silica (open symbols) and methylated (closed symbols) surfaces at ionic strengths of 5 mM (● or ○) and 0.1 M (■ or □).

The hCG binding ratios of adsorbed F(ab')₂ 2A fragments are shown in Fig. 6b. It is observed that the hCG binding ratios for F(ab')₂ 2A are lower than those for F(ab')₂ 1B. The general pattern of the hCG binding ratios with respect to pH variation is similar to that of IgG 2A, although the immunological activity is not absent for adsorption at silica at 5 mM ionic strength and the relatively high ratios at pH 8 and 0.1 M ionic strength are less pronounced for the F(ab')₂ fragments. The similarity between hCG ratios F(ab')₂ and IgG 2A implies that for F(ab')₂ 2A the hCG binding is also opposed by an unfavourable orientation in which the antigen binding sites are located close to the sorbent surface. It is possible that this is caused because the positively charged groups at these pH values are predominantly located close to the antigen binding sites which results in an unequal charge distribution on the F(ab')₂ fragments. The difference in hCG binding ratios IgG 2A compared to that of F(ab')₂ 2A can then be attributed to the presence of the Fc fragment.

6.3.3 The IgG-hCG interaction

Attempts were made to extract more information on the hCG-IgG interaction after the hCG had been bound by the adsorbed IgG or $F(ab')_2$ molecules. This was accomplished by two additional steps. First, the hCG solution was replaced by a constant flow of a buffer solution of the same pH and ionic strength until no further change in the signal was observed. In this way information was obtained about the reversibility of the hCG binding. Second, the IgG or $F(ab')_2$ solution, identical to that used in the first adsorption step, was applied. Since the hCG contains only one strong binding site (epitope) for a monoclonal IgG, the addition of IgG or $F(ab')_2$ to the already adsorbed protein layers enables us to check whether the hCG molecules are directly adsorbed onto the sorbent surface or specifically bound to the antigen binding site.

With respect to the reversibility of the hCG binding it can be noted that for both monoclonals and their respective $F(ab')_2$ fragments only a fraction of the bound hCG molecules was released when a pure buffer solution had been applied. In general, the release of hCG molecules was somewhat lower at 5 mM than that at 0.1 M, indicating that hCG is more strongly bound at low ionic strength. After the desorption step of hCG, the addition of IgG or $F(ab')_2$ did in most cases not lead to a significant increase in the amount of immobilised protein; this fact reduces the possibility that hCG is directly adsorbed on the sorbent surface. However, for IgG 2A and to a lesser extent for $F(ab')_2$ 2A adsorbed at pH 6, a remarkably high amount of IgG or $F(ab')_2$ was adsorbed onto the IgG/hCG or $F(ab')_2$/hCG layer, respectively. Since these large additional adsorbed amounts can not be explained by adsorption on the sorbent surface or by specific binding to hCG molecules, it indicates that hCG binding induces aggregation of IgG and $F(ab')_2$ at this condition. The antigen binding-induced aggregation is called positive cooperativity and this effect has earlier been reported for the same monoclonal IgG by van Erp and co-workers [22].

6.4 Conclusions

The presented results indicate that the adsorption conditions influence the orientation of the adsorbed IgG or $F(ab')_2$, and this is reflected in the effective ratio of antigen binding. The adsorption of Fc fragments is enhanced by their relatively low structural stability. At conditions In which adsorption of $F(ab')_2$ fragments is hampered due to unfavourable interactions with the sorbent surface, this leads to higher hCG binding ratios for IgG 1B. Furthermore, it was concluded that for IgG 2A, which possesses an unequal

charge distribution over the different domains, the orientation of the final adsorbed state can strongly be influenced by electrostatic interactions. When the Fab parts of IgG 2A are strongly electrostatically attracted by the sorbent surface, this results in low hCG binding ratios.

6.5 References

1   M. Muratsugu, S. Kurosawa, Y. Mori, and N. Kamo, *Chem. Phar. Bull.*, **40** (1992) 501.

2   F.V. Bright, T.A. Betts, and K.S. Litwiler, *Anal. Chem.*, **62** (1990) 1065.

3   H. Kawaguchi, K. Sakamoto, Y. Ohtsuka, T. Ohtake, H. Sekiguchi and H. Iri, *Biomaterials*, **10** (1989) 225.

4   A.B. Pereira, A.N. Theofilopoulos, and F.J. Dixon, *J. Immunol.*, **125** (1980) 763.

5   S. Matsuzawa, Y. Itoh, H. Kimura, R. Kobayashi, and C. Miyauchi, *J. Immunol. Methods*, **60** (1983) 189.

6   B. Longhi, B. Chichehian, A. Causse, and J. Caraux, *J. Immunol. Methods*, **92** (1986) 89.

7   J.C. Dijt, M.A. Cohen Stuart, and G.J. Fleer, *Adv. Colloid Interface Sci.*, **50** (1994) 79.

8   P. Frantz, and S. Granick, *Langmuir*, **8** (1992) 1176.

9   L. Bousse, S. Mostarshed, B. van der Shoot, N.F. de Rooij, P. Gimmel, and W. Göpel, *J. Colloid Interface Sci.*, **147** (1991) 22.

10   W. Norde, and E. Rouwendal, *J. Colloid Interface Sci.*, **139** (1990) 169.

11   O.H. Lowry, N.J. Rosebrough, A.L. Farr, and R.J. Randall, *J. Biol. Chem.*, **193** (1951) 265.

12   T. Dabros, and T.G.M. van de Ven, *Colloid Polymer Sci.*, **261** (1983) 694.

13   A.V. Elgersma, R.L.J. Zsom, J. Lyklema, and W. Norde, *J. Colloid Interface Sci.*, **152** (1992) 410.

14   W. Norde, and J. Lyklema, *J. Colloid Interface Sci.*, **66** (1978) 257.

15   A.V. Elgersma, R.L.J. Zsom, W. Norde, and J. Lyklema, *J. Colloid Interface Sci.*, **138** (1990) 145.

16   S. Oscarsson, *J. Colloid Interface Sci.*, **165** (1994) 402.

17   R. van Erp, T.C.J. Gribnau, A.P.G. van Sommeren, and H.P.J. Bloemers, *J. Immunoassay*, **12** (1991) 425.

18   L. Vroman, A.L. Adams, and M. Klings, *Federation Proc.*, **30** (1971) 1494.

19   P. Bagchi, and M. Birnbaum, *J. Colloid Interface Sci.*, **83** (1981) 460.

20   T. Suzawa, and H. Shirahama, *Adv. Colloid Interface Sci.*, **35** (1991) 139.

21   R. van Erp, Y.E.M. Linders, A.P.G. van Sommeren, and T.C.J. Gribnau, *J. Immunol. Methods*, **152** (1992) 191.

22   R. van Erp, T.C.J. Gribnau, A.P.G. van Sommeren and H.P.J. Bloemers, *J. Immunol. Methods*, **140** (1991) 235.

Summary and Perspectives

Summary

Adsorption of immunoglobulin G (IgG) is a common step in the production of immunological tests and biosensors. The use of IgG in these applications stems from its ability to specifically bind all kinds of molecules (antigens). In these tests the IgG molecules are immobilised onto solid surfaces, which is necessary to make visible the IgG-antigen binding. Upon adsorption, however, the IgG molecules may lose their ability to bind antigens. If the antigen binding sites are located close to the sorbent surface, this could reduce the accessibility for antigens. A second problem which may occur upon adsorption is related to structural rearrangements of the protein which could also cause a reduction in the antigen binding capacity.

The purpose of the present work was to acquire more insight into the role of the various interactions between IgG molecules and sorbent surfaces on the adsorption behaviour and, especially, how these interactions determine the adsorbed state of the IgG molecules.

After a general introduction in Chapter 1, in Chapter 2 an overview is given of the physical properties and some general aspects of the adsorption behaviour of IgG.

The different types of protein-sorbent interactions are systematically studied by performing experiments under various system conditions. The influence of the sorbent surface hydrophobicity is investigated using both a hydrophobic and a hydrophilic surface. Chapter 3 describes the adsorption of the proteins onto three polymer latices. Two of these latices are hydrophobic, one being positively and the other negatively charged and the third latex is negatively charged and hydrophilic. The adsorption experiments described in Chapters 4, 5, and 6 are performed using a hydrophilic silica and a hydrophobic methylated surface. Electrostatic interactions are varied by choosing various values for the pH and ionic strength. The experiments are performed using two monoclonal IgGs directed against the pregnancy hormone human chorionic gonadotropin (hCG). These two monoclonals differ in isoelectric point (i.e.p.). As the orientation of the

adsorbed IgG molecules is expected to be influenced by differences in adsorption behaviour of the single domains, experiments are also performed using the fragments, i.e., the $F(ab')_2$ and Fc fragments, of the whole IgG molecule.

Chapter 3 focuses on the equilibrium adsorption of the two IgGs and their corresponding $F(ab')_2$ fragments on polymeric surfaces. Special attention is paid to the electrokinetic properties of the protein/sorbent complexes. Furthermore, the obtained adsorbed amounts at saturation conditions are correlated to the possible orientations of the proteins in the adsorbed state. The proteins show a high affinity for the hydrophobic latices and this affinity is barely influenced by the electrostatic interactions involved. However, at saturation level the adsorbed amount depends on the overall electrostatic interactions resulting in a maximum when the protein charge is to a large extent compensated for by the sorbent surface charge. For the hydrophilic latex, adsorption is absent when the proteins are electrostatically repelled. At hydrophobic polystyrene surfaces, the proteins adsorb mainly in an end-on orientation. In contrast, in the case of a negatively charged hydrophilic latex and high cationic charge densities on the protein, the adsorbed amounts correlate with a closely-packed monolayer of side-on oriented proteins. The trends in the adsorption behaviour are similar for IgG and its corresponding $F(ab')_2$ fragment. Nevertheless, there is some evidence that IgG adsorption is more strongly driven by interactions other than electrostatic ones, hence, by hydrophobic interactions and/or conformational changes.

Dynamic aspects of the adsorption process of the two IgGs and their $F(ab')_2$ and Fc fragments are described in Chapter 4. This information is obtained by monitoring the adsorption process in real-time using reflectometry. Under all conditions, the two IgGs and their $F(ab')_2$ and Fc fragments adsorb onto the silica and methylated surfaces. However, the adsorption rate of IgG and $F(ab')_2$ on a hydrophilic silica surface is retarded when the proteins are electrostatically repelled by the sorbent surface. This effect is stronger for $F(ab')_2$ fragments than for the whole IgG molecule, whereas the adsorption rate of Fc is not significantly affected. This observation shows that there must be an additional driving force for adsorption of the Fc fragments compared to that of the $F(ab')_2$ fragments. On the methylated surface, hydrophobic interactions largely compensate for the retardation of the initial adsorption rate. Both IgGs show a maximum saturation adsorption around their i.e.p. values and these maxima are less pronounced at higher ionic strength. The decrease in adsorbed amounts when the pH is shifted from the i.e.p. of the proteins is probably caused by the formation of a more expanded structure of the protein owing to a rise of its net charge density. Desorption of the proteins after replacement of the protein solution by the pure buffer was determined after fifteen minutes. The desorbed amounts

indicate that the proteins are more tightly bound to methylated surfaces than to silica. Furthermore, a relatively large fraction of IgG and Fc desorbs from silica at low ionic strength around their respective i.e.p. values, whereas this phenomenon is not observed for F(ab')$_2$. This indicates that under these experimental conditions a fraction of the Fc fragments forms rather weak bonds with the sorbent surface, which are easily broken upon dilution.

A quantitative relationship between the adsorption and the secondary structure of the proteins is described in Chapter 5. This information is attained by measuring Fourier Transformed Infrared spectra of adsorbed IgG and F(ab')$_2$ layers. The obtained infrared spectra consist of two absorption bands, the amide I and amide II regions. The amide II region is rather insensitive to the structure of the adsorbed proteins and is related to the adsorbed amounts. The amide I region is sensitive to the secondary structure and is therefore used for the evaluation of this structure. The results show that the amounts of adsorbed IgG decrease with an increasing net charge density on the protein. This decrease is accompanied by a decrease in ß-sheet structure which suggests that IgG adsorbs in a less compact conformation. The adsorption-induced reduction in the ß-sheet content is larger at hydrophobic methylated surfaces than at hydrophilic silica surfaces. At higher ionic strength, the distribution of the amino acid residues over the structural components depends less on the pH. This feature is reflected by a smaller sensitivity of the adsorbed amount on the pH variation. The F(ab')$_2$ fragments contain a higher fraction of ß-sheet than IgG and these fractions are less influenced by adsorption. Therefore, it is concluded that the F(ab')$_2$ fragments have a higher structural stability than whole IgG molecules.

In Chapter 6, the adsorption behaviour of the two IgGs and their F(ab')$_2$ fragments together with the binding of antigen hCG to the adsorbed proteins, is studied using reflectometry. From Chapter 5 it was inferred that the Fc part of an IgG molecule is more flexible than the Fab part. The higher flexibility promotes adsorption of the Fc part, which implies that the Fab parts are directed towards the solution. This is reflected in higher antigen binding ratios under conditions in which the adsorption of F(ab')$_2$ fragments is unfavourable. Furthermore, it is observed that the orientation of an adsorbed IgG molecule with an uneven charge distribution is strongly influenced by electrostatic interactions. When the Fab parts are electrostatically attracted by the sorbent surface, this may even result in a total absence of the antigen binding capacity.

Perspectives

In the present study, we obtained a wealth of information about the interactions involved in IgG adsorption onto solid sorbent surfaces. For practical applications it is desirable to use this information to control the adsorbed state of the IgG molecules. For example, in the production of immunological tests the IgG molecules will have to adsorb with their antigen binding sites accessible for the antigens and without structural changes affecting the antigen binding capacity.

In Chapter 5 it was observed that the $F(ab')_2$ fragments have a relatively high structural stability and that the structure of $F(ab')_2$ remains stable under a wide range of adsorption conditions. This information suggests that in the adsorbed state the $F(ab')_2$ domains retain their ability to bind antigens.

The orientation of the IgG molecules can strongly be influenced by varying the adsorption conditions. In Chapter 3 it is inferred that IgG adsorbs in an end-on orientation at hydrophobic polystyrene latices. For adsorption onto the silica and methylated surfaces, the adsorbed amounts indicate that at least a large fraction of the IgG molecules are adsorbed in such an orientation. In an end-on orientation the antigen binding sites could be directed towards the solution or be attached to the sorbent surface. The differences in adsorption behaviour between $F(ab')_2$ and Fc fragments can now be used to obtain an adsorbed state of the whole IgG molecule in which the antigen binding sites are preferentially directed to the solution. The present study reveals that there are two possible mechanisms for directing the orientation of the adsorbed IgG molecules. First, as shown in Chapter 6, the IgG orientation can be influenced by electrostatic interactions if the charges of the protein are unequally distributed over the Fc and $F(ab')_2$ fragments. Thus, a favourable orientation can be obtained if the Fc fragment is electrostatically attracted while the $F(ab')_2$ fragment is electrostatically repelled by the charges on the sorbent surface. Second, a difference between the structural stabilities of the Fc and $F(ab')_2$ fragments may cause different adsorption affinities of the respective fragments. As the Fc fragment is structurally less stable than the $F(ab')_2$ fragment, the adsorption of an IgG molecule by its Fc fragment is favoured.

However, it should be realised that these two mechanisms for directing the orientation of adsorbed IgG molecules are only effective under conditions in which the adsorption of the $F(ab')_2$ fragment is suppressed. Since the $F(ab')_2$ fragment shows a high affinity for hydrophobic surfaces, this implies that the orientation of the IgG can only be directed by electrostatic interactions if the sorbent surface is hydrophilic. Furthermore, it is observed that the adsorption of the fragments is only influenced by the differences in structural

stability if the adsorption is not promoted by hydrophobic and/or electrostatic interactions.

In conclusion, we can state that the orientation of the adsorbed IgG molecules can be adjusted by the adsorption conditions including modification of the sorbent surface. To obtain an optimal IgG orientation, these conditions require a sorbent surface with a hydrophilic character and a controlled contribution of electrostatic interactions.

Samenvatting

Adsorptie van immunoglobuline aan vaste oppervlakken

Immunoglobuline G (IgG) is een eiwit dat de eigenschap heeft om zeer specifiek biologische molekulen (antigenen) te binden. In het lichaam van mens en dier binden ze lichaamsvreemde stoffen om vervolgens een afweerreactie tot stand te laten komen. Hierdoor spelen ze een belangrijke rol in de natuurlijke bescherming van het lichaam. Buiten het lichaam worden ze toegepast in immunologische testen en biosensoren om bepaalde stoffen te detecteren en te kwantificeren. Zo worden ze bijvoorbeeld gebruikt om in bloed of urine de aanwezigheid van ziekteverwekkers of hormonen vast te stellen. Het huidige onderzoek is uitgevoerd met IgG eiwitten die specifiek het zwangerschapshormoon, human chorionic gonadotropin (hCG), kunnen binden en daarom worden gebruikt in zwangerschapstesten.

In de immunologische testen zijn IgG eiwitten gehecht aan vaste oppervlakken. Dit is gewenst om de binding van de antigenen door IgG op een bepaalde plaats te concentreren. Hierdoor wordt het makkelijker om die binding zichtbaar te maken. Het IgG is een groot 'Y'-vormig molekuul, zoals te zien is in Figuur 1a. Het molekuul heeft drie domeinen. Twee daarvan, de Fab fragmenten, bezitten de antigeenbindingsplaatsen die gesitueerd zijn aan de uiteinden van de fragmenten. Het derde domein is het Fc fragment dat kan binden aan receptoren op celoppervlakken.

Door de wisselwerking van het IgG met het vaste oppervlak kan de eigenschap van het IgG om antigenen te binden verloren gaan. Dit gebeurt bijvoorbeeld doordat de antigeenbindingsplaatsen naar het vaste oppervlak zijn toegekeerd waardoor ze niet meer toegankelijk zijn voor de antigenen. Het is ook mogelijk dat de wisselwerking van het IgG met het oppervlak een ontvouwing (denaturatie) van het eiwit tot gevolg heeft. Dit kan leiden tot verlies van de bindingsactiviteit. Deze verschillende geadsorbeerde toestanden zijn schematisch weergegeven in de Figuren 1b en 1c.
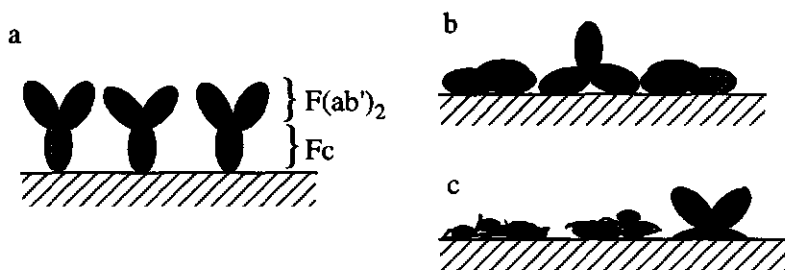
Fig. 1. Schematische weergave van de verschillende toestanden waarin de geadsorbeerde IgG-molekulen zich kunnen bevinden. De antigeenbindingsplaatsen zijn weergegeven door zwarte stippen op de uiteinden van de F(ab')$_2$-fragmenten (twee aan elkaar gekoppelde Fab-fragmenten).

a) In de ideale situatie staan alle antigeenbindingsplaatsen van de IgG-molekulen naar de oplossing gericht.

b) De oriëntatie van de IgG-molekulen is zodanig dat de antigeenbindingsplaatsen niet meer toegankelijk zijn voor antigenen.

c) Een complete of gedeeltelijke ontvouwing is opgetreden, die in vele gevallen leidt tot een verlies van de bindingsactiviteit.

Voor een optimale werking van de immunologische testen is het nodig dat de Fab-fragmenten gericht zijn naar de oplossing en dat eventuele struktuursveranderingen van het IgG, met name in de Fab-fragmenten, beperkt blijven. Dit is schematisch weergegeven in Figuur 1a.

Om de problemen die bij het adsorptieproces kunnen optreden beter te begrijpen en uiteindelijk te voorkomen is het nodig om een goed inzicht te krijgen in de wisselwerkingen tussen het IgG en het vaste oppervlak.

Wisselwerkingen tussen IgG en vaste oppervlakken

Adsorptie van eiwitten wordt voornamelijk bepaald door een drietal factoren, namelijk: elektrostatische wisselwerkingen, hydrofobe wisselwerkingen en de struktuurstabiliteit van het eiwit.

Elektrostatische wisselwerkingen zijn het gevolg van de aanwezigheid van geladen groepen op zowel het eiwit als het vaste oppervlak. De lading van het eiwit wordt bepaald door de ionisatie van zwak zure en zwak basische groepen. Afhankelijk van de

pH (zuurgraad) van de oplossing kan het eiwit netto positief, netto negatief of ongeladen zijn. Indien het eiwit en het oppervlak een tegengestelde lading hebben, wordt het eiwit elektrostatisch aangetrokken door het oppervlak. De elektrostatische wisselwerking wordt sterk beïnvloed door de aanwezigheid van ionen in de oplossing. De ionen schermen de ladingen op het eiwit en op het vaste oppervlak af, zodat bij een hoge ionenconcentratie de elektrostatische wisselwerking pas merkbaar is als het eiwit het oppervlak zeer dicht genaderd is. Verder kunnen de ionen ook ingebouwd worden in de geadsorbeerde laag om op die manier het overschot aan geladen groepen in die laag te compenseren.

Hydrofobe wisselwerkingen ontstaan doordat water niet graag in de buurt van een hydrofoob (waterafstotend) oppervlak zit. Hierdoor wordt de bewegingsvrijheid van de watermolekulen beperkt. De beperking van bewegingsvrijheid is entropisch gezien ongunstig. De toename in entropie, die optreedt als eiwitten de plaats innemen van de aan het oppervlak gebonden watermolekulen, kan een drijvende kracht zijn voor adsorptie.

De struktuurstabiliteit van het eiwit wordt bepaald door een balans van de verschillende wisselwerkingen binnen het eiwit en van het eiwit met zijn omgeving. Indien het eiwit in de buurt komt van een vast oppervlak verandert zijn omgeving en daardoor kan de struktuur van het eiwit veranderen. Indien het IgG een gedeelte van zijn compacte struktuur verliest, wordt daarmee een toename van de entropie verkregen. Een grotere flexibiliteit van het IgG kan er bovendien voor zorgen dat de elektrostatische en hydrofobe wisselwerkingen optimaler worden. De verschillende wisselwerkingen zijn dan ook niet onafhankelijk.

Opzet van het onderzoek

In dit promotieonderzoek is gekeken naar de invloed van de verschillende wisselwerkingen op het adsorptiegedrag van IgG. Hiervoor is gebruik gemaakt van twee verschillende, gekloneerde IgG's die beide specifiek het zwangerschapshormoon hCG binden. Om de invloed van de bovengenoemde wisselwerkingen te bestuderen, is bij de verschillende adsorptie-experimenten de grootte van de wisselwerkingen gevarieerd. Om elektrostatische interakties te variëren zijn adsorptie-experimenten uitgevoerd bij verschillende waarden voor zowel de pH als de ionensterkte. Om de invloed van hydrofobe wisselwerkingen te bestuderen zijn verschillende facetten van het

adsorptiegedrag bestudeerd op hydrofobe en hydrofiele oppervlakken. Voor toepassingen in immunologische testen is het essentieel om te weten of de IgG eiwitten in geadsorbeerde toestand immunologisch actief zijn. Voor deze immunologische activiteit is behalve de struktuur van het IgG ook de oriëntatie op het oppervlak van groot belang. Deze oriëntatie zal in grote mate beïnvloed worden door het adsorptiegedrag van de verschillende domeinen. Daarom is veel aandacht besteed aan de adsorptie van de afzonderlijke fragmenten. Hiertoe is het IgG geknipt in zijn F(ab')$_2$-fragment en het Fc-fragment.

Inhoud van dit proefschrift

Na een algemene introductie in *Hoofdstuk 1*, wordt in *Hoofdstuk 2* aandacht besteed aan eigenschappen van IgG die van belang zijn voor het adsorptiegedrag. Verder wordt een aantal fysische grootheden van de twee gebruikte IgG's gekarakteriseerd. Ook wordt beschreven hoe de F(ab')$_2$- en Fc-fragmenten verkregen zijn door middel van het enzymatisch knippen van de hele IgG-molekulen.

In *Hoofdstuk 3* worden de resultaten beschreven van adsorptie van de twee IgG's en de bijbehorende F(ab')$_2$-fragmenten op een drietal verschillende soorten latexdeeltjes. Twee van deze latexdeeltjes zijn hydrofoob, waarbij één latex negatief en het andere positief geladen is. Het derde latexdeeltje is negatief geladen en hydrofiel. Er is voornamelijk gekeken naar de hoeveelheid eiwit die adsorbeert bij een bepaalde eiwitconcentratie in oplossing. De rol van elektrostatische wisselwerkingen is verder bestudeerd door de invloed van de geadsorbeerde eiwitlaag op de wandpotentiaal na te gaan. In dit onderzoek is ook veel aandacht besteed aan de oriëntaties die het eiwit kan aannemen aan het oppervlak.

Het blijkt dat de IgG's en de F(ab')$_2$-fragmenten een hoge affiniteit tonen voor de hydrofobe latexdeeltjes en dat die affiniteit nauwelijks beïnvloed wordt door de elektrostatische wisselwerking. De geadsorbeerde hoeveelheden zijn echter wel afhankelijk van de elektrostatische wisselwerkingen. Er wordt een maximum in de geadsorbeerde hoeveelheid gevonden als de lading van het eiwit een gedeelte van de tegengestelde lading van het latexoppervlak compenseert. Er kan worden afgeleid dat de relatief grote geadsorbeerde hoeveelheden op de hydrofobe oppervlakken corresponderen met een oriëntatie van de IgG's waarin ze voornamelijk rechtop staan. Op hydrofiele latexdeeltjes treedt geen adsorptie van IgG en F(ab')$_2$ op indien de eiwitten elektrostatisch worden afgestoten door de lading van het latexoppervlak. Als de geladen groepen van de

eiwitten worden aangetrokken door de lading van het latexoppervlak vindt adsorptie wel plaats, maar in kleinere hoeveelheden dan op het hydrofobe latex. In dit geval blijkt dat de geadsorbeerde hoeveelheid correspondeert met een platte oriëntatie van het IgG of F(ab')$_2$-fragment. Alhoewel de IgG's en de F(ab')$_2$-fragmenten in grote lijnen hetzelfde adsorptiegedrag vertonen, blijkt dat de adsorptie van IgG sterker gedreven wordt door wisselwerkingen die niet van elektrostatische origine zijn, dus door hydrofobe wisselwerkingen en/of door een geringere struktuurstabiliteit.

Dynamische aspecten van het adsorptiegedrag worden beschreven in *Hoofdstuk 4*. Deze informatie is verkregen door de geadsorbeerde hoeveelheid in de tijd te volgen met behulp van een reflectometer. Tevens is gekeken naar de desorptie van de eiwitten als de eiwitoplossing vervangen wordt door een bufferoplossing. De twee IgG's en de bijbehorende F(ab')$_2$- en Fc-fragmenten zijn bij verschillende waarden voor de pH en ionensterkte geadsorbeerd op zowel een hydrofiel silica-oppervlak als op een hydrofoob gemethyleerd silica-oppervlak.

Uit dit onderzoek blijkt dat de eiwitten onder alle omstandigheden adsorberen, maar dat de adsorptiesnelheid sterk wordt vertraagd als de IgG en de F(ab')$_2$-fragmenten elektrostatisch worden afgestoten door het hydrofiele silica. Deze vertraging is veel sterker voor het F(ab')$_2$-fragment dan voor het hele IgG, terwijl de adsorptiesnelheid van het Fc-fragment nauwelijks wordt vertraagd. Hier kwam dus naar voren dat, vergeleken met het F(ab')$_2$-fragment, het Fc-fragment een extra drijvende kracht heeft voor adsorptie. Deze verschillen waren niet te zien bij adsorptie op de hydrofobe oppervlakken omdat bij alle pH's en ionensterktes de adsorptiesnelheid hierop maximaal is. Dit betekent dat elk eiwitmolekuul adsorbeert als het in de buurt komt van een leeg oppervlak. Bij beide oppervlakken treedt maximale adsorptie van IgG op indien het eiwit netto ongeveer ongeladen is. Verder is de invloed van de pH op de geadsorbeerde hoeveelheid kleiner bij hoge zoutsterktes. Dit duidt op een sterke invloed van elektrostatische wisselwerkingen. Aangezien de geadsorbeerde hoeveelheid weinig wordt beïnvloed door het soort oppervlak, lijkt het erop dat deze hoeveelheid voornamelijk wordt bepaald door de lading van het eiwit.

Bij desorptiemetingen blijkt dat onder alle experimentele omstandigheden desorptie optreedt, maar dat de eiwitten steviger zijn gebonden aan het hydrofobe gemethyleerde oppervlak dan aan het hydrofiele silica. Verder wordt waargenomen dat een relatief groot gedeelte van de IgG-molekulen en de Fc-fragmenten desorbeert van het silica-oppervlak. Met name bij een lage zoutsterkte en een pH-waarde die in de buurt ligt van het iso-elektrisch punt van de eiwitten. Aangezien onder deze omstandigheden geen desorptie

van F(ab')$_2$-fragmenten optreedt, kan geconcludeerd worden dat in ieder geval een gedeelte van de IgG-molekulen via het Fc-fragment met een relatief zwakke binding is gehecht aan het oppervlak.

In *Hoofdstuk 5* wordt het adsorptiegedrag gekoppeld aan veranderingen die optreden in de secundaire struktuur van de geadsorbeerde IgG- en F(ab')$_2$-molekulen. Deze informatie is verkregen met behulp van Fourier-getransformeerde infrarood spectroscopie. Dit is een methode die het mogelijk maakt om zowel de geadsorbeerde hoeveelheid eiwit als de hoeveelheid van de verschillende struktuurcomponenten waaruit de eiwitten bestaan te kwantificeren. Aangezien de secundaire struktuur van het IgG voornamelijk bestaat uit ß-sheets, is het gehalte hiervan bepaald onder verschillende adsorptieomstandigheden.

Het blijkt dat bij een lage zoutsterkte de geadsorbeerde hoeveelheid afneemt indien de netto lading op het eiwit toeneemt. Deze afname gaat gepaard met een verlies in het gehalte van de ß-sheets. Dit suggereert dat de lagere geadsorbeerde hoeveelheid in ieder geval gedeeltelijk wordt veroorzaakt omdat het IgG in een minder compacte struktuur adsorbeert. Als de zoutsterkte toeneemt, wordt de invloed van pH op het ß-sheetgehalte minder. Ook is gevonden dat het gehalte aan ß-sheets lager is bij adsorptie op het hydrofobe gemethyleerde silica dan op het hydrofiele silica. Dit wordt waarschijnlijk veroorzaakt door de sterkere wisselwerking van het eiwit met hydrofobe oppervlakken dan met hydrofiele oppervlakken.

Er was een opvallend verschil tussen het ß-sheetgehalte van de geadsorbeerde F(ab')$_2$-fragmenten en de hele IgG-molekulen. Bij lage zoutsterkte is het ß-sheetgehalte van de F(ab')$_2$-fragmenten onder alle adsorptieomstandigheden groter dan dat van de hele IgG-molekulen. Tevens blijft het ß-sheetgehalte relatief constant als het F(ab')$_2$-fragment geadsorbeerd wordt bij verschillende pH-waarden. Hieruit blijkt dat het F(ab')$_2$-fragment een grotere struktuurstabiliteit heeft dan het hele IgG-molekuul. Dit verschil in struktuurstabiliteit is dan ook zeer waarschijnlijk de oorzaak van het verschil in adsorptiegedrag zoals waargenomen en beschreven in de Hoofdstukken 3 en 4.

Tenslotte wordt in *Hoofdstuk 6* beschreven hoe de verschillende adsorptie-omstandigheden de antigeenbindingscapaciteit van de geadsorbeerde IgG- en F(ab')$_2$-molekulen beïnvloeden. Deze bindingscapaciteit is bestudeerd door aan een laag met geadsorbeerde IgG- of F(ab')$_2$-molekulen het zwangerschapshormoon hCG toe te voegen. De geadsorbeerde hoeveelheden worden bepaald met de reflectometer en omgerekend naar het aantal molekulen hCG gebonden door een IgG- of F(ab')$_2$-molekuul.

In principe kan elk IgG- en F(ab')$_2$-molekuul maximaal twee hCG-molekulen binden. Het blijkt echter dat de verhouding bij alle adsorptie-omstandigheden beneden de één ligt. Uit dit onderzoek komt naar voren dat de oriëntatie van een IgG-molekuul met een ongelijke ladingsverdeling sterk beïnvloed kan worden door de lading op het oppervlak. De negatieve lading op het silica oppervlak is in staat om een IgG met een negatief geladen Fc-fragment en een positief geladen F(ab')$_2$-fragment zodanig te richten, dat het IgG adsorbeert met zijn F(ab')$_2$-fragment. Dit heeft tot gevolg dat er totaal geen hCG gebonden wordt. Ook blijkt dat de lagere struktuurstabiliteit van het Fc-fragment ten opzichte van het F(ab')$_2$-fragment ervoor kan zorgen dat het IgG er de voorkeur aan geeft om met zijn Fc-fragment aan het oppervlak te binden. Dit resulteert in een hogere hCG-bindingsverhouding wanneer het IgG adsorbeert onder elektrostatisch afstotende omstandigheden aan een hydrofiel oppervlak.

Met betrekking tot de immunologische testen kunnen we concluderen dat door de hoge structuurstabiliteit van het F(ab')$_2$-fragment de bindingsactiviteit behouden blijft onder een groot aantal omstandigheden waarbij adsorptie wordt uitgevoerd. Tevens is het mogelijk om de oriëntatie van de geadsorbeerde IgG-molekulen te beïnvloeden door de keuze van de adsorptieomstandigheden. Dit kan bij voorkeur door gebruik te maken van een systeem met hydrofiele oppervlakken en elektrostatische afstoting tussen het oppervlak en het F(ab')$_2$-gedeelte van het IgG-molekuul.

Nawoord

De afgelopen vier jaar heb ik regelmatig het idee gehad dat ik in mijn eentje bezig was met mijn promotieonderzoek. Zonder een goede werkomgeving zou het echter onmogelijk geweest zijn om het onderzoek uit te voeren. Zo'n goede werkomgeving was zeker te vinden bij de vakgroep fysische- en kolloïdchemie en hiervoor wil ik alle (ex-) medewerkers van de vakgroep bedanken.

Natuurlijk hebben een groot aantal mensen direct of indirect meegewerkt aan het tot stand komen van dit proefschrift.

Allereerst wil ik mijn begeleiders, Willem en Hans, bedanken. Ik vond het zeer prettig dat ik mijn onderzoek in grote vrijheid kon uitvoeren. Ik heb altijd een groot vertrouwen gehad in jullie kennis van het vakgebied en heb veel geleerd van jullie kritische commentaren.

Het onderzoek werd financieel mogelijk gemaakt door Akzo Nobel (Arnhem). Hiervoor mijn dank. De samenwerking met het Centrale Research Laboratorium van Akzo Nobel (ARLA) en Organon Teknika heb ik als zeer prettig ervaren en de constructieve werkbesprekingen hebben veel bijgedragen aan de totstandkoming van dit proefschrift. Ook heb ik altijd een beroep kunnen doen op de aanwezige kennis, apparatuur en materialen, hiervoor wil ik James, Rob, Mirjam, Pieter, Bert en Roberta van Akzo Nobel en David van Organon Teknika bedanken. Verder is het Ron en André van Organon Teknika gelukt om mij in de eerste twee maanden van mijn onderzoek wegwijs te maken in de eiwitchemie. Dat was behalve een gezellige ook een zeer leerzame periode.

In het kader van een afstudeervak hebben Petra, Karin, Toine en Dries in grote mate bijgedragen aan dit onderzoek. Zonder jullie hulp was het nooit gelukt!

De afgelopen vier jaar heb ik met enkele onderbrekingen mijn kamer gedeeld met Marc en Luc. Hoezeer ik dat op prijs heb gesteld, merk ik pas nu ik al een paar maanden alleen op deze kamer zit. Verder wil ik Janet bedanken voor de motiverende en relativerende gesprekken en Jeanette, Marcel en Jenny voor het meezwemmen om de werkstress te ontladen.

Op een meer indirecte manier hebben familie en vrienden mij bijgestaan tijdens mijn promotieopdracht. Zonder jullie steun was het zeker niet gelukt om de motivatie te vinden die nodig was voor het voltooien van dit proefschrift.

En tenslotte: Elles, er zijn zoveel dingen waarvoor ik jou zou willen bedanken dat ik het maar houd op een simpel "bedankt" !

Jos

Curriculum Vitae

Jos (J.A.G.) Buijs was born in Arnhem, The Netherlands, on 17 March 1967. He graduated from the Liemers College (high school), Zevenaar in 1985. Subsequently, he started studying molecular sciences at the Wageningen Agricultural University. He specialised in physical chemistry and graduated (M.Sc.) in March 1991. His main subjects were physical chemistry and physics, and he took mathematics as a secondary course. He spent a practical training period of four months at the Department of Photophysics, Institute of Isotopes of the Hungarian Academy of Sciences, Budapest, Hungary. From April 1995 he worked as a research assistant at the Department of Physical and Colloid Chemistry of the Wageningen Agricultural University. The research project was a collaboration with the Akzo Nobel Central Research Institute and Organon Teknika. From October 1995 he will work as a post-doc at the Center for Biopolymers at Interfaces, Salt Lake City, U.S.A. For this post-doctoral position he received a grant (Talent-stipendium) from the Netherlands Organization for Scientific Research (NWO).